DEVELOPMENT OF ORGANIC-INORGANIC COMPOSITE MEMBRANES FOR FUEL CELL APPLICATIONS

A THESIS SUBMITTED TO
THE GRADUATE SCHOOL OF NATURAL AND APPLIED SCIENCES
OF
MIDDLE EAST TECHNICAL UNIVERSITY

BY

HÜLYA ERDENER

IN PARTIAL FULFILLMENT OF THE REQUIREMENTS
FOR
THE DEGREE OF MASTER OF SCIENCE
IN
CHEMICAL ENGINEERING

JUNE 2007

Approval of the Graduate School of Natural and Applied Sciences

Prof. Dr. Canan ÖZGEN
Director

I certify that this thesis satisfies all the requirements as a thesis for the degree of Master of Science.

Prof. Dr. Nurcan BAÇ
Head of Department

This is to certify that I have read this thesis and that in my opinion it is fully adequate, in scope and quality, as a thesis for the degree of Master of Science.

Prof. Dr. Hayrettin YÜCEL	Prof. Dr. Nurcan BAÇ
Co-Supervisor	Supervisor

Examining Committee Members

Prof. Dr. İnci EROĞLU	(METU, CHE)	
Prof. Dr. Nurcan BAÇ	(METU, CHE)	
Prof. Dr. Hayrettin YÜCEL	(METU, CHE)	
Prof. Dr. Güniz GÜRÜZ	(METU, CHE)	
Asst. Prof. Dr. Mehmet SANKIR	(TOBB, CHEM)	

I hereby declare that all information in this document has been obtained and presented in accordance with academic rules and ethical conduct. I also declare that, as required by these rules and conduct, I have fully cited and referenced all material and results that are not original to this work.

Name, Last name: Hülya ERDENER

Signature

ABSTRACT

DEVELOPMENT OF ORGANIC-INORGANIC COMPOSITE MEMBRANES FOR FUEL CELL APPLICATIONS

Erdener, Hülya
M.S., Department of Chemical Engineering
Supervisor : Prof. Dr. Nurcan BAÇ
Co-Supervisor: Prof. Dr. Hayrettin YÜCEL

June 2007, 116 pages

Hydrogen is considered to be the most promising energy carrier of the 21st century due to its high energy density and sustainability. The chemical energy of hydrogen can be directly converted into electricity by means of electrochemical devices called fuel cells. Proton exchange membrane fuel cells (PEMFC) are the most preferred type of fuel cells due to their low operating temperatures enabling fast and easy start-ups and quick responses to load changes. One of the most important components of a PEMFC is the proton conducting membrane. The current membrane technology is based on perfluorosulfonic acid membranes and the most common one being Nafion. Although these membranes have good thermal and chemical stability, mechanical strength and high proton conductivities, they tend to dehydrate very fast at high temperatures and low relative humidity leading to poor fuel cell performances. Moreover, the high manufacturing cost of these membranes limits the mass-production of PEMFC's in near future.

The aim of this study is to develop alternative PEMFC membranes that have sufficient thermal and chemical stability, mechanical strength and comparable proton conductivity and fuel cell performances with Nafion membranes at relatively low cost. In this context, organic-inorganic composite membranes and blends were developed. A relatively cheap and commercially available polymer, polyether ether ketone, (PEEK), was chosen as the membrane matrix for its high thermal and mechanical stability and improvable proton conductivity via post-sulfonation. The proton conductivity of SPEEK membrane (at DS 68%) was 0.06 S/cm at 60°C, and this conductivity was further increased to 0.13 S/cm with the introduction of zeolite beta crystals as inorganic fillers. The conductivity of a SPEEK blend (25wt% SPES-75wt% SPEEK) membrane was 0.08 S/cm at 90°C. In PEMFC performance tests, 397 mA/cm^2 was obtained for SPEEK membrane (DS 56%) at 0.6V for a H_2/O_2 PEMFC working at 1 atm and 80°C. This result is promising when compared to the performance of Nafion 112® of 660mA/cm^2 under same conditions. These results are welcomed since the target for commercially viable alternate membranes are reached.

Keywords: PEM Fuel Cells, Organic-inorganic composite membranes, Sulfonated Aromatic Hydrocarbon Membranes, Blend membranes

ÖZ

YAKIT PİLİ UYGULAMALARI İÇİN ORGANİK-İNORGANİK KOMPOZİT MEMBRAN GELİŞTİRİLMESİ

Erdener, Hülya
Yüksek Lisans, Kimya Mühendisliği Bölümü
Tez Yöneticisi : Prof. Dr. Nurcan BAÇ
Ortak Tez Yöneticisi: Prof. Dr. Hayrettin YÜCEL

Haziran 2007, 116 sayfa

Hidrojen yüksek enerji yoğunluğu ve sürdürülebilir olması nedeniyle 21. yüzyılın en olası enerji taşıyıcısı olarak görülmektedir. Hidrojenin içerdiği kimyasal enerji, yakıt pili adı verilen elektrokimyasal araçlar vasıtasıyla doğrudan elektiriğe dönüştürülebilir. Proton değişim membranlı yakıt pilleri (PEMFC), hızlı ve kolay başlatılmalarına olanak veren düşük çalışma sıcaklıkları ve yük değişikliklerine verdikleri hızlı tepkiler nedeniyle en çok tercih edilen yakıt pili çeşididir. PEMFCnin en önemli parçalarından biri proton iletken membrandır. Günümüz zar teknolojisi en yaygın kullanılanı Nafyon olmak üzere, perflorosulfonik asit bazlı membranlara dayanmaktadır. Bu membranlar iyi ısıl, kimyasal ve mekanik dayanıklılık, yüksek proton iletkenlikleri ve yakıt pili performanslarına sahip olmalarına rağmen, yüksek sıcaklıkta ve düşük nemde hızla kururlar ve yakıt pili performansları düşer. Bunun yanısıra, bu membranların yüksek üretim maliyetleri, PEM yakıt pillerinin yakın bir gelecekte yaygın üretime geçilmesini kısıtlamaktadır.

Bu çalışmanın amacı yeterli ısıl, kimyasal ve mekanik dayanıklılıkta Nafyon membranlarla karşılaştırılabilir proton iletkenlikleri, yakıt pili performansı ve daha düşük üretim maliyetleri olan alternatif PEM yakıt pili membranları geliştirmektir.
Bu amaçla, organik-inorganik kompozit ve karışım membranlar geliştirilmiştir. Ucuz ve kolay bulunabilen bir polimer olan, polieter eter keton, (PEEK), polimeri yüksek ısıl ve mekanik dayanımı ve iyileştirilebilir proton iletkenliği nedeniyle membran matrisi olarak seçilmiştir. SPEEK membranın proton iletkenliği 60°C'de 0.06 S/cm'dir ve bu iletkenlik inorganik dolgu malzemesi olan zeolite beta kristallerin eklenmesi sonucu 0.13 S/cm'e kadar yükselmiştir. %25 SPES içeren SPEEK karışım membranın 90°C'deki iletkenliği ise 0.08 S/cm'dir. 1 atm 80°C'de yapılan H_2/O_2 PEM yakıt pili performans testlerinde SPEEK membranının 0.6 V'da 397 mA/cm^2 akım verdiği görülmüştür bu değer aynı şartlarda 660 mA/cm^2 akım veren Nafyon 112 membranla karşılaştırıldığında umut vericidir. Ticari olarak kullanılabilır alternatif membran hedefine ulaşıldığı için bu sonuçlar memnuniyet vericidir.

Anahtar Kelimeler : PEM Yakıt Pilleri, organik-inorganik kompozit membranlar, sülfonlanmış aromatik hidrokarbon membranlar, karışım membranlar

This work is dedicated to my family.

ACKNOWLEDGEMENTS

I would like to express my gratitude to Prof. Dr. Nurcan BAÇ, Prof. Dr. Hayrettin YÜCEL and Prof. Dr. İnci EROĞLU for their continuous supervision, invaluable guidance, encouragement and patience during all stages of this work.

I am grateful to my laboratory co-workers Gültekin Akay, Kübra Kamışoğlu and the members of fuel cell research group. It was my pleasure to work with each of these people. Moreover, I would like to thank to Erce Şengül, Serdar Erkan and Ayşe Bayrakçeken for their help in MEA preparation and fuel cell performance tests. Furthermore, I would like to thank to the technical staff of METU, Chemical Engineering Department and Central Laboratory personnel for the characterization analysis.

The scholarship and funding of project (number 104 M 364) from TÜBİTAK are gratefully acknowledged.

Finally, I would like to express all my love to my family and close friends for their support and patience.

TABLE OF CONTENTS

ABSTACT……iv
ÖZ……..vi
ACKNOWLEDGEMENTS……ix
TABLE OF CONTENTS……x
LIST OF TABLES…….....xiii
LIST OF FIGURES……...xiv
NOMENCLATURE…….....xvii
CHAPTER …….....1
INTRODUCTION…….....1
1.1 Fuel Cells……...2
1.2 Types of Fuel Cells……3
1.2.1 Proton Exchange Membrane Fuel Cells…….....4
1.2.2 Alkaline Fuel Cells.....4
1.2.3 Phosphoric Acid Fuel Cells.....4
1.2.4 Molten Carbonate Fuel Cells……..5
1.2.5 Solid Oxide Fuel Cells.....5
2 LITERATURE SUMMARY.....7
2.1 Technology behind PEM Fuel Cells.....7
2.2 Solid Polymer Electrolyte Membrane…….10
2.3 A Closer Look to SPEEK Membrane……..14
2.3.1 Sulfonation of PEEK Polymer……..15
2.3.2 The Influence of Sulfonation Level on Crystallinity and Solubility of PEEK Polymer……...22
2.3.3 Thermal Stability of PEEK Polymer and its Sulfonated Derivatives……..24

2.3.4 Water Uptake of PEEK Polymer and its Sulfonated Derivatives……..…27
2.3.5 Proton Conductivities of PEEK Polymer and its Sulfonated Derivatives……..……28
2.4 Proton Transfer Mechanism……35
2.5 Effect of Inorganic Additives on Proton Conductivity……...39
2.6 Zeolite Beta……45
3 EXPERIMENTAL……49
3.1 Zeolite Synthesis……49
3.2 Characterization of Zeolite Beta……51
3.2.1 X-Ray Powder Diffraction Analysis……..51
3.2.2 Scanning Electron Microscopy Analysis……...51
3.3 Polymer Sulfonation……...51
3.3.1 Sulfonation of PEEK Polymer……...51
3.3.2 Sulfonation of PES Polymer……..53
3.4 Characterization of Sulfonated Polymers……...53
3.4.1 Titration Analysis.....53
3.4.2 H-NMR Analysis……...53
3.5 Composite Membrane Casting and Incorporation of Zeolite Beta Particles…….....54
3.6 Blend Membrane Casting……55
3.7 Membrane Characterization……55
3.7.1 Differential Scanning Calorimetry analysis……...55
3.7.2 Thermogravimetric Analysis……..55
3.7.3 Water Uptake Measurements……56
3.7.4 Swelling Measurements…….....56
3.7.5 Proton Conductivity Analysis……....56
3.7.6 Fuel Cell Tests……...58
4 RESULTS& DISCUSSIONS……....59
4.1 Zeolite Synthesis.....59
4.2 Polymer Sulfonation.....64
4.3 Composite Membranes.....68
4.4 Swelling Problem.....75

4.5 Blend Membranes……...76
4.6 Fuel Cell Performance Tests……...79
5 CONCLUSIONS...…….85
6 RECOMMENDATIONS FOR FUTURE WORKS…...……...88

REFERENCES…...…….90

APPENDICES…….....96

LIST OF TABLES

Table 1.1: Comparison of Various Types of Fuel Cells…….6
Table 2.1: Sulfur Content of Different Sulfonated SPEEK Samples……17
Table 2.2: Characterization of PEEK Polymers of Different Brands……...31

LIST OF FIGURES

Figure 1.1: Gaseous Voltaic Battery……...3
Figure 2.1: The Components of PEMFC……9
Figure 2.2: Structure of Nafion® Membrane…….11
Figure 2.3: Structure of Aciplex-S Developed by Asahi Chemicals……11
Figure 2.4: Development of Solid Polymer Electrolyte Membranes……12
Figure 2.5: The Structure of Dow Membrane……...12
Figure 2.6: Plain and Sulfonated Structure of PEEK Polymer…….14
Figure 2.7: Ion Exchange Capacity of PEEK as a function of Reaction Time at Room Temperature……...……15
Figure 2.8: Nomenclature of Protons in SPEEK Structure……..….16
Figure 2.9: H-NMR Spectra of SPEEK Polymers with Different DS Values……..18
Figure 2.10: Degree of Sulfonation of SPEEK as a function of Reaction Time at Room Temperature……...19
Figure 2.11: FT-IR Spectra of PEEK and its Sulfonated Derivative……20
Figure 2.12: FT-IR Spectra of PEEK and its Sulfonated Derivatives……..21
Figure 2.13: Wide Angle X-Ray Diffractogram of PEEK and its Sulfonated Derivatives……....23
Figure 2.14: Tg of SPEEK as a Function of DS……...24
Figure 2.15: TGA and DTG Curves of PEEK and SPEEK Polymers……..26
Figure 2.16: Water Uptake of Sulfonated PEEK Membranes……..27
Figure 2.17: Conductivity of SPEEK Membranes at Ambient Conditions……..28
Figure 2.18: Proton Conductivity of Different SPEEK Membranes as a Function of Temperature……..…30
Figure 2.19: Temperature Dependence of Gatone™ PEEK (DS 58%) and Vitrex™ PEEK (DS 59%) ……...32
Figure 2.20: Schemes of Co-axial and Longitudinal Conductivity Cells…….34

Figure 2.21: Comparison of Conductivities of the Same Membrane Measured in Transversal and Longitudinal Directions……..34
Figure 2.22: Comparison of Structures of Nafion and SPEEK Polymers……36
Figure 2.23: Proton Transfer Mechanism in Different Membrane Configurations..37
Figure 2.24: Transfer Mechanism of a Protonic Defect in Water…….37
Figure 2.25: Influence of HPAs on the Proton Conductivity of a) SPEEK with DS 70%, b) SPEEK with DS 74%.....40
Figure 2.26: Proton Conductivity of BPO_4/SPEEK Composite Membranes……41
Figure 2.27: Polarization Curves of Nafion 115, SPEEK and SPEEK-Laponite membranes in H_2-O_2 PEMFC……...42
Figure 2.28: Conductivity of Nafion based Composite Membranes at RT……..43
Figure 2.29: Conductivity of Nafion based Composite Membranes as a function of Temperature……..…44
Figure 2.30: Conductivity of SPES-40 based Composite Membranes as a function of Temperature……..……44
Figure 2.31: Structure of Zeolite Beta……..45
Figure 2.32: The Effect of Acid Treatment on Zeolite Beta Structure…….47
Figure 2.33: TGA Analysis of as Synthesized and Acid Treated Zeolite Beta Samples...……..…47
Figure 2.34: Schematic diagram of three pore structures obtained by introduction of zeolite particles in a film……...48
Figure 3.1: The Introduction of Synthesis Gel into Teflon-lined Autoclaves……..50
Figure 3.2: Introduction of Grinded PEEK Polymer into H_2SO_4…….52
Figure 3.3: Stopping the Post-Sulfonation Reaction…….....52
Figure 3.4: Bruker Biospin NMR Spectrometer……...54
Figure 3.5: Membrane Casting onto Petri-Dishes…….54
Figure 3.6: Conductivity Cell……57
Figure 3.7: Fuel Cell Test Station…….58
Figure 4.1: XRD pattern of As-synthesized Zeolite Beta (SiO_2/Al_2O_3= 20).....60
Figure 4.2: XRD pattern of As-synthesized Zeolite Beta (SiO_2/Al_2O_3= 12).....60
Figure 4.3: XRD pattern of As-synthesized Zeolite Beta Treated with 95-98 wt% H_2SO_4.....61
Figure 4.4: TGA Graph of Zeolite Beta Crystals.....62

Figure 4.5: SEM Micrographs of Synthesized Zeolite Beta Crystals.....63
Figure 4.6: Degree of Sulfonation of PEEK Polymer as a function of Reaction Time.....65
Figure 4.7: H-NMR Spectra of SPEEK Polymer (DS 68%).....66
Figure 4.8: Thermal Stability of PEEK Polymer as a Function of Sulfonation Level.....67
Figure 4.9: Water Uptake Capacities of Plain and Composite SPEEK Membranes.....68
Figure 4.10: Teflon Conductivity Cell.....69
Figure 4.11: Proton Conductivity of Plain and Composite SPEEK Membranes.....70
Figure 4.12: Proton Conductivity of SPEEK and Composite Membranes as a function of Temperature.....72
Figure 4.13: Influence of Zeolite Beta Loading on Proton Conductivity.....74
Figure 4.14: TGA Graph of 25 wt% SPES + 75 wt% SPEEK Blend Membrane…76
Figure 4.15: TGA Graph of 50 wt% SPES + 50 wt% SPEEK Blend Membrane…77
Figure 4.16: TGA Graph of 75 wt% SPES + 25 wt% SPEEK Blend Membrane…77
Figure 4.17: Water Uptake Capacities of Blend Membranes……...78
Figure 4.18: Proton Conductivities of Plain and Blend Membranes……79
Figure 4.19: Comparison of Nafion Solution and SPEEK Solution for SPEEK based MEAs……....80
Figure 4.20: Effect of Operating Temperature on the Performance of SPEEK based MEAs……..…..81
Figure 4.21: Effect of Operating Temperature on the Performance of Blend Membranes……..…….81
Figure 4.22: Effect of Sulfonation Level on the Performance of SPEEK based MEAs……..……..82
Figure 4.23: Effect of Acid Treatment on the Performance of SPEEK based MEAs……..……..…83
Figure 4.24: The comparison of Nafion and SPEEK Membrane's Performances....84

NOMENCLATURE

AFC: Alkaline Fuel Cell

CSA: Chlorosulfonic Acid

DMA: Dimethyl Amine

DMAc: Dimethyl Acetamide

DMAm: Dimetyl Aminium hydrogen Sulfate

DMF: Dimethyl Formamide

DMSO: Dimethyl Sulfoxide

DS: Degree of Sulfonation

DSC: Differential Scanning Calorimetry

EIS: Electrochemical Impedance Spectroscopy

FT-IR: Fourier Transform Infrared

H-NMR: Proton Nuclear Magnetic Resonance

HPA: Heteropoly Acid

IEC: Ion Exchange Capacity

MCFC: Molten Carbonate Fuel Cell

MEA: Membrane Electrode Assembly

MMT: Montmorillonite

MPA: Molybdo-phosphoric Acid

Na-TPA: Disodium Salt of Tungstophosphoric Acid

PAFC: Phosphoric Acid Fuel Cell

PEMFC: Proton Exchange Membrane (or Polymer Electrolyte Membrane) Fuel Cell

PFCA: Perfluoro carboxylic acid

PFSA: Perfluorosulfonic acid

RH: Relative Humidity

RT: Room Temperature

SEM: Scanning Electron Microscopy

SOFC: Solid Oxide Fuel Cell

SPEEK: Sulfonated Polyether Ether Ketone

SPES-C: Sulfonated Polyether Sulfone with Cardo

SPBI: Sulfonated Polybenzimidazole

SPPBP: Sulfonated Polyphosphazene

SPS: Sulfonated Polysulfone

T_d: Thermal Decomposition Temperature

T_g: Glass Transition Temperature

TGA: Thermogravimetric Analysis

TPA: Tungstophosphoric Acid

σ : Proton Conductivity

CHAPTER 1

INTRODUCTION

Energy concept was introduced by the discovery of fire and became crucial in everyday life especially after the industrial revolution. Fossil fuels, such as coal, lignite, natural gas, petroleum and their derivatives are used as the main energy resources. However, there are two main drawbacks of the continued fossil fuel utilization. Firstly, the time periods required for the formation of fossil fuel resources are very long thus these reserves are getting scarce day by day. It is estimated that, there will be an increase in the production of the most commonly used fossil fuels, petroleum and natural gas sometime in between 2015 -2020 [1]; then the production rate will decrease. Therefore there may be depletion in the liquid fuels beginning around 2015 [1]. The second drawback is the environmental problems caused by the consumption of fossil fuels. It is known that, greenhouse gases such as CO, CO_2, SO_2, NO_x are produced during the combustion of fossil fuels. These greenhouse gases trap excess heat from the sun's irradiation within the atmosphere and cause environmental problems such as global warming, climate changes, acid rains, pollution and ozone layer depletion, so on. In order to get over these drawbacks, there is an active interest in the researches of alternate energy resources.

Hydrogen is seen as one of the most promising candidates of these alternate energy resources for being the lightest, cleanest and most efficient fuel. The most important property of hydrogen energy is its direct conversion into electricity in fuel cells with higher efficiencies than conversion of fossil fuels in traditional combustion engines or to electrical energy in thermal power plants [1].

Because of this property, hydrogen fuel cells find a wide application area of use from portable applications such as cellular phones, laptops, portable military applications to transportation and stationary applications. Since hydrogen fuel cells are electrochemical devices and not heat engines, their performance is independent of Carnot cycle limitations, thus they have higher efficiencies than other heat engines (internal combustion engines, gas turbines, steam turbines, etc) [1].

In conclusion, petroleum and natural gas were the leading energy resources of the 20^{th} century and hydrogen energy is believed to take their place in the 21^{st} century, thus fuel cell technology may eventually replace the traditional heat engines.

1.1 Fuel Cells

Fuel cells are electrochemical devices that directly convert the chemical energy of fuel into direct current electricity. Their working principle is just the reverse of water hydrolysis; in which pure hydrogen and oxygen are produced from water as a result of an applied potential difference. The operating principle of fuel cells, the gaseous fuels that generate electricity, was first discovered by Sir William Robert Grove and Christian Friedrich Schönbein independently in 1839 [1] and first fuel cell was made by Sir William Grove in 1843 [2] and this fuel cell was named as 'Gaseous voltaic battery'. However, no other researches on fuel cells were recorded almost over a century.

It was not until 1937, Francis T. Bacon has started working on fuel cells and in 1950's he developed 5kW fuel cell [1]. The first practical fuel cell applications were in the U.S. space program. In early 1960's, polymer electrolyte membrane fuel cells developed by General Electrics were used in the Gemini space program. This was followed by the Apollo Program which used fuel cells to supply electricity and drinking water [1]. The fuel cells in Apollo Program were fabricated by Pratt and Whitney based on licensed Bacon's patents [2].

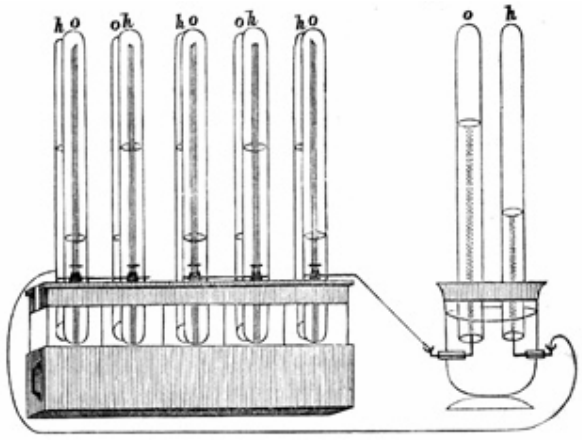

Figure 1.1: Gaseous Voltaic Battery [2]

Until 1990's, fuel cells were considered mainly in space programs. After 1990's, fuel cells have found a wide application area. In 1989, the first polymer electrolyte fuel cell (PEMFC) powered submarine was demonstrated by Ballard, Perry Energy systems and an emerging Canadian company [1]. In 1993, Ballard established fuel cell powered busses and in the same year the first passenger car running on fuel cell power was produced by Perry energy systems [1], which took the attention of other car companies on fuel cells. Fuel cells applications are then broadened to portable devices such as cellular phones, laptops and military equipments thus fuel cells became an active research area for both scientific and engineering communities.

1.2 Types of Fuel Cells

Fuel cells are classified according to the type of the electrolyte used in the fuel cell. The electrolyte basically determines the kind of the chemical reactions occurring within the cell; the type of the catalyst used; the operating temperature range of the cell and the fuel required [3]. There are five main types of fuel cells;

1.2.1 Proton Exchange Membrane (PEM) Fuel Cells

PEM fuel cells have a solid organic polymer membrane which plays an active role in proton transport between anode and cathode compartments. The most commonly used solid polymer membranes are Perfluorosulfonic acid (PFSA) type membranes or per fluorinated carboxylic acid type membranes (PFCA). PEM fuel cells operate at low temperatures (60-100°C), that enables for quick start-up resulting in less wear on the system components, hence better durability. However, these fuel cells require expensive platinum catalyst which is very sensitive to the fuel impurities.
For this reason, pure hydrogen and pure oxygen are generally utilized as fuel in PEMFC's. PEMFC's are mainly used in portable applications, transportation and some stationary applications.

1.2.2 Alkaline Fuel Cells (AFC)

Alkaline fuel cells were one of the pioneer fuel cell technologies developed and first used in Apollo space craft. AFC's use a potassium hydroxide (KOH) solution in water as the electrolyte and the operating temperature of AFC depends on the concentration of this solution. Concentrated solutions (~85 wt %) can perform at high temperatures (100-250 °C), where as less concentrated solutions (35-50 wt %) can work at lower temperatures (<120°C) [1]. Various non-precious metals can be used as catalyst. However, these fuel cells can be easily poisoned by carbon dioxide (CO_2).

1.2.3 Phosphoric Acid Fuel Cells (PAFC)

PAFC's use liquid phosphoric acid soaked in either ceramic matrix or Teflon-based silicon carbide as the electrolyte and platinum catalyst containing electrodes. Operating temperature is typically between 175-200°C. 200 kW PAFC packages are commercially available for stationary electricity generation (UTC fuel cells) [1].

1.2.4 Molten Carbonate Fuel Cells (MCFC)

MCFC's are high temperature fuel cells (~650 °C) which use molten carbonate salts as electrolyte. At such high temperatures precious catalysts are not required. These fuel cells are in pre-commercial stage for stationary power applications [1].

1.2.5 Solid Oxide Fuel Cells (SOFC)

These fuel cells usually use solid, non-porous metal oxide (usually ytrria stabilized zirconium-oxide) as electrolyte. They work at very high operating temperatures, around 800-1000°C where ionic conduction takes place by oxygen ions [1]. Similar to MCFC's, these fuel cells are also in pre-commercial demonstration stage for stationary power applications.

A brief comparison of various fuel cells can be found in Table 1.1. Proton exchange membrane (or polymer electrolyte membrane) fuel cells are mostly preferred among the other types, due to their low operating temperature, fast, easy start-up and quick response to the load changes. PEM fuel cells have a wide application area especially in transportation, stationary applications and portable use such as cellular phones, laptops, military equipment and so on. Thus, the scope of this work is narrowed down to PEM fuel cells.

One of the main components of a PEM fuel cell is the membrane which facilitates the proton transfer between the anode and the cathode sides. The current membrane technology is based on perfluorosulfonic acid membranes having good thermal and chemical stability, mechanical strength and high proton conductivities on the order of 10^{-1} S/cm. However, these membranes tend to dehydrate very fast at high temperatures and low relative humidity leading to low proton conductivity and poor fuel cell performance. Besides, the high manufacturing cost of these membranes limits the mass-production of PEM fuel cells in the near future. Hence, the objective of this work is to develop alternate membranes that possess comparable properties with PFSA based membranes at a relatively low cost.

Table 1.1: Comparison of Various Types of Fuel Cells [4]

	Electrolyte	Operating Temperature (°C)	Advantages	Disadvantages	Applications
Proton Exchange Membrane (PEM)	Solid organic polymer membrane (perfluorosulfonic acid)	60-100	-Solid Electrolyte -Low temperature -Quick start-up -High power density	-Expensive Pt catalyst -Sensitive to fuel impurities (CO, S)	-Portable power -Transportation -Electric Utilities
Alkaline (AFC)	Liquid solution of potassium hydroxide soaked in a ceramic matrix	90-100	-High Performance	-Intolarent to CO_2 -Requires pure H_2/O_2 -Liquid Electrolyte	-Military -Space
Phosphoric Acid (PAFC)	Liquid phosphoric acid soaked in a ceramic matrix	175-200	-Higher grade waste heat can be used in cogeneration applications	-Corrosive liquid electrolyte	-Electric Utilities -Transportation
Molten Carbonate (MCFC)	Liquid solution of lithium, sodium & potassium carbonates soaked in a matrix	~650	-Internal reforming -High Efficiency -High grade of waste heat available for bottoming cycle	-Materials (corrosion) -Intolarance to S -Liquid electrolyte -Slow start-up	-Electric Utilities
Solid Oxide (SOFC)	Solid zirconium oxide to which a small amount of ytrria is added	800-1000	-Internal reforming -High Efficiency -High grade of waste heat available for bottoming cycle	-Materials (corrosion) -Slow start-up -Intolarance to S	-Electric Utilities

CHAPTER 2

LITERATURE SUMMARY

2.1 The Technology behind PEM Fuel Cells

PEM fuel cells usually use hydrogen as fuel and oxygen (or air) as the oxidant. A PEM fuel cell is composed of a proton conductive membrane in the middle, catalyst layers surrounding the membrane on both sides, then gas diffusion layers and flow field plates respectively, as shown in Figure 2.1.

Hydrogen gas is supplied to the anode side of the cell through the flow field (or bi-polar) plates and diffuses through the gas diffusion layers. At the anode side platinum catalyst, hydrogen splits into its protons and electrons. Protons are conducted to the cathode side through the proton conducting polymer membrane and electrons are forced to travel through the outer circuit since the membrane is electrically insulating. The passage of electrons through the outer circuit creates the current.

In the meanwhile, oxygen (or air) is supplied to the cathode side through the flow field plates and pass through the gas diffusion layers. At the cathode catalyst, oxygen combines with the electrons coming from the outer circuit and the protons transferred through the membrane and produce water and heat.

These redox reactions can be stated as;

Anode side:

$$2H_2 \rightarrow 4H^+ + 4e^- \quad (1)$$

Cathode side:

$$O_2 + 4H^+ + 4e^- \rightarrow 2H_2O \quad (2)$$

Net reaction

$$2H_2 + O_2 \rightarrow H_2O \quad (3)$$

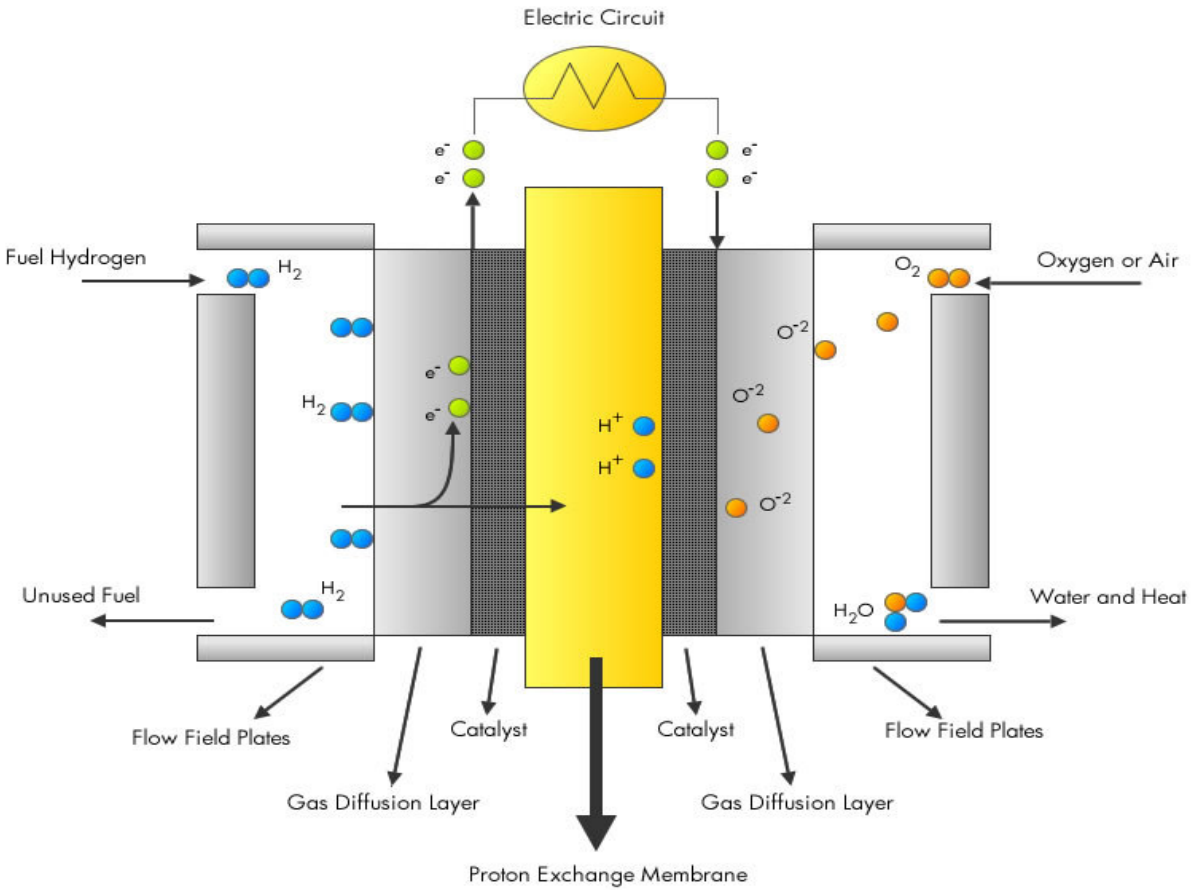

Figure 2.1: The Components of PEMFC [5]

2.2 Solid Polymer Electrolyte Membrane

The solid polymer electrolyte membrane is one of the most important components of a PEM fuel cell, since it facilitates the proton transfer between the anode and cathode compartments.

A good solid polymer electrolyte membrane must have;

- Good separation between the anode and cathode compartments, thus low fuel cross-over rates
- High proton conductivity (around 0.1 S/cm at 80°C) to enhance the proton transfer and must be electrically insulating
- Good thermal and chemical stability to overcome the harsh environment of the fuel cell.

Grubb, was the first to use a solid organic electrolyte membrane in fuel cells in 1959 [6]. The first operational application of a PEMFC membrane was the GE-Built 1 kW Gemini Power Plant. This was the primary source of Gemini spacecraft during mid-1960s. Polystyrene sulfonic acid based membrane was utilized as the solid polymer electrolyte, and the fuel cell performance and lifetime of Gemini PEMFC was limited due to degradation of the membrane [6]. The second unit was a 350kW module powered the Biosatellite spacecraft in 1969, whose electrolyte was the Nafion® membrane, developed by DuPont in 1966. Nafion® is a long chain per fluorinated ionomer which provide conductivities around 0.1 S/cm at optimum fuel cell operating temperature 80°C [6]. It possesses good chemical and thermal stability in the operating temperature range. The structure of Nafion® is given in Figure 2.2, where x= 6-10 and y=z=1[7].

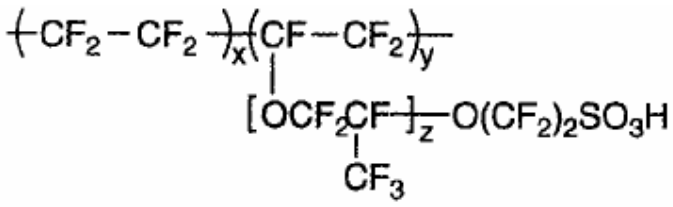

Figure 2.2: Structure of Nafion® Membrane [7]

The fluorinated hydrophobic backbone introduces thermal and chemical stability whereas the hydrophilic side chains act as proton carriers between anode and cathode.

There are many other long-chained perfluorinated membranes developed with similar properties to Nafion®. These membranes are called Perfluorinated carbonic acid (PFCA) membranes. One such membrane is called Aciplex-S developed by Asahi Chemicals Company in Japan whose structure is given in Figure 2.3, where x=6-8, y=0-1, and z=1[7]

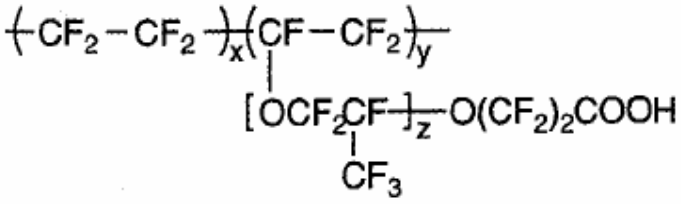

Figure 2.3: Structure of Aciplex-S Developed by Asahi Chemicals [7]

Another membrane developed by Asahi Chemicals Company, which has similar properties with Nafion® is Flemion® [8].

However, these PFSA membranes have low glass transition temperature around 110-130°C which limits the fuel cell operating temperature below 100°C. Above this temperature the membrane tends to dehydrate very fast, leading to not only low proton conductivities but also poor fuel cell performances.

Hence there is an active interest in developing alternate fuel cell membranes that could perform at higher temperatures. The materials and development of polymer electrolyte membranes for fuel cell applications has increased drastically within the last 20 years [9].

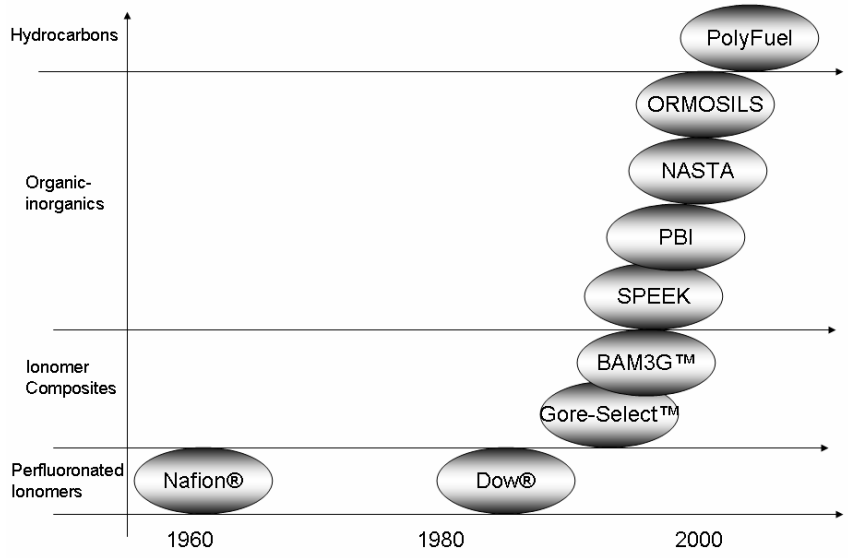

Figure 2.4: Development of Solid Polymer Electrolyte Membranes [9]

The Dow Membrane was developed in 1988 to further improve the capacity of Nafion, while operating at the same temperature [10].

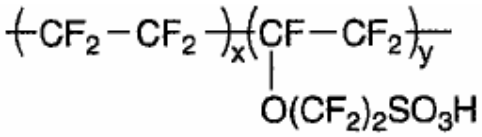

Figure 2.5: The Structure of Dow Membrane [7]

Instead of long chain per fluorinated ionomer, the conductive chain of Dow membrane is shorter as in Figure 2.5, where x=3-10, and y=1.

Using the same proton conduction mechanism, the Dow membrane speeds up the ionic transfer by giving the protons a short distance to travel [10]. Dow membrane has better water retention properties than Nafion.

However, these membranes are still very expensive as the other PFSA membranes. Typical costs of these membranes are on the order US$ 800 to US$ 2000 per m^2. The high manufacturing costs of these membranes and their toxic production processes limit the mass production of PEM fuel cells in the near future. Thus, development of alternate membranes is receiving more attention.

Organic membranes were developed to improve the proton conductivity of polymer electrolyte membranes at high temperatures, because the reaction kinetics is enhanced by the increasing temperature. Moreover, above 130°C, the risk of catalyst poisoning with the pollutants in the reactant gases become negligible, thus reformate gases can be utilized instead of pure hydrogen. Likewise, the precious metal catalysts required for the Redox reactions can be replaced by cheaper metal alloys for high temperature applications.

Since the conductivity of the ionomer or ionomer composite membrane is profoundly dependent on humidification, these organic membranes are designed to maintain their ionic conductivities at low relative humidity and high temperature applications, by creating strong bonds with water molecules absorbed in the membrane. Moreover, these organic membranes can be designed to have sufficient thermal and chemical stability and mechanical strength.

Polyaromatic hydrocarbon backboned compounds can meet all these qualifications and comprise the bulk of the organic composite membranes [11]. In this respect, Sulfonated polyether ether ketone, (SPEEK), [12-15], sulfonated poly-phenoxybenzoyl phenylene, (SPPBP), [13], sulfonated poly ether sulfone with cardo, (SPES-C), [16], sulfonated poly sulfone, (SPS), [17-19], sulfonated polybenzimiadazole, (SPBI), [20, 21], Sulfonated poly phosphazene [22], and composite membranes with inorganic supports have been studied [23-25].

Poly-aromatic hydrocarbon polymers possess various advantages which takes attention as an active research area [6];

- Hydrocarbon polymers are commercially available at lower costs than per-fluorinated ionomers.
- Hydrocarbon polymers consists of polar groups that retain water within the membrane, hence these polymers could work at a wide temperature range.
- Decomposition of these polymers could be controlled by proper design.
- Hydrocarbon polymers do not require complex recycling processes and no toxic gases are produced during the recycling process.

2.3 A Closer Look to SPEEK Membrane

Among the various polymers with miscellaneous mechanical properties, durability, efficiency and cost, membranes based on polyether ether ketone have significant promise for their sufficient thermal and chemical stability, suitable mechanical strength and improvable proton conductivity [26]. Sulfonated polyether ether ketone polymer was originally designed for water electrolysis and first tested for fuel cell application in 1997 [6, 7]. PEEK polymer with its aromatic, nonfluorinated back-bone, in which 1, 4-disubstituted phenyl groups are separated by ether (-O-) and carbonyl (-CO-) linkages is a thermo stable polymer and is shown in Figure 2.6 [14].

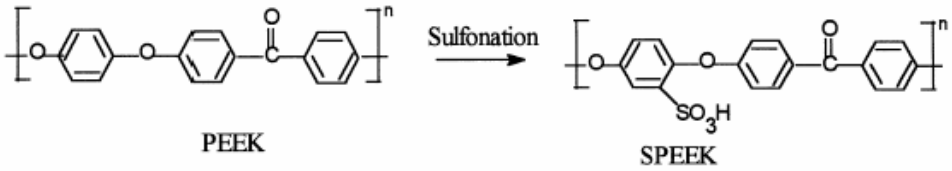

Figure 2.6: Plain and Sulfonated Structure of PEEK Polymer [14]

2.3.1 Sulfonation of PEEK Polymer

The proton conductivity of PEEK polymer can be functionalized by sulfonation. Sulfonated SPEEK polymer can be obtained either by the polymerization reaction of previously sulfonated monomers or by post-sulfonation. Post-sulfonation is an electrophilic substitution reaction in which a sulfone group is attached to the polymer backbone. Its application depends on the substituents present on the ring. The electron donating substituents will favor the reaction whereas electron accepting substituents will not. The number of sulfonic acid groups per repeating unit is defined as Degree of Sulfonation (DS) [14]. The Degree of sulfonation of a polymer can be either found by titration (ion exchange capacity), H-NMR (Proton Nuclear Magnetic Resonance) spectroscopy or by elemental analysis. The ion exchange capacity (IEC) is a measure of counter ions exchangeable in SPEEK and found to increase with increasing reaction time as given in Figure 2.7 [14].

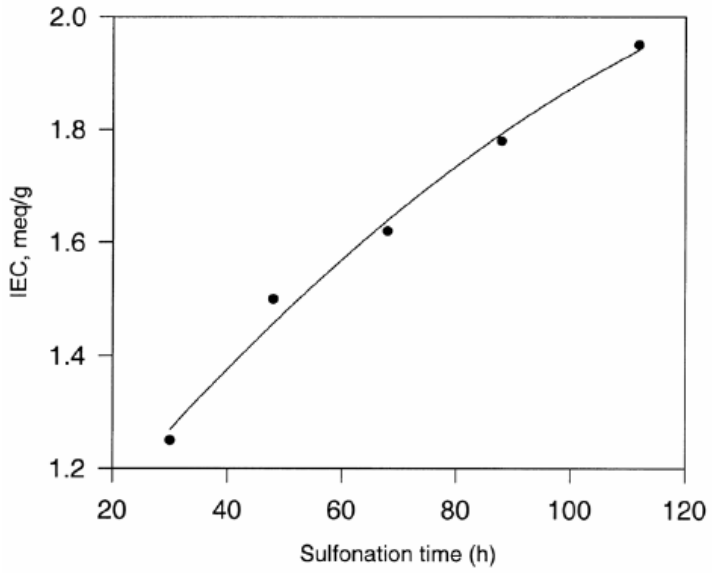

Figure 2.7: Ion Exchange Capacity of PEEK as a Function of Reaction Time at Room Temperature [14]

The degree of sulfonation can be determined quantitatively by using H-NMR spectroscopy. 'In H-NMR the presence of sulfonic acid group's results in a 0.25 ppm down-field shift of the hydrogen H_E compared to H_C, H_D in the hydroquinone ring' [14]. The nomenclature of the aromatic protons for the SPEEK repeat unit is given in Figure 2.8.

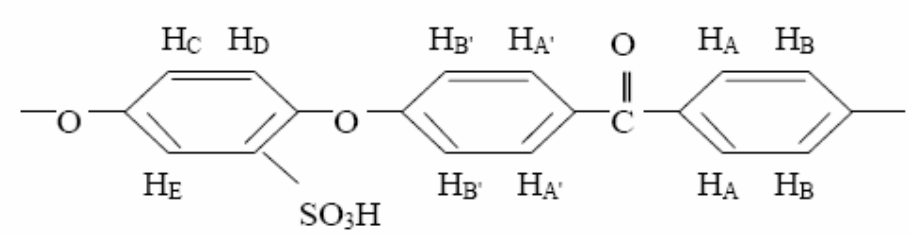

Figure 2.8: Nomenclature of Protons in SPEEK Structure [14]

The presence of sulfonic acid groups in the structure causes a distinct signal for protons at E position. Estimates for the H_E content which is equal to the sulfonic acid group content can be done according to the intensity of this signal [14].The H-NMR signal for sulfonic acid group is difficult since the proton is labile. The ratio of peak area of distinct H_E signals (AH_E) and integrated areas of the signals corresponding to all the other aromatic hydrogens ($AH_{A,A',B,B',C...}$)are expressed as [14]:

$$n/(12-2n) = AH_E / \sum AH_{A,A',B,B',C...}, \qquad (0 \le n \le 1) \tag{4}$$

The H-NMR spectra of different SPEEK samples are shown in Figure 2.9. 'In low sulfonated SPEEK, a significant proportion of repeat units are non-sulfonated and the H_C and H_D of the unsubstituted ring of PEEK repeat units in the SPEEK polymer appears as a singlet at 7.25 ppm' [14].

Two new signals increasing in intensity with higher DS were associated with the Hydroquinone ring of the SPEEK unit. H_C is a doublet of doublets at 7.20 ppm and two $H_{B'}$ protons are a doublet at 7.00 ppm shifted up field by the proximity of sulfonic acid groups [14]. The intensities of both H_C and two $H_{B'}$ increase proportionally with the intensity of H_E [14].

DS also can be found by elemental analysis. DS calculated from H-NMR analysis and elemental analyses are compared in Table 2.1 and they are found to be in good agreement [14].

Table 2.1: Sulfur Content of Different Sulfonated SPEEK Samples [14]

Sample	Degree of Sulfonation (DS) by NMR, mol%	Sulfur Content (wt %) by Elemental analysis	Sulfur content (wt %) Calculated from DS
PEEK	0.0	0.0	0.0
JZ2	48	3.90	4.30
JZ3	51	4.45	4.63
SP3	56	5.15	5.06
SP4	68	6.60	6.08
JZ5	72	7.00	6.40

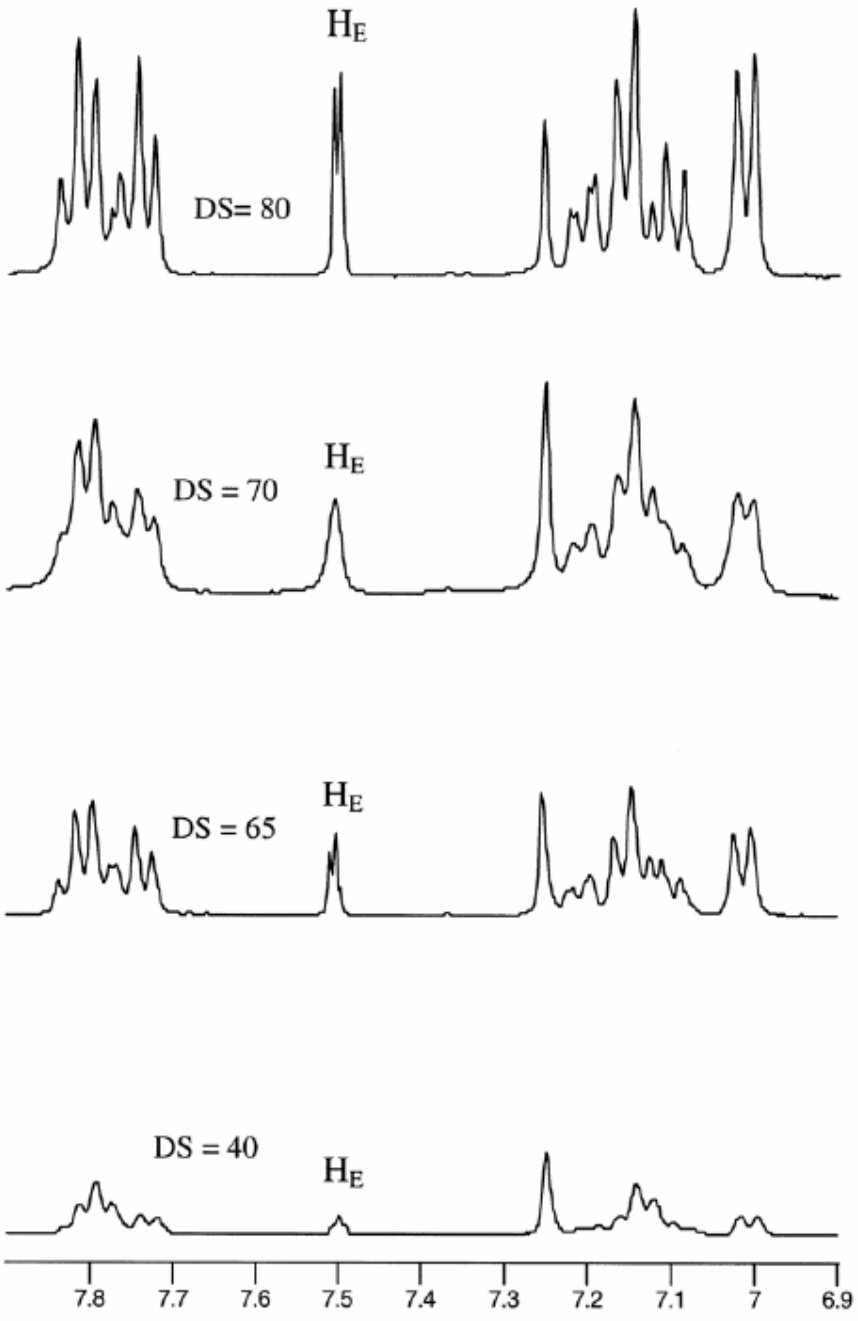

Figure 2.9: H-NMR Spectra of SPEEK Polymers with Different DS Values [14]

The DS can be adjusted by controlling the reaction time, temperature, the amount and concentration of the sulfonating agent [14]. The effect of reaction time on the sulfonation degree of PEEK can be seen in Figure 2.10.

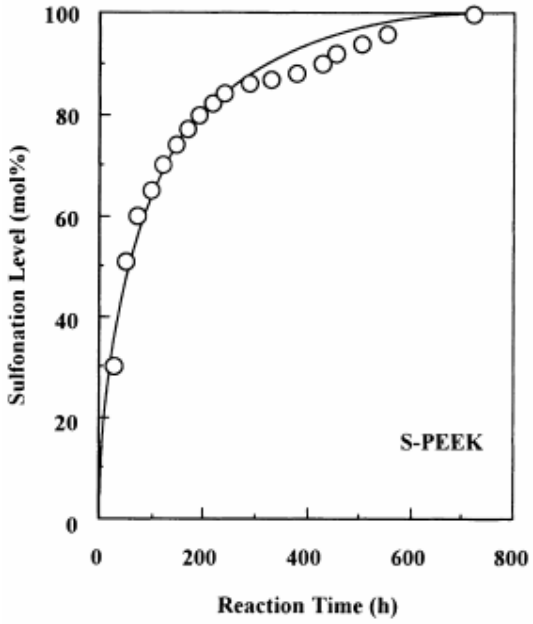

Figure 2.10: Degree of Sulfonation of PEEK as a Function of Reaction Time at Room temperature [14]

PEEK polymer is easily sulfonated by concentrated sulfuric acid, chlorosulfonic acid, pure or complexed sulfur trioxide, and acetyl sulfate [6]. However, sulfonation with chlorosulfonic acid and fuming sulfuric acid is known to cause degradation and cross-linking of the polymer structure. Cross-linking presumably involves sulfone groups, the concentration of which is negligible when sulfuric acid contains a few percent water, since water decomposes the aryl pyrosulfate intermediate required for the sulfone formation [27]. Concentrated sulfuric acid is a better sulfonating agent since the water content in the acid prevents degradation and cross-linking problems. When concentrated sulfuric acid is utilized as the sulfonating agent, the sulfonation range of PEEK polymer can be provided in the range of 30-100% DS by adjusting the reaction time and temperature [6].

However, it is not possible to obtain truly random copolymers at sulfonation degrees less than 30% by this method. This is due to the dissolution and sulfonation, in sulfuric acid in a heterogeneous environment which causes an increase in the viscosity of the polymer [6]. In order to prevent the heterogeneous sulfonation, the dissolution period of the polymer must be short. Grinding the polymer prior to the reaction can provide shorter dissolution period.

The sulfonation of PEEK at room temperature in concentrated sulfuric acid places a limit of one sulfonic acid group per repeating unit and PEEK polymer can be sulfonated up to 100% DS without any degradation or cross-linking at room temperature [6]. Fourier Transform Infrared (FT-IR) spectra of PEEK and its sulfonated form are given in Figure 2.11.

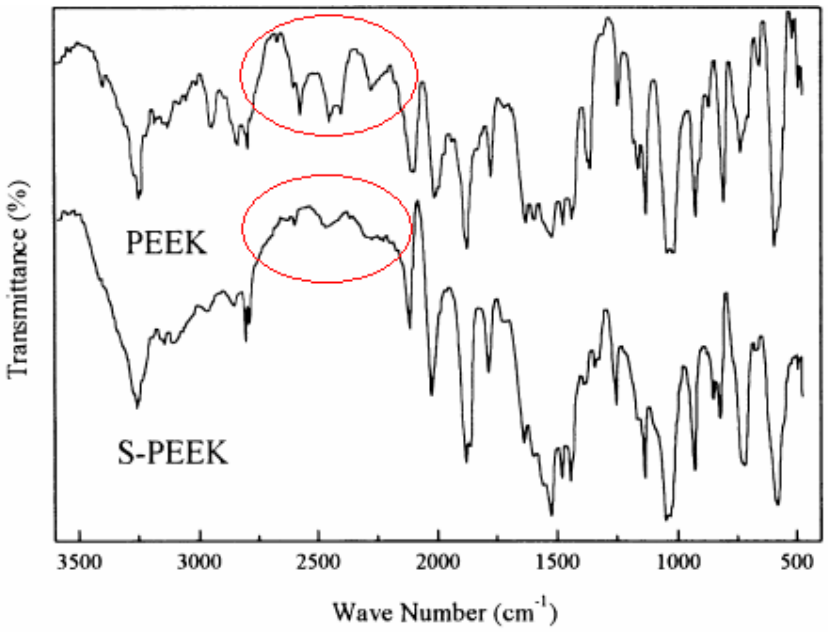

Figure 2.11: FT-IR Spectra of PEEK and its Sulfonated Derivative [6]

From Figure 2.11, it is clear that PEEK is sulfonated at one position on the phenylene ring between the ether groups [6]. The FT-IR Spectra of PEEK and its sulfonated derivatives also studied with different sulfonation degrees as in Figure 2.12.

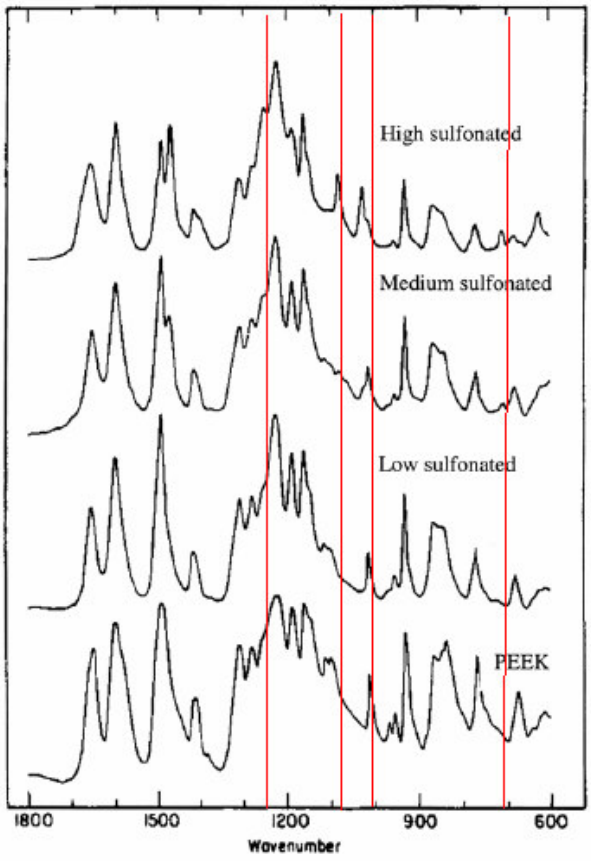

Figure 2.12 FT-IR Spectra of PEEK and its sulfonated derivatives [27].

According to Figure 2.12, significant differences are observed in the FT-IR spectrum of pure PEEK and its sulfonated derivatives. 'The presence of sulfonic acid groups is observed with the absorption bands at 1252, 1080, 1024 and 709cm^{-1}' [27]. The intensities of these bands increased with increasing level of sulfonation. In conclusion, the changes in the spectra indicate the presence of sulfonic acid groups in the structure.

2.3.2. The Influence of Sulfonation Level on Crystallinity and Solubility of PEEK polymer

The content of sulfonic acid groups within the membrane directly affects the chemical and mechanical properties of the membrane; which tend to deteriorate with increasing degree of sulfonation. Sulfonation modifies the chemical character of the polymer, reduces its crystallinity and as a result affects its solubility [14]. The crystal structure of PEEK and its sulfonated form has been previously investigated by wide-angle X-ray diffraction as shown in Figure 2.13 [27].

For low sulfonated PEEK sample, X-ray diffraction pattern shows weaker and less intense crystalline peaks. This indicates the effect of sulfonation on crystallinity, even when DS is very low. The diffractograms of medium and highly sulfonated PEEK shows only a broad amorphous scattering background [14]. The introduction of sulfonic acid groups into the structure modifies the chain conformation and packing thus causes loss of crystallinity and the polymer becomes soluble. For instance, SPEEK polymer with DS around 30% is only soluble in strong acids like sulfuric acid, chlorosulfonic acid, etc at room temperature. However when DS reaches 40% it becomes soluble in solvents such as Dimetyl Sulfoxide (DMSO), dimethyl formamide (DMF) and Dimetyl Acetamide (DMAc) at room temperature. When DS exceeds 70%, the polymer becomes soluble in hot water, thus above this sulfonation degree it is inappropriate for fuel cell applications [14].

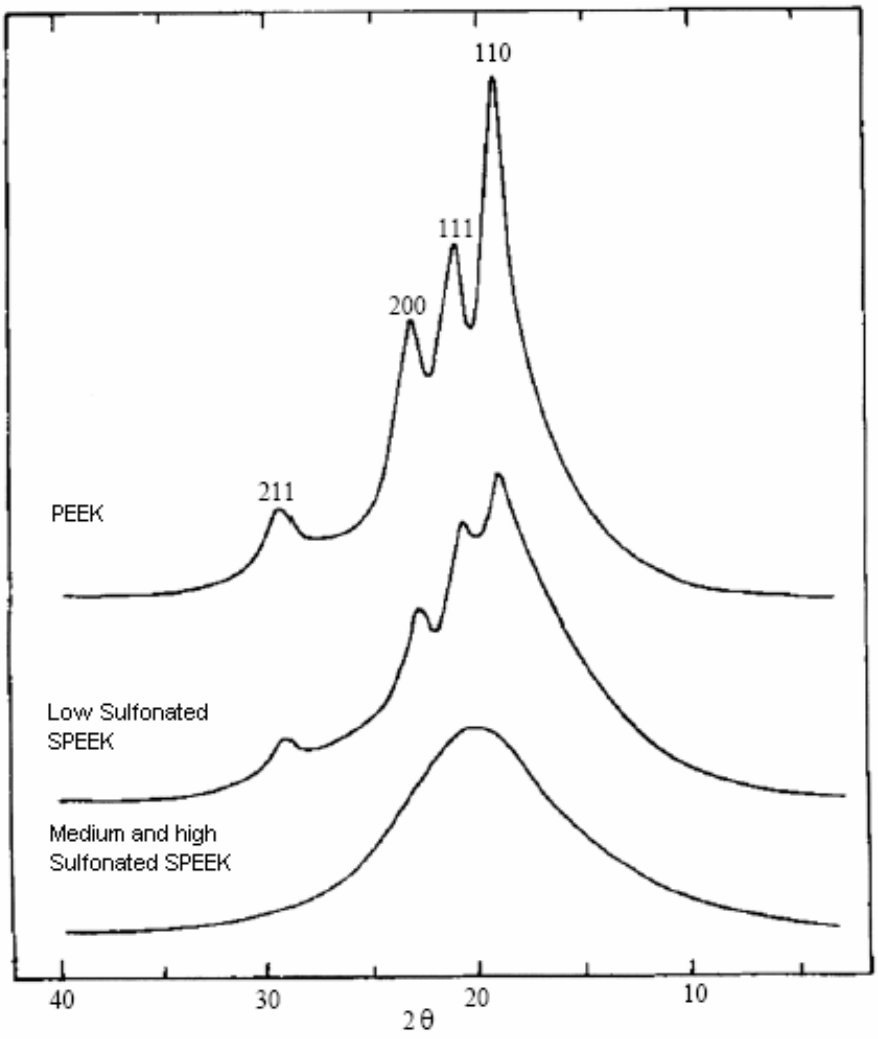

Figure 2.13 Wide-angle X-ray diffractogram of PEEK and its sulfonated forms [27]

2.3.3. Thermal Stability of PEEK Polymer and its Sulfonated Derivatives

The glass transition temperature and the thermal stability of PEEK polymer are also strongly dependent on the sulfonic acid content of the structure. The effect of sulfonation level on glass transition temperature of the polymer is given in Figure 2.14.

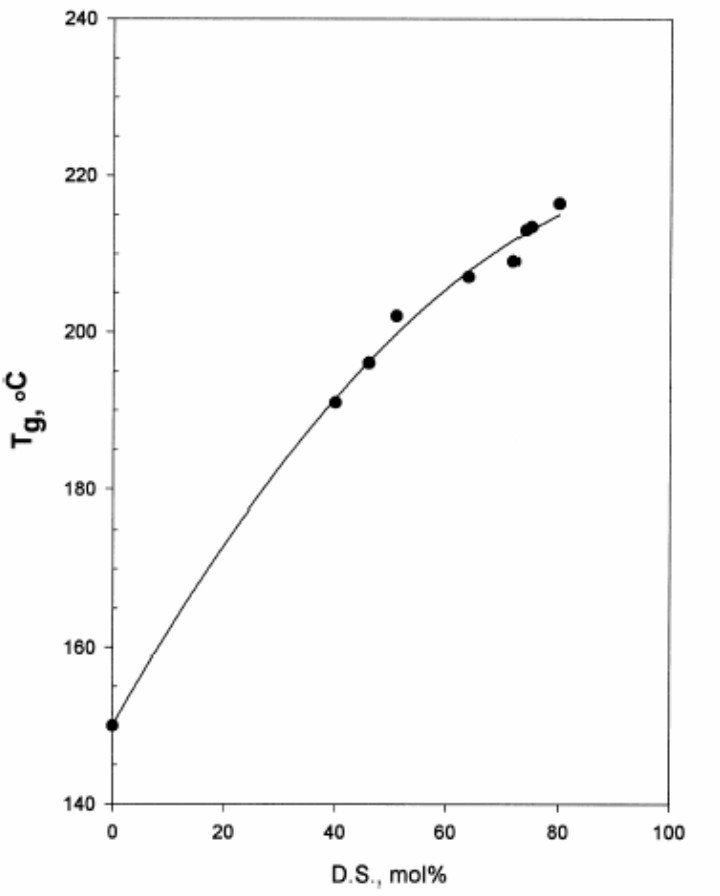

Figure 2.14: T_g of SPEEK as a function of DS [14]

According to the Figure 2.13, the glass transition temperature of SPEEK polymer increases with increasing level of sulfonation. This increase results from the increased intermolecular interaction with the hydrogen bonding of sulfonic acid groups which is known as 'ionomer effect'. These intermolecular forces are likely to hinder the internal rotations which occur in case of pure PEEK [14].

The thermal stability of PEEK membrane is also influenced by the sulfonic acid content of the membrane. Thermal gravimetric analysis showed that, the thermal stability of the polymer tends to deteriorate with increasing level of sulfonation. The TGA and DTG curves of pure PEEK polymer and its sulfonated form are given in Figure 2.15.

PEEK polymer is a thermostable polymer with an onset of weight loss around 520°C as can be seen in Figure 2.15. The pyrolytic degradation of PEEK results in formation of benzene and phenols which occurs in early scission involving ether linkages [14]. In sulfonated form of SPEEK polymer, two weight lost steps are observed. The first weight loss peak is supposed to be formed as a result of splitting of the sulfonic acid groups from the structure. The maximum of the second peak resembles the thermal decomposition temperature, and for all SPEEK samples it is shifted to 560°C from 600°C for PEEK. The maximum temperature at which first sulfonic acid decomposition is observed was found to be 360°C [14].

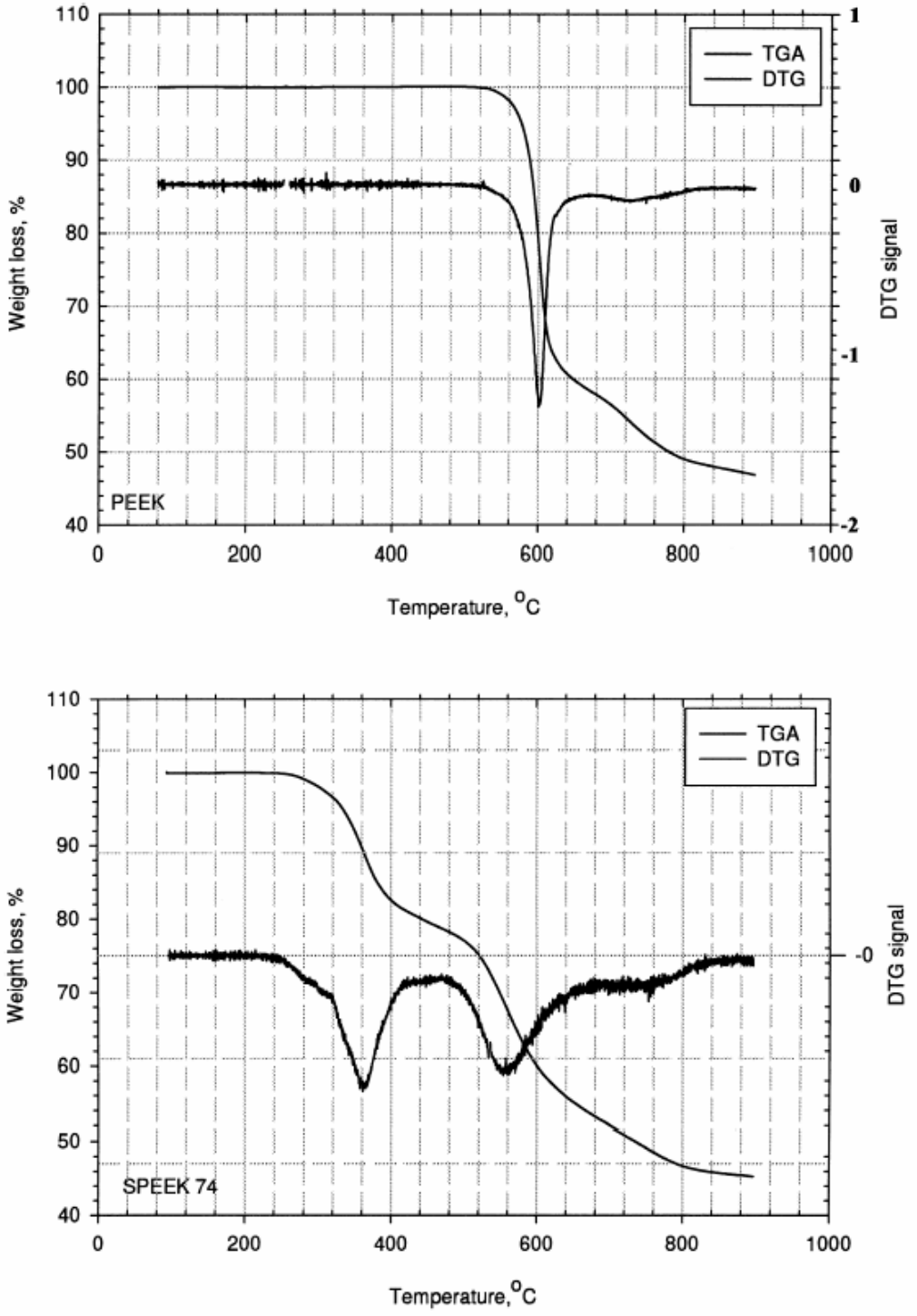

Figure 2.15: TGA and DTG curves of PEEK and SPEEK polymers [14].

2.3.4 Water Uptake of PEEK Polymer and its Sulfonated Derivatives

The main objective of sulfonation is to introduce hydrophilic sulfonic acid groups into the polymer structure and improve the polymers water retention property. The presence of sulfonic acid groups in PEEK structure facilitates proton transfer and increases proton conductivity in presence of water [14]. The improvement of hydrophilicity of the polymer as a function of sulfonic acid group density can be seen in Figure 2.16.

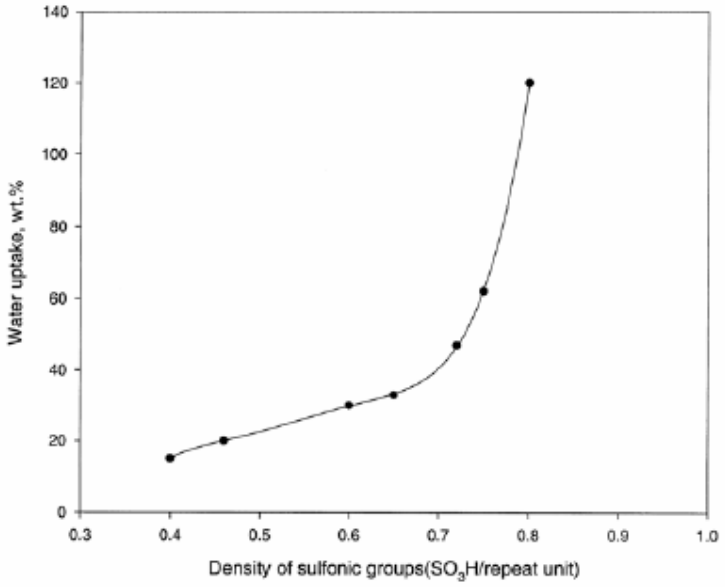

Figure 2.16: Water Uptake of Sulfonated PEEK membranes [14]

The water uptake increases as a function of sulfonic acid group density and reaches 120 wt % for DS 80% (0.8 -SO_3H group/ repeating unit) [14]. The results show that water uptake of PEEK membranes increases linearly up to DS 65%, then increases dramatically after DS 70%. The reason for this dramatic increase resulting at high sulfonation levels is the high density of sulfonic acid groups which may cause clustering and agglomeration [14].

The clustered ionomers absorbs more water, therefore high water uptakes may be suggestive of the presence of ion-rich regions where proton transfer is facilitated. Sulfonation not only increases the sulfonic acid content of the structure but also forms water mediated pathways for easier proton transfer. The water content of SPEEK membranes is higher than in Nafion117 membranes (34%), Dow membranes (56%), NASTA Membranes (48%) and polyimide membranes (30%) [14, 27].

2.3.5 Proton Conductivities of PEEK polymer and its Sulfonated Derivatives

The effect of DS on proton conductivity was studied at room temperature and the results are given in Figure 2.17 [27].

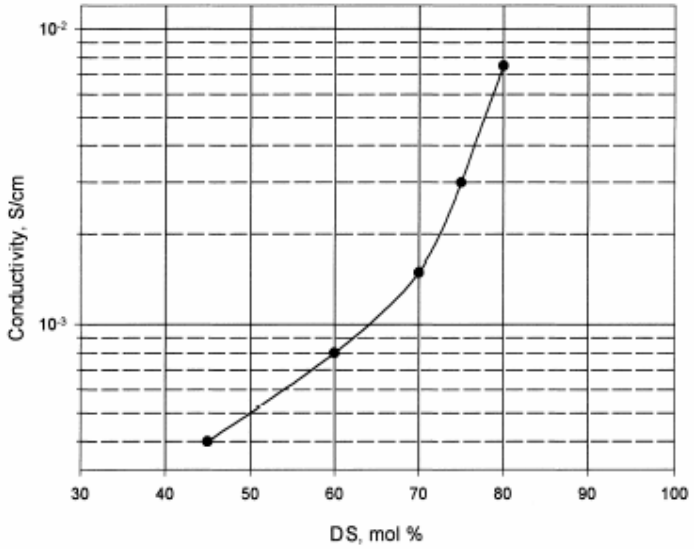

Figure 2.17: Conductivity of SPEEK Membranes at Ambient Conditions [27]

The conductivity is found to increase with increasing degree of sulfonation and reached $8x10^{-3}$ S/cm for 80% DS. With increasing DS, the crystallinity of the polymer decreases, as a result, it becomes hydrophilic and absorbs more water which facilitates proton transfer [27].

As sulfonic acid content of the membrane increases, not only the number of protonated sites increase but also ionomer clusters and agglomerates form water mediated pathways which enhance proton transfer.

The influence of temperature on proton conductivity has been also explored and the results are given in Figure 2.18. According to the figure, proton conductivity of the membrane with 40% DS decreased with increasing temperature. On the other hand, the conductivity of the membrane with DS 48% increased up to 85°C and then decreased very sharply. The membranes with 70% and 74% DS have showed a steady increased up to 100°C and than decreased gradually. The temperature dependence of SPEEK conductivity suggests the presence of two conducting mechanisms, one of which enhances the proton transfer whereas the other reduces [27]. Since the proton conductivity is thermally stimulated, a rise in proton conductivity is expected with increasing temperature. However, the increase in the temperature causes dehydration of the membrane which slows down the proton transfer. At low DS values, the water uptake capacity of the membrane is less so it dehydrates very fast leading to a sharp decrease in proton conductivity, but at high temperatures the water retention of the membranes are better so their proton conductivities are not affected much from dehydration.

In literature, very different proton conductivity values were reported for SPEEK membranes. For instance, Rikukawa and co-workers found the conductivity of SPEEK membrane with DS 65 % around 10^{-5} S/cm at room temperature and 100% relative humidity and $\sigma = 7x10^{-4}$ to $8x10^{-4}$ S/cm at 60°C [6, 13]. A thousand times higher conductivity of $\sigma = 6.4x10^{-2}$ S/cm at 25°C was reported by Cui and co-workers for SPEEK membranes with even lower DS 60% [28]. With the same DS a three times lower conductivity $\sigma = 2x10^{-2}$ S/cm was reported in work [29], while a

similar conductivity of $\sigma = 6.6x10^{-2}$ S/cm was registered for SPEEK samples with a higher DS of 73% in works [30, 31].

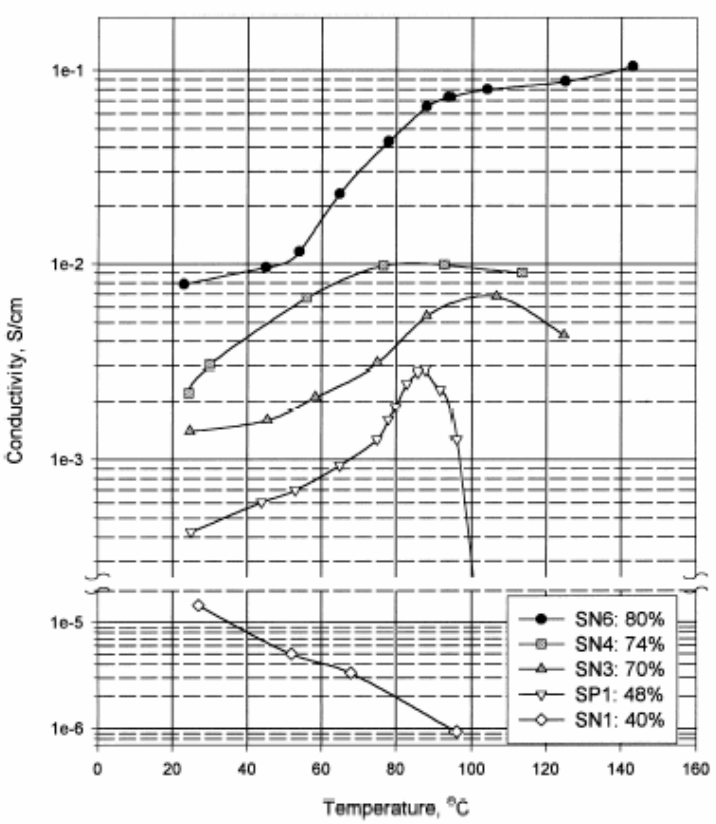

Figure 2.18: Proton Conductivity of Different SPEEK Membranes as a Function of Temperature [27]

In other works, [14, 15, 27] for a variety of SPEEK membranes with DS ranging from 45 to 80% have shown proton conductivity values from $\sigma = 4x10^{-4}$ to $8x10^{-3}$ S/cm at 25°C, which is lower than the values reported in references [28-31], but higher than that was observed in references [6, 13]. These discrepancies in the reported values could be resulted from the origin of the polymer, utilization of different solvents upon membrane casting, the measuring technique and conditions utilized in determining the proton conductivity.

In the work of Kaliaguine and co-workers, the properties of PEEK polymers of different brands were explored with using different solvents such as DMF and DMAc and the results are tabulated at Table 2.2 [32].

Table 2.2: Characterization of PEEK Polymers of Different Brands [32]

Polymer	Solvent	DS	Sample	T_g (°C)	T_{dec} (°C), loss onset	$\sigma_{25°C}$ (S/cm)	Water Uptake at 25°C (wt %)
Vitrex® PEEK™	DMF	59	V59F	200	185	$8.7x10^{-4}$	20.7
		67	V67F	196	214	$2.0x10^{-3}$	21.6
		69	V69F	199	184	$3.8x10^{-3}$	23.0
		79	V79F	-	-	$3.6x10^{-3}$	29.0
		88	V88F	206	209	$3.3x10^{-3}$	47.6
		96	V96F	214	-	$3.5x10^{-3}$	94.0
	DMAc	69	V69A	196	260	$2.2x10^{-2}$	28.0
		79	V79A	-	258	$3.9x10^{-2}$	40.0
		88	V88A	206	253	$5.1x10^{-2}$	58.2
		96	V96A	214	185	$1.1x10^{-1}$	90.1
Gatone™ PEEK	DMF	48	G48F	196	168	$6.8x10^{-4}$	14.1
		58	G58F	216	207	$2.5x10^{-3}$	18.9
		67	G67F	219	182	$2.6x10^{-3}$	19.7
	DMAc	59	G59A	-	259	$1.7x10^{-2}$	13.0
		79	G79A	220	246	$2.6x10^{-2}$	47.0

As can be seen from Table 2.2, the Gatone™ PEEK has conductivity several times higher than Vitrex™ PEEK. The effect of temperature on conductivity of similarly sulfonated Gatone™ PEEK and Vitrex™ PEEK were explored and the results are given in Figure 2.19 [32].

The Figure 2.19 indicates that Gatone™ PEEK always shows better conductivities than Vitrex™ PEEK and begins to dehydrate after 100°C whereas Vitrex™ PEEK dehydrates above 80°C. This behavior can be explained by the difference in their molecular weights. Gatone™ PEEK has a lower molecular weight (M_w =31000) compared to Vitrex™ PEEK (M_w =34000), thus it dissolves more quickly in sulfuric acid and is more homogenous.

On the other hand, it takes days for the dissolution of Vitrex™ PEEK under the same conditions leading a more heterogeneous product [32].

Homogeneity is important since it provides more uniform route for proton transfer within the membrane. Homogeneity of the sulfonated PEEK can be improved by using pulverized PEEK during the post-sulfonation process.

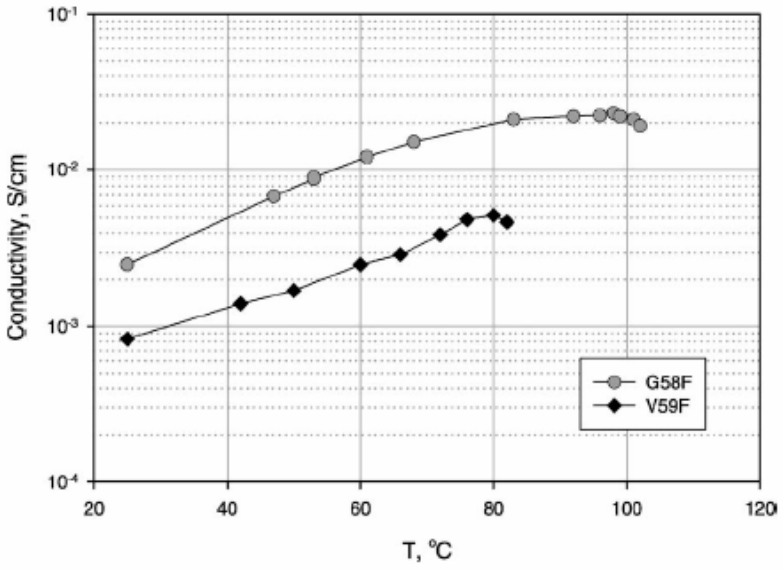

Figure 2.19: Temperature Dependence of Gatone™ PEEK (DS 58%) and Vitrex™ PEEK (DS 59%) [32]

Another important parameter affecting the proton conductivity of the membrane is the type of the solvent utilized in membrane casting. It is known that DMF forms strong hydrogen bonding complex with sulfonic acid groups starting at temperatures as low as 60°C, whereas this temperature increases above 140°C in case of DMAc [32, 33]. This will explain the higher proton conductivities of both Gatone™ and Vitrex™ PEEKs when DMAc is utilized as the casting solvent as tabulated in Table 2.2.

Both solvents are prone to thermally activated decomposition catalyzed with sulfonic acid functions leading to dimetylamine (DMA) production which forms strong bonds with SPEEK polymer [33]. Thus the residual sulfuric acid originating from improper washing of the polymer in the post-sulfonation process will catalyze the decomposition of the solvents. This results the formation of N,N-dimetylaminium hydrogen sulfate (DMAm) which lowers the proton conductivity [33].

Another reason of the discrepancies of the proton conductivity values reported in literature will be the measuring technique and the conditions utilized while determining the proton conductivity. There exist several experimental schemes which have their own cons and pros.

For example, in the work of Cui and co-workers, the membrane is equilibrated in a liquid electrolyte solution, which can affect its chemistry due to ion exchange [32]. This approach seems appropriate for electro-dialysis; however, it is far from reality for fuel cell applications [32]. In the work of Bonnet and co-workers [29], the proton conductivity was measured in longitudinal direction on one membrane side whereas in other references [6, 13, 28-31] it was measured in transversal direction. In the longitudinal conductivity cell, the membrane can better equilibrate with its environment than a co-axial cell and avoids the parasitic inductance response from the leads which occurs in the case of a coaxial cell [32]. However, it can strongly overestimate the true conductivity if the bulk humidification is lower than that of the surface where moisture absorbs [32]. On the other hand, in co-axial type conductivity cells there is the risk of dehydration of the membrane during the measurements which may lead to underestimated results [14, 32]. Conductivity measurements in co-axial conductivity cells are simple and useful for conductivity measurements above 100°C and below 0°C, however, the water uptake of the hydrated sample in such a cell may change during the measurements, so longitudinal cells are better in this temperature range [6]. The schemes of both co-axial (transverse) and longitudinal conductivity cells are given in Figure 2.20

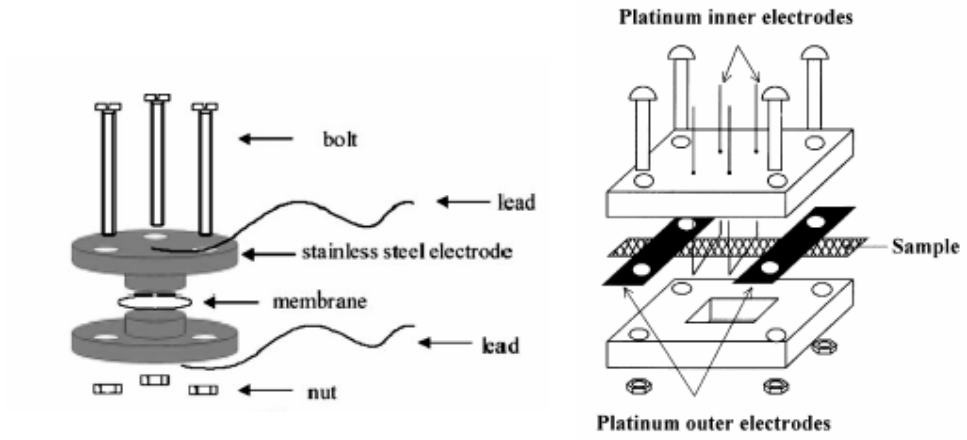

Figure 2.20: Schemes of Co-axial [34] and Longitudinal [6] Conductivity Cells

The comparison of the proton conductivity measurements performed in transverse and longitudinal directions in the measurement cells described above are given in Figure 2.21.

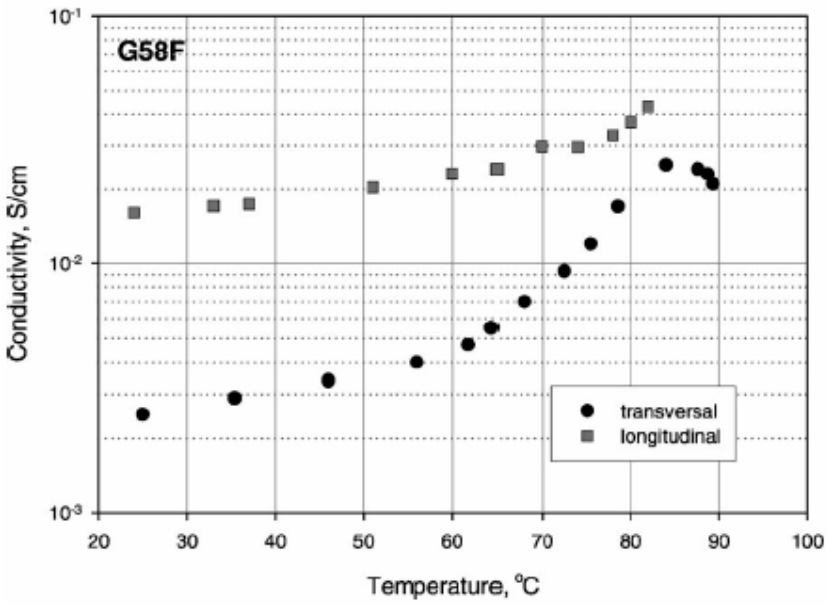

Figure 2.21: Comparison of conductivities of the same membrane measured in transversal and longitudinal directions [32].

When Figure 2.21 is examined a difference of almost one order of magnitude can be observed which reveals that the measuring technique is of great significance and affects the results [32].

2.4 Proton Transfer Mechanism

Proton is the only ion which has no electronic shell, thus it is strongly affected by the electron density of the environment. Proton transfer phenomena follows two transfer mechanism where the proton remains shielded in the electron density of the environment, so existence of a free proton can not be seen. The most trivial case of proton transfer is known as vehicular mechanism in which the proton transfers through the medium with a vehicle (for example, H_2O as H_3O^+) [35]. The counter diffusion of unprotonated vehicles (H_2O) allows the net transport of protons. The observed conductivity is strongly dependent on the diffusion velocity of the vehicle [35].

In the other mechanism, the vehicles show local dynamics and reside on their sides. The protons are conducted from one vehicle to another by hydrogen bonds (also known as proton hopping) [35]. This mechanism is known as the Grotthuss Mechanism. These two principle mechanisms show the difference in the nature of hydrogen bonds between the proton and the environment. If the media supports strong hydrogen bonding than Grotthuss Mechanism is preferred. On the contrary, the vehicular mechanism becomes more pronounced in the media of weaker hydrogen bonding. As a result, Grotthuss mechanism is progressively dominated by vehicular mechanism with increasing temperature [35].

Degree of hydration is the factor that influences the proton conductivity of a membrane. The hydration is dependent on the phase separation between the hydrophobic polymer backbone and hydrophilic side chains [35]. Nafion and SPEEK polymers both exhibit phase separated domains consisting of an extremely hydrophobic backbone which gives morphological stability and extremely hydrophilic side chains [35].

These functional groups aggregate to form hydrophilic nano-domains which act as water reservoirs [35]. The structure of Nafion and polyether ketone based polymers can be seen in Figure 2.22.

Proton transport in water is a result of protonic defects and occurs via breaking and reformation of bonds [35]. In a PEM, the hydrated environment acts as a solvent for the diffusion of hydronium ion which is formed. This diffusion like transfer together with the hopping model (Grotthuss Mechanism) which may play a role at reduced hydrations is shown in Figure 2.23.

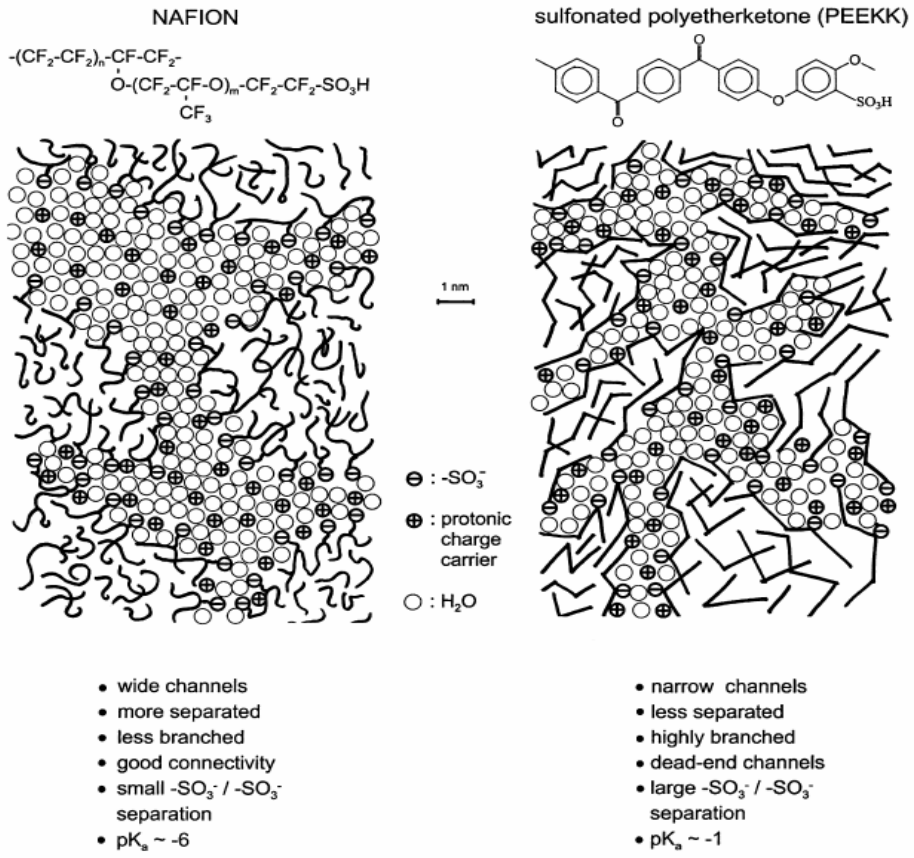

Figure 2.22: Comparison of structures of Nafion and SPEEK polymers [35].

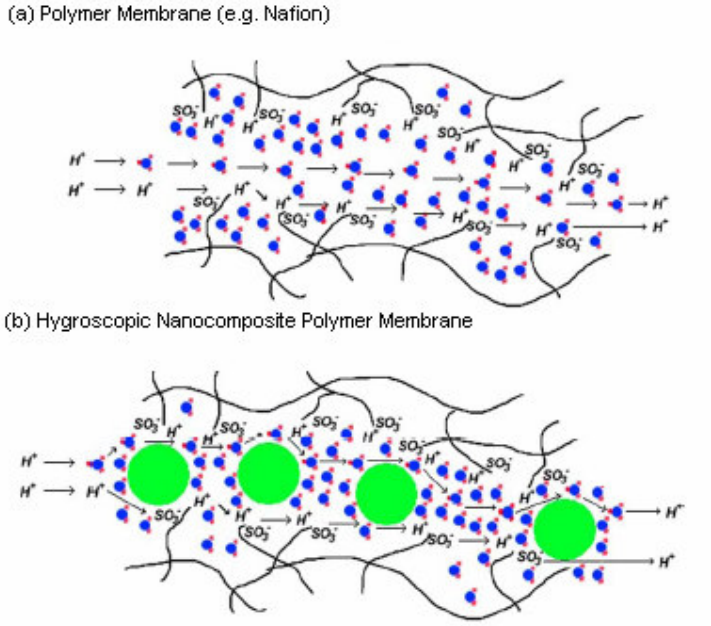

Figure 2.23: Proton transfer mechanisms in different membrane configurations [35]

The transfer of a protonic defect in water is more clearly demonstrated in Figure 2.24.

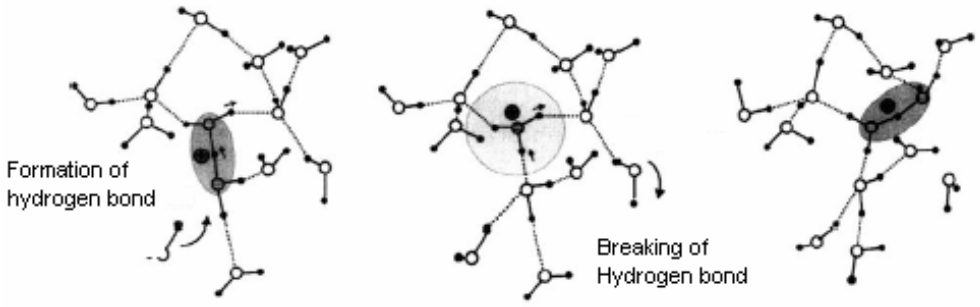

Figure 2.24: Transport mechanism of a protonic defect in water [35]

The transport of the protonic defect pulls other water molecules through the membrane which is called electro-osmotic drag and caused by the size of the molecule and by the molecular attractions between the molecules [35].

Another competing force to proton conduction is back diffusion from the cathode which occurs as a result of driving forces formed as water is removed from the anode due to electro-osmotic drag.

The proton transport in composite membranes is more complex and could be examined in three parts;

- Hygroscopic composites: These membranes are formed by the introduction of a hygroscopic material (such as silica, etc.) within the polymer matrix. This hygroscopic materials dramatically increases the swelling of the membranes at low relative humidity and prevents fuel cross over. This increases the proton conductivity while reducing methanol permeability in direct methanol fuel cells.
- Conductive Composites: These membranes are formed by the introduction of a second proton conducting species (such as ZrP, etc.) into the polymer matrix to reduce the methanol and water permeability of the membrane. The introduced conductive specie is assumed to make up for conduction losses due to reduced water in the membrane [35]
- Water substituted composites: These composites consist of the polymer matrix to which alternative proton transporter is added (such as heteropolyacids, acid doped polybenzimiadazole, etc.) [35]. The objective is to introduce a highly conductive acid into the structure so that proton conductivity may not depend on hydration and electro-osmotic effect is reduced. However, the substituted composite tends to leach from the membrane over time [35].

2.5 Effect of Inorganic Additives on Proton Conductivity

There is an active interest in exploring the effect of inorganic additives on proton conductivity. The inorganic additives may prevent water losses from the ionic regions (pores) in the membrane, thereby will maintain same level of hydration at elevated temperatures and low relative humidity.
Moreover, these inorganic additives will contribute to the proton conductivity of the membrane by introducing their own conductivities and these additives will enhance the thermal, chemical stability and mechanical strength of the polymer matrix. In this context, several inorganic materials such as; heteropolyacids (HPA), Boron phosphate (BPO_4), SiO_2 and zeolites such as montmorillonite, laponite, Zeolite Beta and Zeolite 4A were considered in literature [14, 15, 25, 36].

In the work of Zaidi and co-workers, the effect of different heteropolyacids (tungstophosphoric acid (TPA), molybdo-phosphoric acid (MPA) and disodium salt of tungstophosphoric acid, (Na-TPA)) on the proton conductivity of SPEEK membrane was explored [14]. The incorporation of HPAs resulted in improved proton conductivities for SPEEK membranes with DS 70 and 74%. The influence of inorganic additives became less pronounced with increasing DS of SPEEK given in Figure 2.25.

In another work, Mickhailenko and co-workers, utilized boron phosphate as the inorganic additive into SPEEK polymer matrix [15]. The incorporation of BPO_4 additives has increased the proton conductivity, but this increase becomes more pronounced for composite membranes with low DS as shown in Figure 2.26 [15].

The properties of composite membranes prepared by embedding layered silicates such as Laponite and Montmorillonite (MMT) into SPEEK polymer were studied by Chang and co-workers. They reported that, the introduction of these inorganic into the structure reduced swelling in hot water significantly and decreased methanol permeability [36]. These membranes showed thermal stabilities up to 240°C and a proton conductivity of 3-3.5x 10^{-3} S/cm at room temperature [36].

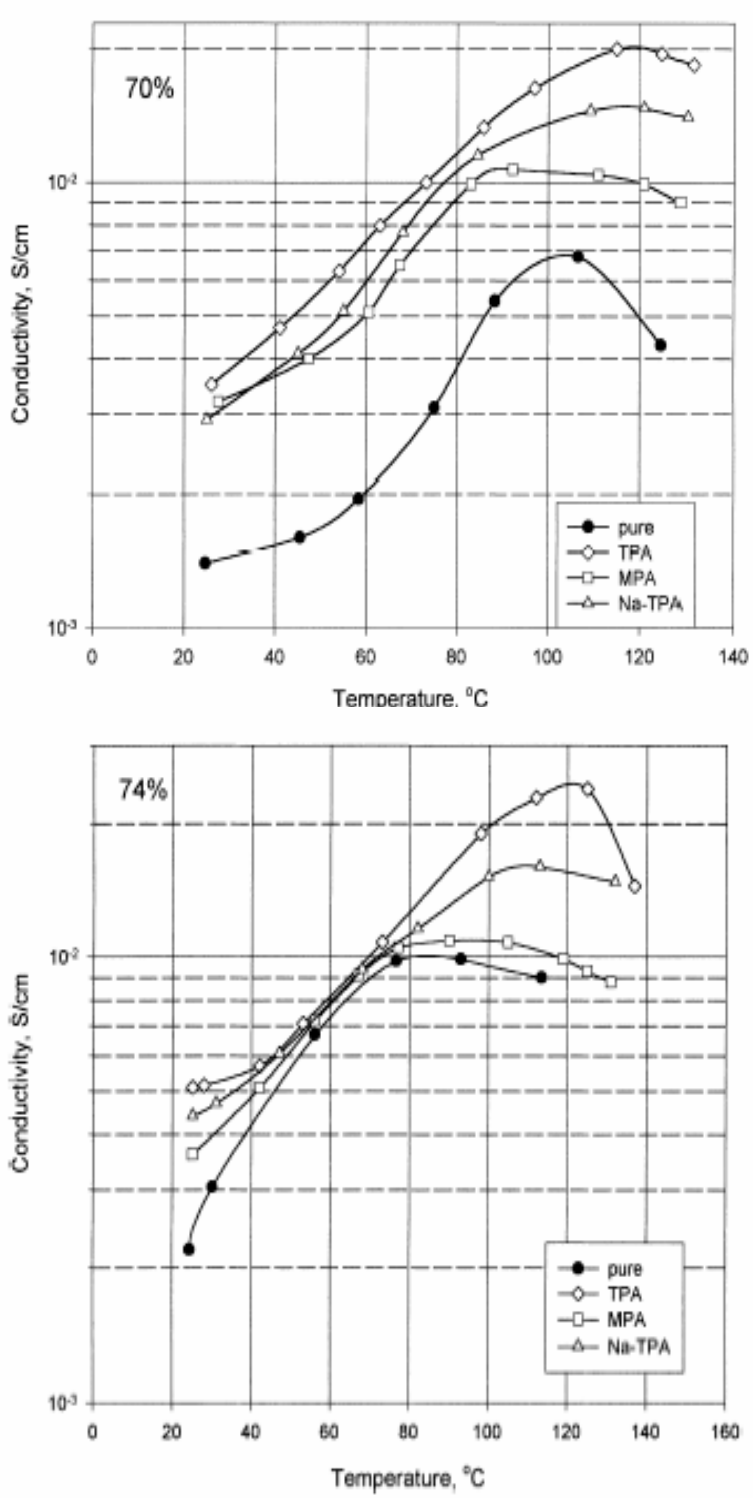

Figure 2.25: Influence of HPAs on proton conductivity of a) SPEEK with DS 70%, b) SPEEK with DS 74% [14]

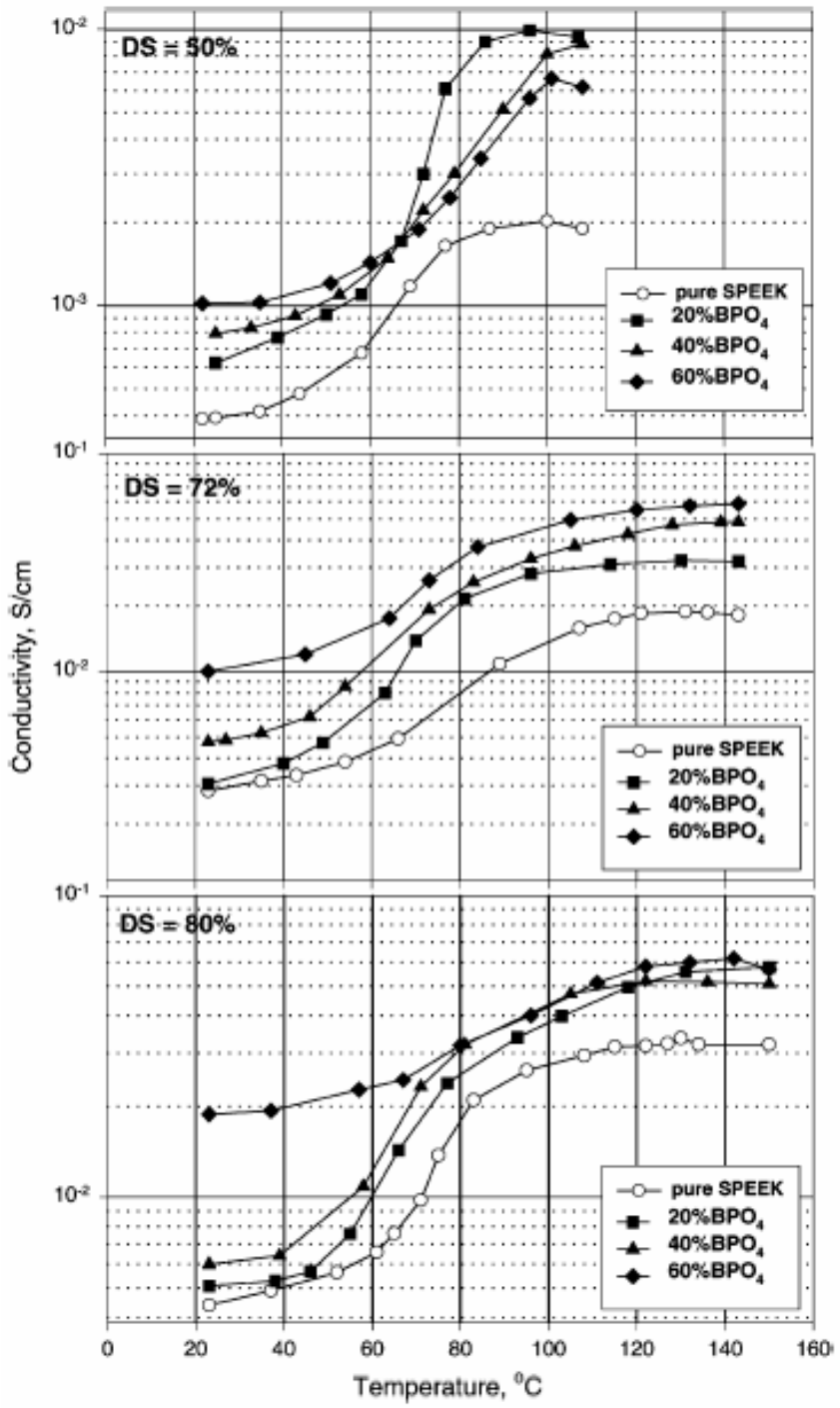

Figure 2.26: Proton Conductivity of BPO_4/ SPEEK Composite Membranes [15].

The polarization curve of pure SPEEK and SPEEK-Laponite composite membranes are compared with Nafion 115 membrane as given in Figure 2.27 [36]. As seen in Figure 2.27, the composite membrane exhibits better performance than the pure SPEEK membrane.

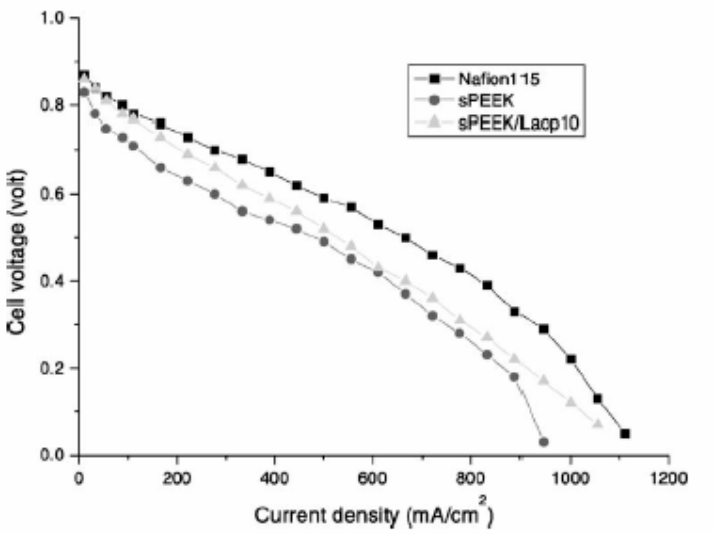

Figure 2.27: Polarization Curves of Nafion 115, SPEEK and SPEEK-Laponite membranes in H_2-O_2 PEMFC (Cell temperature 60°C) [36]

In the work of Baç and co-workers, the effect of inorganic additives such as silica, zeolite 4A and zeolite beta on the proton conductivity of Nafion membrane were studied. All these inorganic additives are found to increase the proton conductivity of Nafion membrane as a function of temperature and relative humidity as given in Figure 2.28 and 2.29 [25].

The inorganic additive which resulted in the best proton conductivity was Zeolite beta. Another composite membrane was prepared by the introduction of zeolite beta into SPES-40 polymer matrix, and showed better proton conductivities than pure Nafion 117 membrane as given in Figure 2.30.

These results indicate that, zeolite beta provides a nano-sized pore structure through the inorganic portion of the composite membrane and also adds hydrophilic particles into the structure thus increase the hydrogen bonding sites for water in membrane [25]. Moreover, zeolite H-Beta has the effect of providing extra proton conductivity [25].

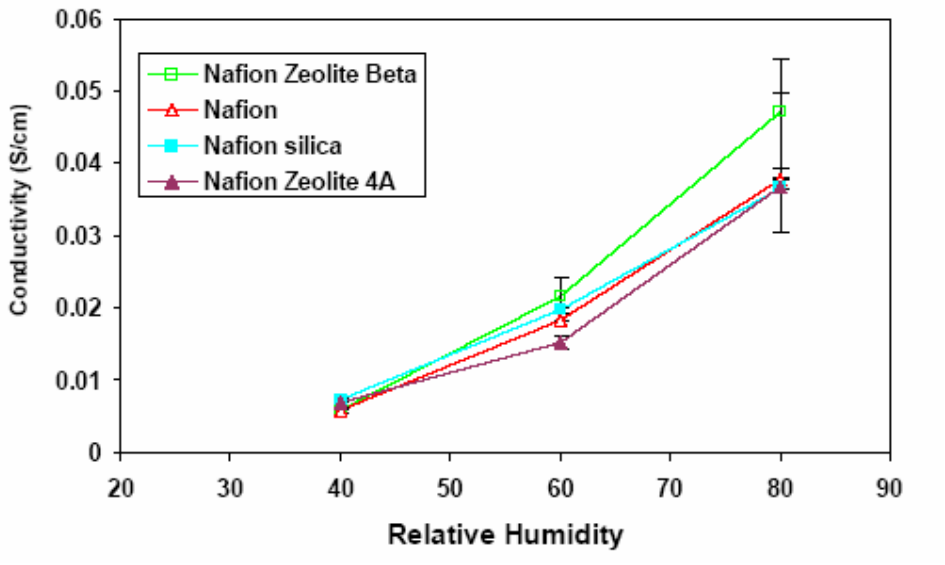

Figure 2.28: Conductivity of Nafion based composite membranes at room temperature [25]

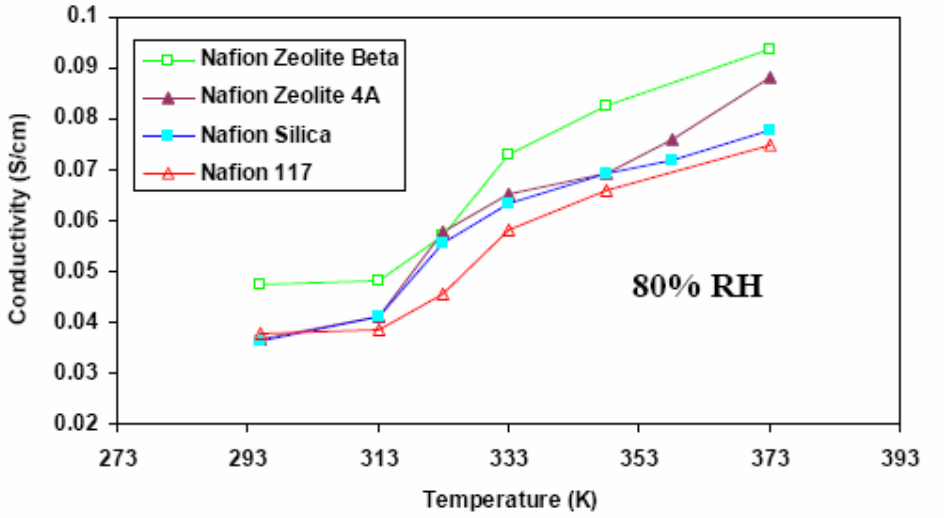

Figure 2.29: Conductivity of Nafion based composite membranes as a function of temperature [25]

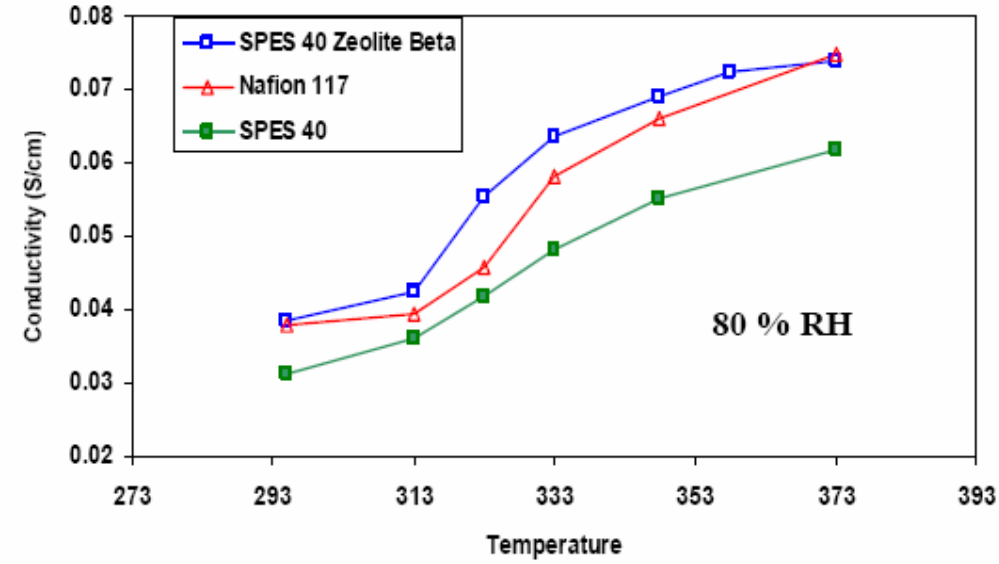

Figure 2.30: Conductivity of SPES-40 based composite membranes as a function of temperature [25]

2.6 Zeolite Beta

Zeolite beta is a high silica, large pore crystalline aluminosilicate material which was first synthesized by Wadlinger and co-workers in 1964 [37]. Zeolite Beta has a three-dimensional tetragonal structure with straight 12-membered ring pores crossed with 10-membered ring-channels with an interconnected channel system as given in Figure 2.31

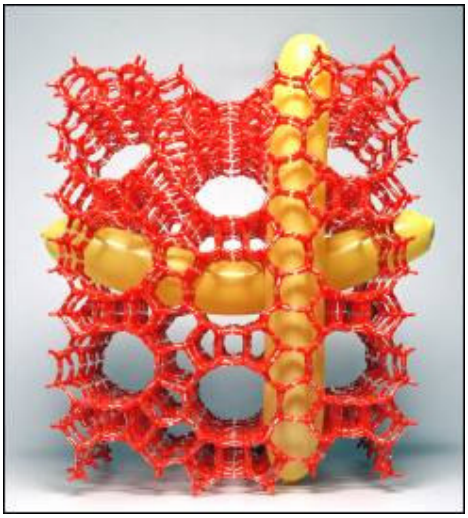

Figure 2.31 Structure of Zeolite Beta [38]

Zeolite beta has a wide application area as a catalyst, ion exchanger and adsorbent. It can easily be synthesized hydrothermally at different SiO_2/Al_2O_3 ratios, from 20-60, with the batch composition 2.2 Na_2O: 1.0 Al_2O_3: x SiO_2: 4.6 $(TEA)_2O$: 440 H_2O [39]. The synthesis procedure involves gelation and crystallization of a silica precursor solution with an alumina precursor solution and a structure directing agent (either tetraethyl ammonium hydroxide (TEAOH) or tetraethyl ammonium bromide (TEABr)). Different silica sources such as colloidal silica, TEOS (tetraethyl orthosilicate) or fumed silica can be used during the synthesis and each resulted in pure crystalline zeolite beta phase [40].

Aluminum sulfate, aluminum isopropoxide and sodium aluminate can be used as the aluminum sources among which sodium aluminate gives the biggest synthesis yield [37].

The parent Zeolite beta obtained from hydrothermal synthesis is Na-Beta which is in the Na^+ form and can be converted into more conductive H^+ form H-Beta by acid treatment. The treatment with sulfuric acid causes ion exchange and also removes some of the structure directing agent (or the organic template) from the zeolite structure.

Holmberg and co-workers, has investigated the proton conductivity of sulfonic acid functionalized zeolite beta nano-crystals [41]. They have emphasized that, zeolite beta particles could be effective as an inorganic additive when introduced into PEMFC membrane matrix and could enable high temperature operations around 110-150°C due to their strong acid stability and enhanced hydrophilicity at high temperatures. Also, zeolite beta could prevent fuel cross-over in direct methanol fuel cells and membrane swelling problems. Moreover, these inorganic additives will contribute to the proton conductivity of the membrane by introducing their own proton conductivities. Ordinary aluminosilicate crystals are moderate proton conductors with conductivities around 10^{-4} S/cm and this conductivity can be further improved by acid treatment up to 10^{-1} S/cm [41]. Also, these inorganic additives will retain water within the membrane thus will facilitate the proton transfer.

Zeolite beta with high silica content is very stable in the acid environment. The XRD patterns of as synthesized and acid treated zeolite beta samples are given in Figure 2.32 [41].

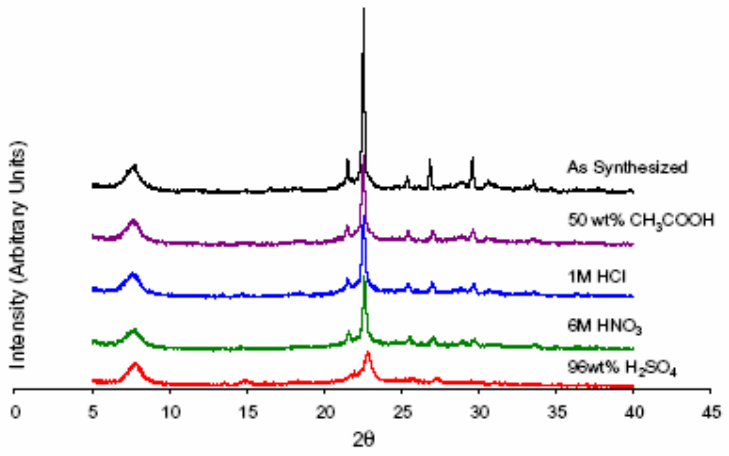

Figure 2.32: The effect of Acid treatment on Zeolite Beta Structure [41]

The zeolite samples were treated in the above mentioned acids overnight at 80°C with stirring. Even with the strongest acid (96 wt% H_2SO_4), the characteristic peaks of zeolite beta are still strong [41]. This result suggests that, zeolite beta can withstand the harsh acidic environment of the fuel cell. The 96 wt% H_2SO_4 acid treatment most effectively removed the structure directing agent as shown in Figure 2.33 [41].

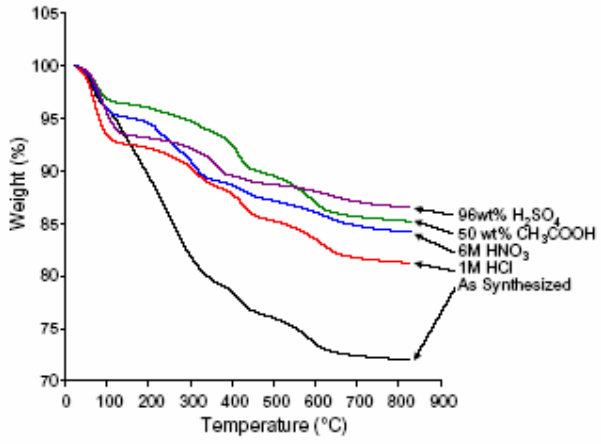

Figure 2.33: TGA analysis of as synthesized and acid treated zeolite beta samples [41]

It can be concluded that, zeolite beta nano-crystals could be good additive for fuel cell membranes due to their significant proton conductivity, excellent water retention at high temperatures and molecular sieving capabilities [41].

Three configurations will arise upon introduction of zeolite beta additives into an amorphous polymer matrix, which can be seen in Figure 2.34 [42].

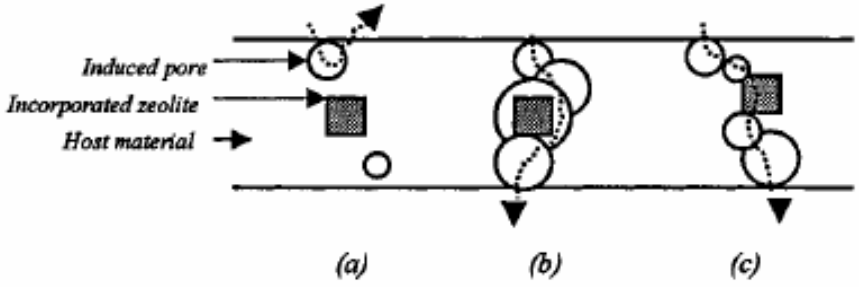

Figure 2.34: Schematic diagram of three pore structures obtained by introduction of zeolite particles in a film: (a) poorly formed pore structure result in a non-accessible zeolite particle; (b) void spaces around a zeolite particle which permits its circumvention; (c) traversing the pore network necessarily includes passage through a zeolite particle [42].

The pores created in the matrix should allow diffusing species to reach the zeolite crystals but the zeolite crystals must still be the gate keepers to transport through the entire film, which is just the case in case (c) shown in Figure 2.34 [42].

CHAPTER 3

EXPERIMENTAL

3.1 Zeolite Synthesis

Zeolite beta crystals were synthesized hydrothermally according to the batch composition 2.2 Na_2O: 1.0 Al_2O_3: x SiO_2: 4.6 $(TEA)_2O$: 440 H_2O at various SiO_2/Al_2O_3 ratios [39]. In hydrothermal synthesis, an alkaline precursor solution was prepared by dissolving sodium aluminate (52.9 wt% Al_2O_3, 45.3 wt% Na_2O, Riedel de Haën) in deionized water prior to addition of the structure directing agent, tetraethyl ammonium hydroxide (TEAOH) solution (20 or 35 wt% in water, Aldrich). Additional sodium was supplied by sodium hydroxide (NaOH) pellets (J.T. Baker). The solution was kept in a high density polyethylene (HDPE) bottle at 60˚C and mixed vigorously under magnetic stirring to obtain a homogenous solution. The silica precursor solution, mainly composed of colloidal silica (SiO_2), (Ludox 40 wt% suspension in water, Sigma-Aldrich), was added to the alumina precursor solution and gelation was observed. A homogenous gel was obtained by vigorously shaking this mixture for 15 minutes at 60˚C. This homogenous gel was poured into Teflon-lined steel autoclaves as shown in Figure 3.1 and the autoclaves were kept at constant temperature (150˚C) under static pressure for a reaction period of 5-15 days.

Figure 3.1: The introduction of synthesis gel into Teflon-lined steel autoclaves [43]

The degree of crystallization depends on the reaction temperature and time. After keeping the autoclaves at desired temperature for a predetermined time period, the autoclaves were taken out of the oven. As synthesized zeolite crystals were filtered either by vacuum filtration or centrifuge and washed to neutralize the pH of the zeolite crystals. The zeolites were then dried at 80˚C.

As synthesized zeolites still contain the structure directing agent; thus the zeolite beta crystals were calcined at 550˚C for 6 hours to remove the structure directing agent from the zeolite framework. The as-formed zeolite beta is in the Na^+ form and can be converted into more proton conductive H^+ form after acid treatment with 95-98 wt% H_2SO_4 (Merck).

Acid treatment of zeolite beta crystals is just an ion-exchange process. The zeolite beta particles are introduced into a 95-98 wt% H_2SO_4 containing beaker and stirred for 24 hours by magnetic stirrer to enable complete ion-exchange. After the acid treatment, the zeolite particles were washed with deionized water until their pH became neutral and filtered by vacuum filtering. The H^+-Beta zeolite crystals obtained were then dried at 80˚C and became ready to use.

3.2 Characterization of Zeolite Beta

3.2.1 X-ray Powder Diffraction (XRD) Analysis

The synthesized zeolites were characterized by a Philips PW 1729 X-ray diffractometer using CuKα radiation. The XRD analyses were performed for zeolite beta samples before calcinations and characteristic peaks of zeolites were observed around 2θ~ 7.8° and 2θ~ 22.4° as reported in literature [41].

3.2.2 Scanning Electron Microscopy (SEM) Analysis

The morphology and particle size distributions of the zeolite beta crystals synthesized at different SiO_2/Al_2O_3 ratios were monitored by scanning electron microscopy analyses (NORAN Instrument, JSM 640 Scanning Microscope).

3.3 Polymer Sulfonation

3.3.1 Sulfonation of PEEK Polymer

PEEK polymer was obtained as pellets (Polyoxy-1,4-pheneyleneoxy-1,4-pheneyelene carbonyl-1,4-phenylene, Aldrich, Mw= 20,800). The pellets were ground to reduce the dissolution time of the polymer in the sulfonating agent and prevent heterogeneous polymer sulfonation as shown in Figure 3.2.

The ground polymers were dried at 100°C in vacuum oven overnight prior to post-sulfonation. 95-98wt% H_2SO_4 (Merck) was used as the sulfonating agent since it is known not to cause polymer degradation or cross-linking. In the post-sulfonation reaction, 20g polymer was dissolved in 400mL H_2SO_4 to give a dark, viscous solution and the reaction temperature was kept constant at 50°C during the desired reaction time [36].

Figure 3.2: Introduction of Grinded PEEK polymer in to H_2SO_4 [43].

Reaction was stopped by pouring the polymer solution in excess ice-cold water and white polymer strings were obtained as shown in Figure 3.3.

Figure 3.3 Post-Sulfonation Reaction of PEEK was stopped by pouring into ice-cold water [43].

The decanted polymer strings were washed with deionized water until a pH around 6 was obtained. Then the sulfonated polymer was dried in vacuum oven at 80°C for 12 hours followed by drying at 120°C for another 12 hour.

3.3.2 Sulfonation of PES polymer

PES polymer cannot be easily sulfonated as PEEK in H_2SO_4. Therefore chlorosulfonic acid (CSA) was used in the sulfonation reaction. The polymer was first dissolved in H_2SO_4 (usually 1/10 w/v) then a predetermined amount of CSA was added dropwise into the solution. Reactions were carried out at 5°C or room temperature if the room temperature was below 20°C. At the end of the predetermined reaction time solution was poured into cold ice-water and the precipitate was filtered and washed until excess acid is removed and dried at 90°C.

3.4 Characterization of Sulfonated Polymers

The sulfonation level of PEEK polymer can be characterized either by H-NMR analysis or by titration.

3.4.1 Titration Analysis

For titration analysis, 1gr of sulfonated polymer was placed in 3M NaCl solution and kept for one day [14]. The solution was then titrated with 0.1M NaOH solution. Thus the ion exchange capacity of the polymer can be easily found as mili-equivalents per gram polymer and can be used to find the degree of sulfonation of the PEEK polymer according to;

$$DS = \frac{M_w * IEC}{1000 - 81 * IEC} \tag{5}$$

3.4.2 H-NMR Analysis

The H-NMR spectra were obtained by using Bruker Biospin NMR spectrometer with a resonance frequency of 300MHz as shown in Figure 3.4. Samples were prepared by dissolving 10-20 mg polymer in DMSO-d6. The DS was determined by integration of distinct aromatic signals [14].

Figure 3.4: Bruker Biospin NMR spectrometer in Central Laboratory, METU

3.5 Composite Membrane Casting and Incorporation of Zeolite Beta

The SPEEK polymer was dissolved in n-n, dimethyl-Acetamide (DMAc, Merck) and stirred overnight with magnetic stirrer. Then, zeolite H^+-Beta was added to the solution at proper loadings. The solution was mixed under ultrasonic mixing overnight and then drop-casted onto petri dishes as shown in Figure 3.5. The casted membranes were dried in vacuum oven at 60°C to 120°C for 24 hours.

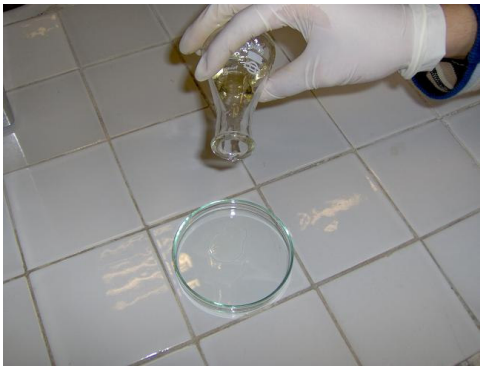

Figure 3.5: Membrane Casting onto Petri-Dishes [43]

3.6 Blend Membrane Casting

Proportional amounts of sulfonated PEEK and PES polymers were dissolved in dimethylacetamid (DMAc) to give a 10 wt % polymer solution. The solution was stirred by magnetic stirrer overnight prior to mixing in ultrasonic water bath to obtain a homogenous solution. After mixing, the homogenous solution was casted onto Petri dishes and dried from 60°C to 120°C in 24 hours.

3.7 Membrane Characterization

The membranes casted were thermally characterized by differential scanning calorimetry (DSC) and thermogravimetric (TGA) analyses. The water uptakes and swelling ratio of the membranes were measured and proton conductivity analyses were performed by electrochemical impedance technique. Finally, the membranes were tested in the fuel cell test station.

3.7.1 Differential Scanning Calorimetry (DSC) Analysis

DSC analyses were carried out by DuPont-TA 910S at a heating rate of 10°C/min under N_2 atmosphere from 20°C to 300°C. The glass transition temperature (T_g) was calculated from the intersection of the tangents to the corresponding DSC curve [14].

3.7.2 Thermogravimetric Analysis (TGA)

TGA analyses were carried out by DuPont TA 951. Approximately 10-15 mg samples were heated from 20°C to 900°C at a rate of 10°C/min under N_2 atmosphere [14].

3.7.3 Water Uptake Measurements

The SPEEK membranes were dried at 100°C to remove the moisture prior to measurements. The dried membranes were weighed and immersed in H_2O and kept at different temperatures to observe the effect of temperature on membrane water uptake. Membranes were kept in water for a day at each temperature. Then wetted membranes were blotted with dry absorbent paper prior to weighing. The membrane water uptake was calculated with reference to the dry membrane weight [14, 15].

$$Water\ Uptake = \frac{W_{wet} - W_{dry}}{W_{dry}} \times 100\% \tag{6}$$

3.7.4 Swelling Measurements

Swelling ratio analyses were explored similar to water uptake measurements. Firstly, the membranes were dried at 100°C to remove the moisture. Then specimens of 1cm x 4cm were prepared and soaked in water at different temperatures for a day each. Then the percent elongation was calculated with reference to the dry length.

$$Percent\ Elongation = \frac{L_{wet} - L_{dry}}{L_{dry}} \times 100\% \tag{7}$$

3.7.5 Proton Conductivity Analysis

The proton conductivity of the membranes was measured by AC Electrochemical Impedance (EIS) technique over a frequency range of 1-300 kHz with an oscillating voltage using GAMRY PCL40 Potentiostat system. This technique is explained in detail in Appendix A. All measurements were performed in longitudinal direction by using the conductivity cell given in Figure 3.6, under vapor atmosphere at 100% relative humidity either with 2 probes or 4 probe EIS as a function of temperature.

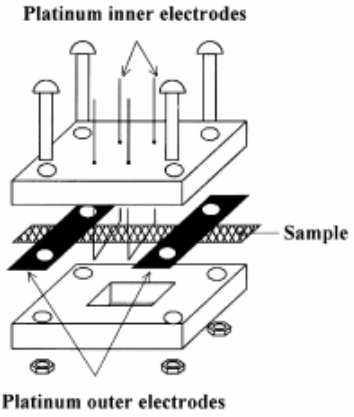

Figure 3.6: Conductivity Cell [6]

The specimens were prepared as 1cm x 5cm membrane strips and sandwiched into a Teflon conductivity cell with Pt electrodes. The specimen and the electrodes were fixed by using bold and nuts [6].

The conductivity, σ, of samples in longitudinal direction was calculated in Siemens per cm from the impedance data by using;

$$\sigma = \frac{L}{R \times W \times d} \tag{8}$$

where; L is the distance between the electrodes, W is the width of the membrane, d is the thickness of the membrane and R is the low intersect of the high-frequency semi-circle on a complex impedance plane with the Re(Z) axis.

3.7.6 Fuel Cell Tests

The casted membranes which resulted in good proton conductivities during electrochemical impedance spectroscopy analyses were further tested by fuel cell tests. The fuel cell tests were carried out by a single cell PEMFC (Electrochem) with an active area of 5cm x 5cm to which pure hydrogen was supplied as the fuel and pure oxygen as the oxidant. The test station can be seen in Figure 3.7. [44] The tests were performed at different operating temperatures in the range of 70˚C-90˚C adjusted according to the thermal stability of the membrane. The membrane electrode assemblies (MEA) were prepared by gas diffusion layer (GDL) spraying method. Carbon paper (SGL 30BC) was used as the gas diffusion layer and catalyst was 20 wt % Pt on Vulcan XC-72 from E-TEK [44].

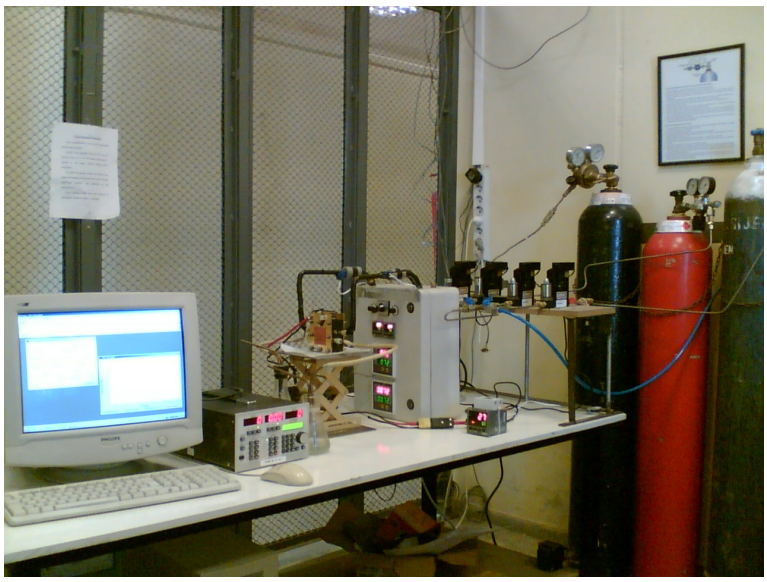

Figure 3.7: Fuel Cell Test Station [44]

CHAPTER 4

RESULTS & DISCUSSION

4.1 Zeolite Synthesis

Zeolite beta crystals were synthesized at different SiO_2/Al_2O_3 ratios according to the batch composition 2.2 Na_2O: 1.0 Al_2O_3: x SiO_2: 4.6 $(TEA)_2O$: 440 H_2O as described in the experimental section [39]. As-synthesized zeolite crystals were characterized by X-ray diffraction analyses (Philips PW 1729, XRD) and the characteristic peaks of zeolite beta were identified as in Figure 4.1.

The XRD pattern of zeolite beta that was hydrothermally synthesized at SiO_2/Al_2O_3 ratio of 20 is given in Figure 4.1. Additional XRD patterns for zeolites synthesized at different SiO_2/Al_2O_3 ratios can be seen in Appendix B.1. The characteristics peaks of zeolite beta crystals were observed at 2θ~ 7.8° and 2θ~ 22.4° as stated in literature [41] for zeolite beta samples synthesized at SiO_2/Al_2O_3 in the range of 20-50. Pure zeolite beta phases could be obtained at SiO_2/Al_2O_3 in the range of 20-50 with high yield; however, beyond this range other zeolite phases were obtained as well as zeolite beta. In Figure 4.2, an XRD pattern of zeolite beta crystals synthesized at SiO_2/Al_2O_3 ratio of 12 is shown. As it can be clearly seen in the figure, the crystals do not only belong to the zeolite beta phase but also some other zeolite phases exist. Hence pure zeolite beta could not be synthesized at this ratio.

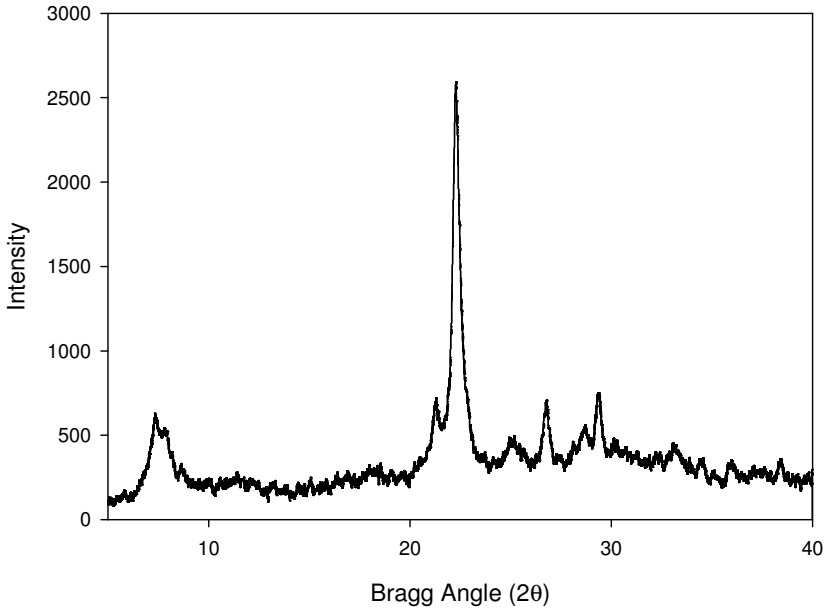

Figure 4.1: XRD pattern of as synthesized zeolite beta (SiO_2/Al_2O_3=20).

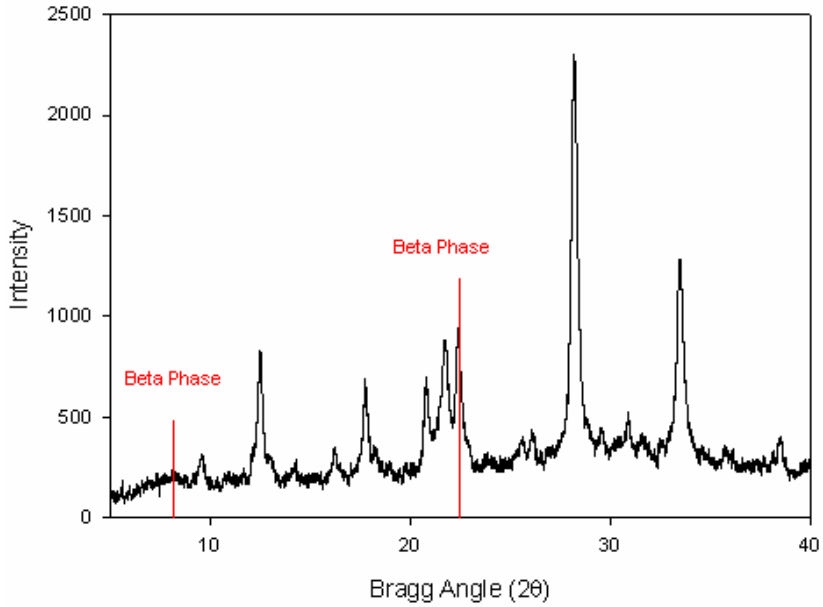

Figure 4.2: XRD pattern of as synthesized zeolite beta (SiO_2/Al_2O_3=12).

The zeolite beta crystals have a strong resistance to the acid environment as stated in literature [41]. The characteristic peaks of zeolite beta could even be identified after the acid treatment with strong sulfuric acid solution of 95-98 wt% as can be seen in Figure 4.3. The acid stability of the zeolite particles is very important, since the fuel cell environment is highly acidic.

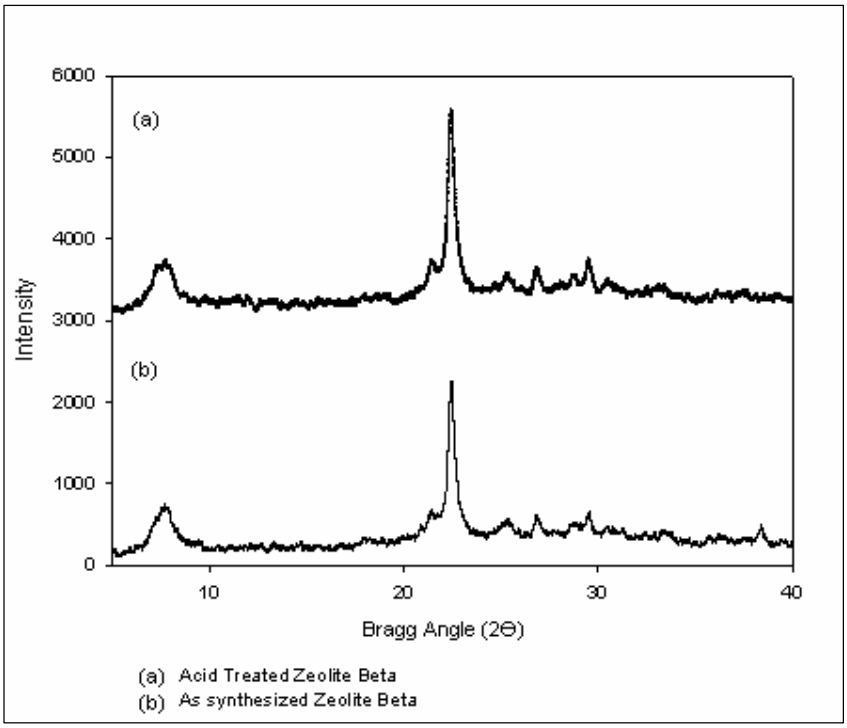

Figure 4.3: XRD pattern of zeolite beta treated with 95-98 wt% H_2SO_4.

Another important characteristic of zeolite beta is its high thermal stability. Thermo gravimetric analyses of zeolite beta crystals showed that the first weight loss was around 465°C as given in Figure 4.4 and it demonstrates the removal of the structure directing agent (SDA) from the zeolite structure. Thus, zeolite crystals were calcined at higher temperatures to remove SDA completely. The thermal decomposition temperature of zeolite beta particles was around 850°C, this means that the zeolite beta particles are stable up to this temperature. Hence, they are suitable for fuel cell applications.

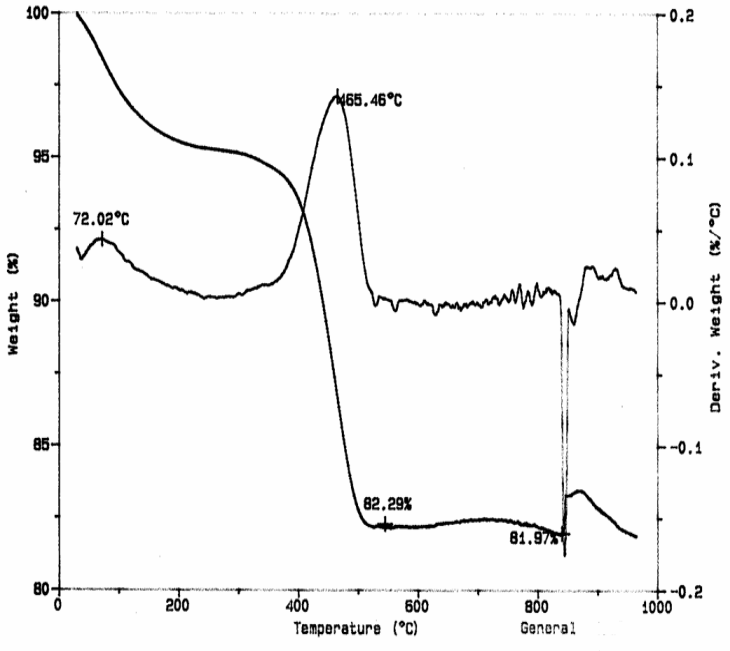

Figure 4.4: TGA graph of zeolite beta crystals.

Moreover, the particle size distribution and morphology of the synthesized zeolite particles were characterized with scanning electron microscopy (SEM) analyses and the SEM micrographs are given in Figure 4.5.

The synthesized zeolite particles showed an even particle size distribution around 1μm.

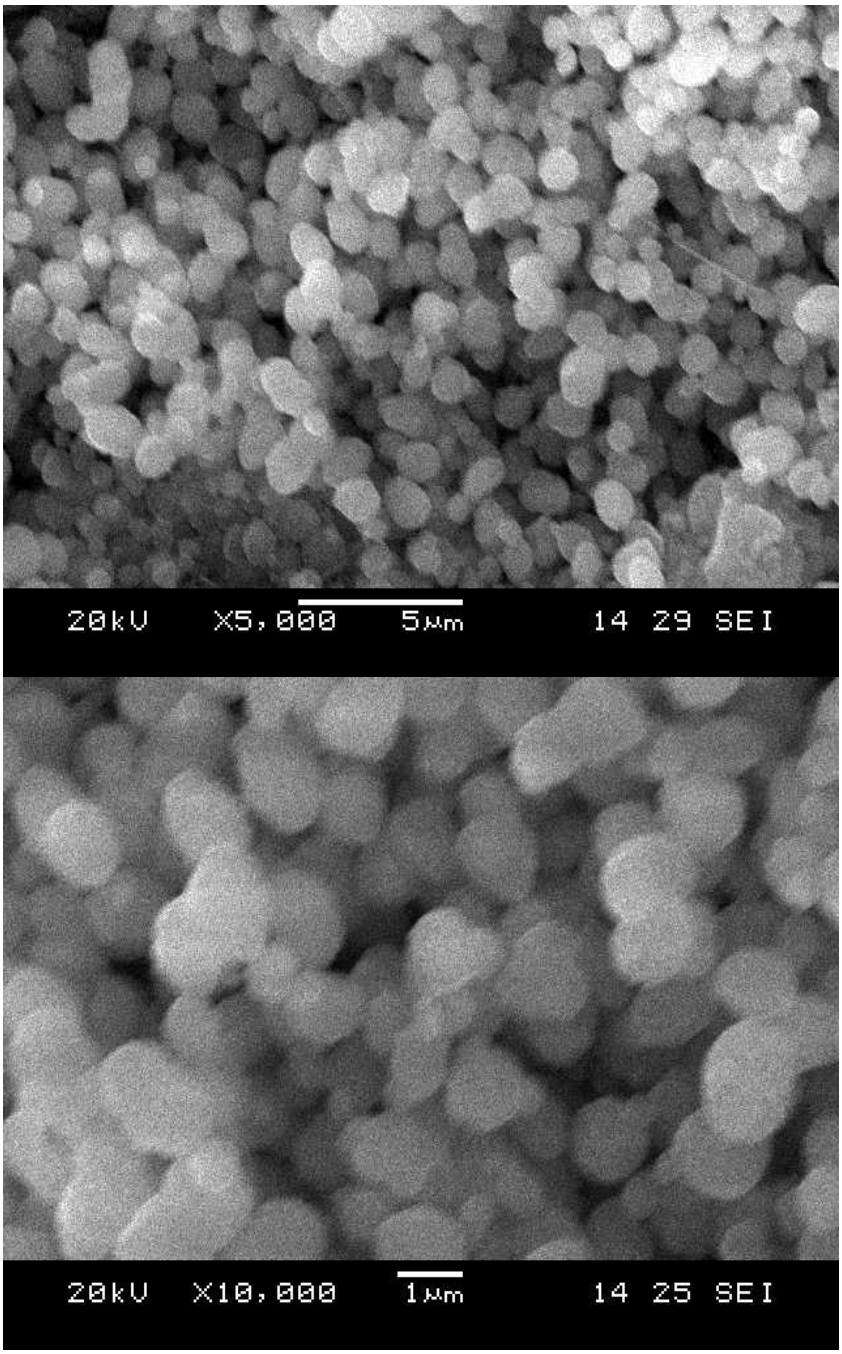

Figure 4.5: SEM micrographs of synthesized zeolite beta crystals.

4.2 Polymer Sulfonation

The objective of polymer sulfonation is to introduce sulfonic acid groups into the structure and increase the number of acid sites available for bonding of the water molecules which enhance the proton transfer. The number of sulfonic acid groups per repeating unit is called as the degree of sulfonation (DS) or sulfonation level (SL). Polyether ether ketone (PEEK) polymer can be easily sulfonated by using concentrated sulfuric acid solution. The reaction time, reaction temperature and the amount of the sulfonating agent plays a key role in controlling the DS of the polymer.

In the beginning of this study, the PEEK polymer pellets were dissolved in 95-98wt% H_2SO_4 solution for 2 hours at room temperature. After this dissolution period, the solution was sieved to remove the PEEK particles that were not dissolved and post-sulfonated at 50°C in the same solution for a predetermined time. However, because of the long dissolution period of 2 hours, the polymer could not be sulfonated homogeneously; hence the dissolution period was shortened. Thus, ground PEEK polymers were used instead of pellets and the dissolution temperature was increased from room temperature up to 50°C. As a result, complete dissolution of polymer was achieved in 10-15 minutes. From that point on, all post-sulfonation experiments were carried out by dissolving ground PEEK in 95-98wt% H_2SO_4 at 50°C.

Another important parameter in polymer sulfonation was the reaction time. A series of experiments were performed to explore the effect of the reaction time on degree of sulfonation. During these experiments the reaction temperature was kept constant at 50°C as mentioned before. The results of these experiments can be seen in Figure 4.6. The degree of sulfonation was found to increase with increasing reaction time. It was as expected result as shown before in Figure 2.10.

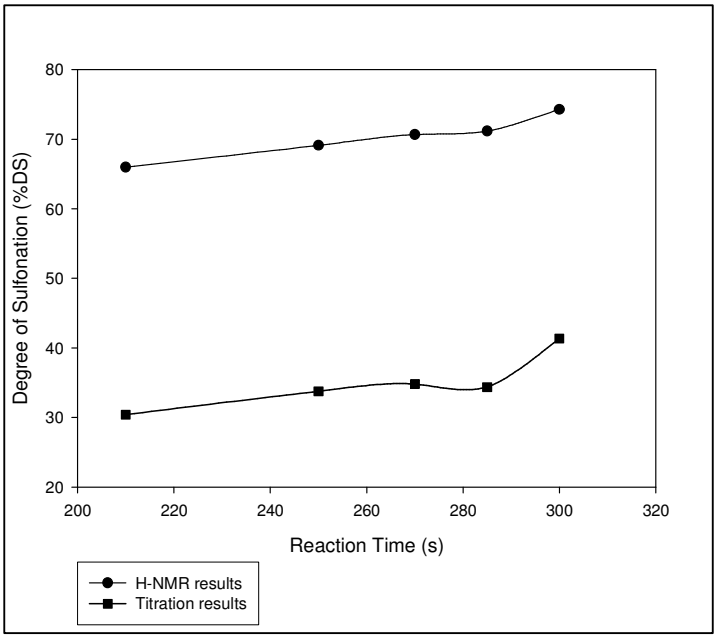

Figure 4.6: Degree of Sulfonation of PEEK polymer as a function of reaction temperature.

The sulfonation level of the polymers can be calculated either by H-NMR or titration analyses. (H-NMR analyses results are given in Appendix B.2). However, there is a high discrepancy between the results obtained from these analyses as demonstrated in Figure 4.6. The H-NMR analyses resulted in higher DS values than titration analyses for the same samples. This difference could be explained as follows; in H-NMR analysis, every sulfonic acid groups within the structure could be monitored, however, in titration analysis only the sulfonic acid groups attached to the polymer surface could be considered. Thus, H-NMR results are more reliable, and from this point forward the DS results are going to be reported according to H-NMR analyses.

The chemical and mechanical properties of PEEK polymer is directly related with the degree of sulfonation of the polymer. As the sulfonic acid group content of the polymer increases, its crystallinity decreases and at high DS values it becomes amorphous and dissolves in hot water.

If DS is less than 30%, the polymer is only soluble in strong acids and it becomes soluble in solvents at room temperature only after 40% DS. When DS exceeds 70%, it becomes soluble in methanol and hot water and becomes inappropriate for fuel cell applications. Hence, DS must be kept between 40 and 70%. In this work, SPEEK polymer with DS 68% was chosen as the membrane matrix due to its high proton conductivity and suitable mechanical strength. The H-NMR spectra of SPEEK polymer with a sulfonation degree of 68% is shown in Figure 4.7.

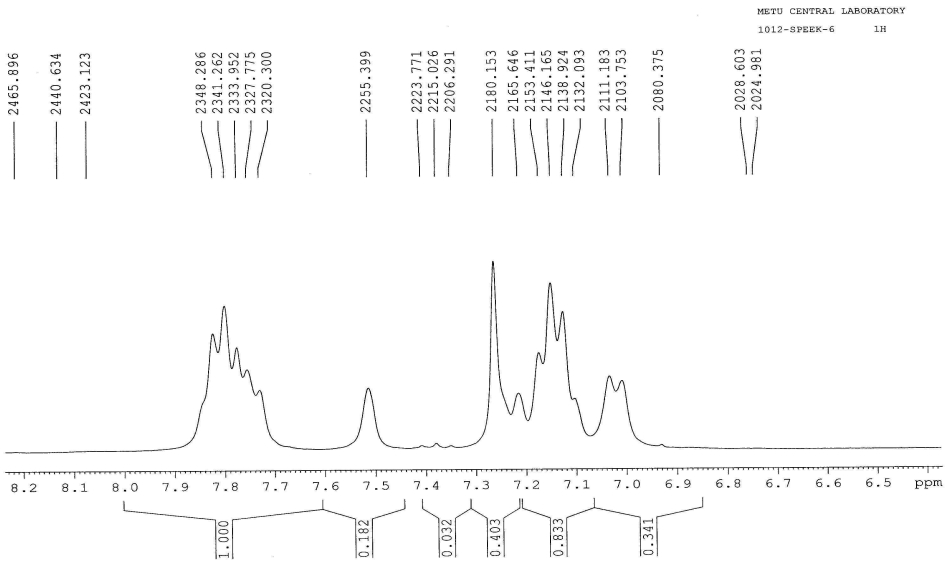

Figure 4.7: H-NMR Spectra of SPEEK polymer (DS 68%)

The thermal behavior of the polymer was explored as a function of degree of sulfonation. The sulfonated derivative of PEEK polymer shows two weight loss steps as given before in Figure 2.15 [14]. The TGA graphs of sulfonated PEEK polymers can be found in Appendix B. The onset of thermal decomposition demonstrates the splitting of the sulfonic acid groups from the polymer structure. As stated in literature [15], a sharp decrease was observed in the thermal decomposition temperature as the sulfonic acid content of the polymer increased. As given in Figure 4.8, the onset of thermal decomposition of PEEK polymer was decreased from 550°C to 340°C upon sulfonation.

TGA graphs of SPEEK polymers with different DS values could be found in Figures B.10- B.13. However, 340°C is still a quite high temperature when PEMFC operating temperature about 80°C is considered.

Moreover, the glass transition temperatures of SPEEK polymers with different DS were found to be in the range of 180°C-250°C and observed to increase after thermal treatment as shown in Figure B.17 and B.18 in Appendix.

Thus, it can be concluded that, PEEK polymer and its sulfonated derivatives are thermally stable and appropriate for fuel cell applications.

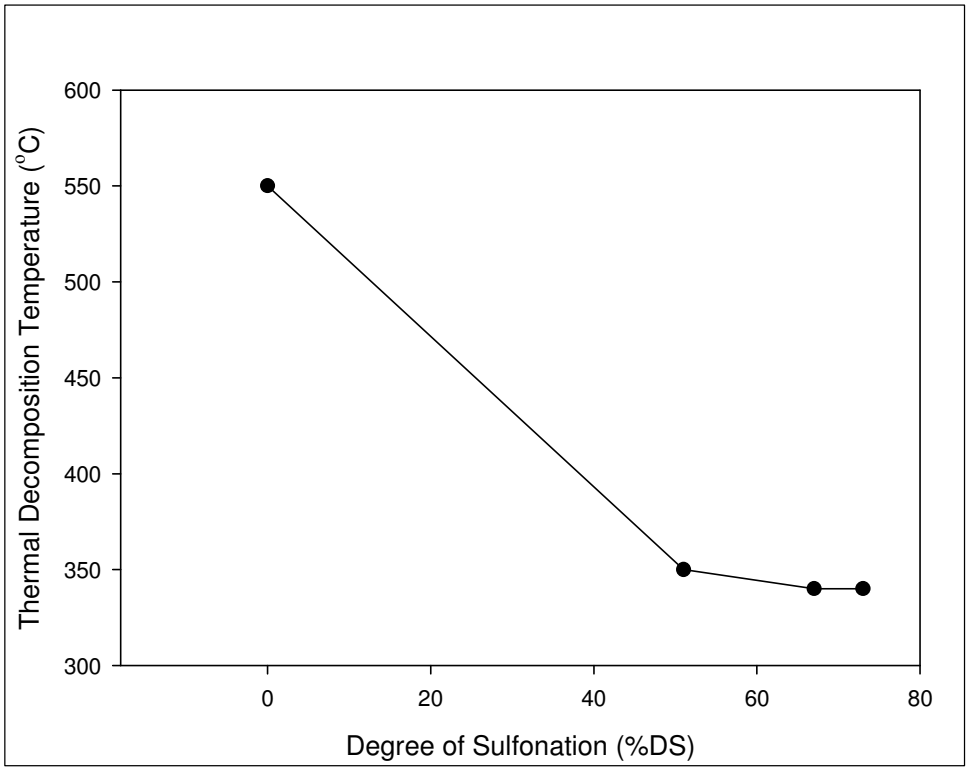

Figure 4.8: Thermal Stability of PEEK polymer as a function of sulfonation level

4.3 Composite Membranes

The objective of introducing zeolite particles into the polymer matrix was to enhance the proton transfer through the membrane by retaining water within the membrane and to create water mediated pathways while contributing their own proton conductivity. The water retention property of the membranes was measured by water uptake measurements as shown in Figure 4.9.

The hydrophilic zeolite particles improved the water retention property of the plain SPEEK membranes. As seen in Figure 4.9, the composite membranes containing zeolites have shown higher water uptake capacities. However, above 60°C, the composite membranes absorbed too much water and swelling problem was observed above this temperature. Thus, the proton conductivity analyses of composite membranes were limited up to this temperature.

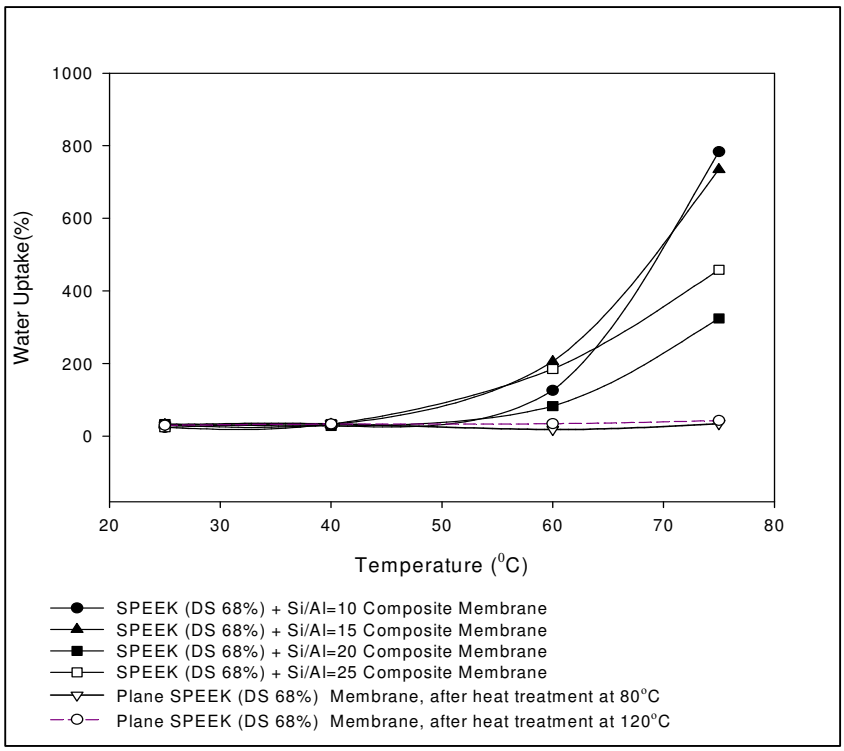

Figure 4.9: Water Uptake Capacities of plain and composite SPEEK membranes.

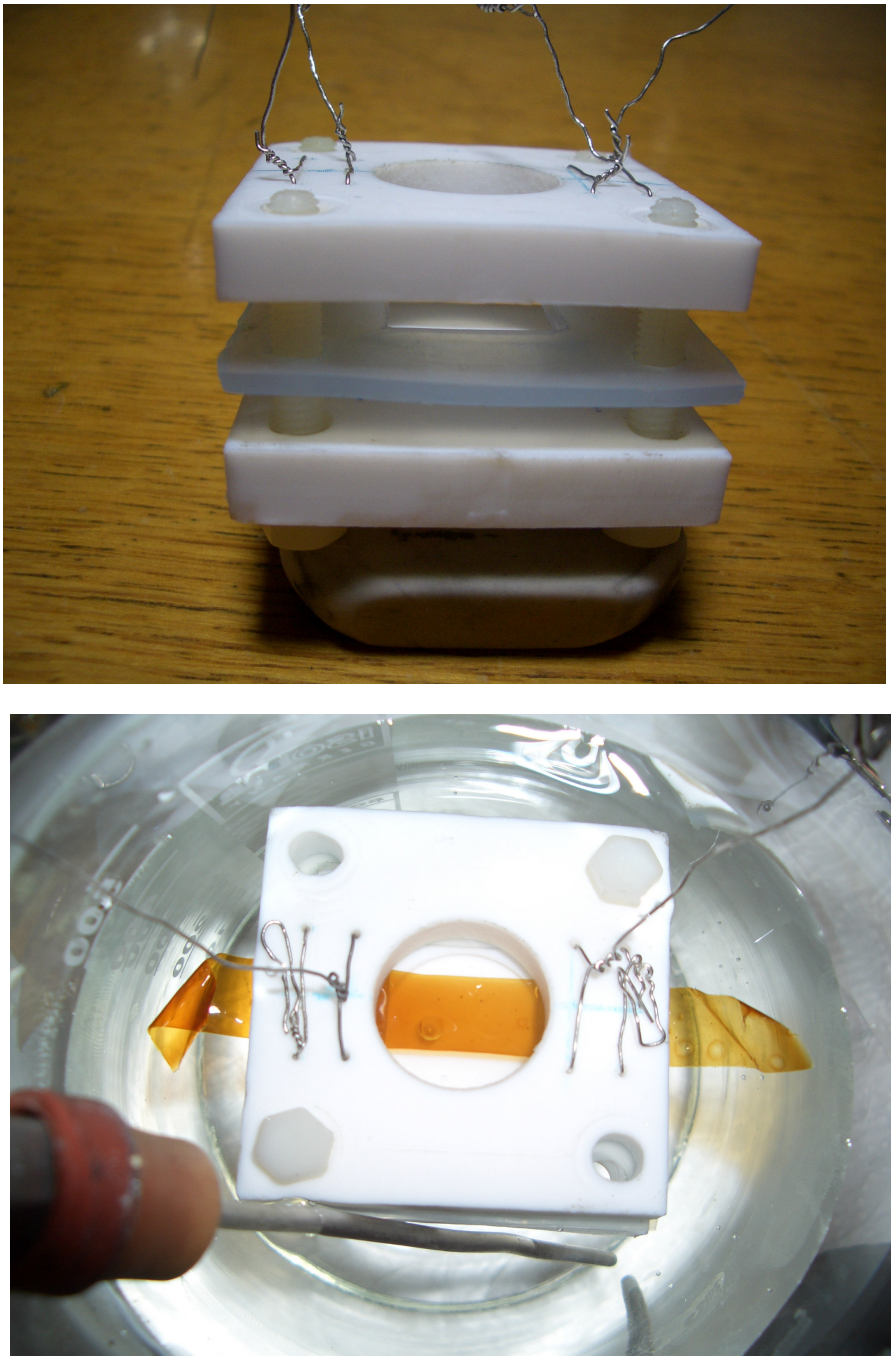

Figure 4.10: Teflon Conductivity Cell

The proton conductivity analyses of these membranes were performed by using electrochemical impedance technique (EIS). The measurements were carried out by a GAMRY PCL40 Potentiostat system, by 2 or 4 probe analyses in air at 100% relative humidity or in fully-hydrated state. The Teflon lined conductivity cell equipped with platinum electrodes and wire is shown in Figure 4.10.

The membrane strips with dimensions of 1cm x 5cm were prepared. The proton conductivities of plain and composite membranes were measured at room temperature before and after treatment with 1 M HCl acid. All membranes were washed and hydrated with deionized water prior to measurements.

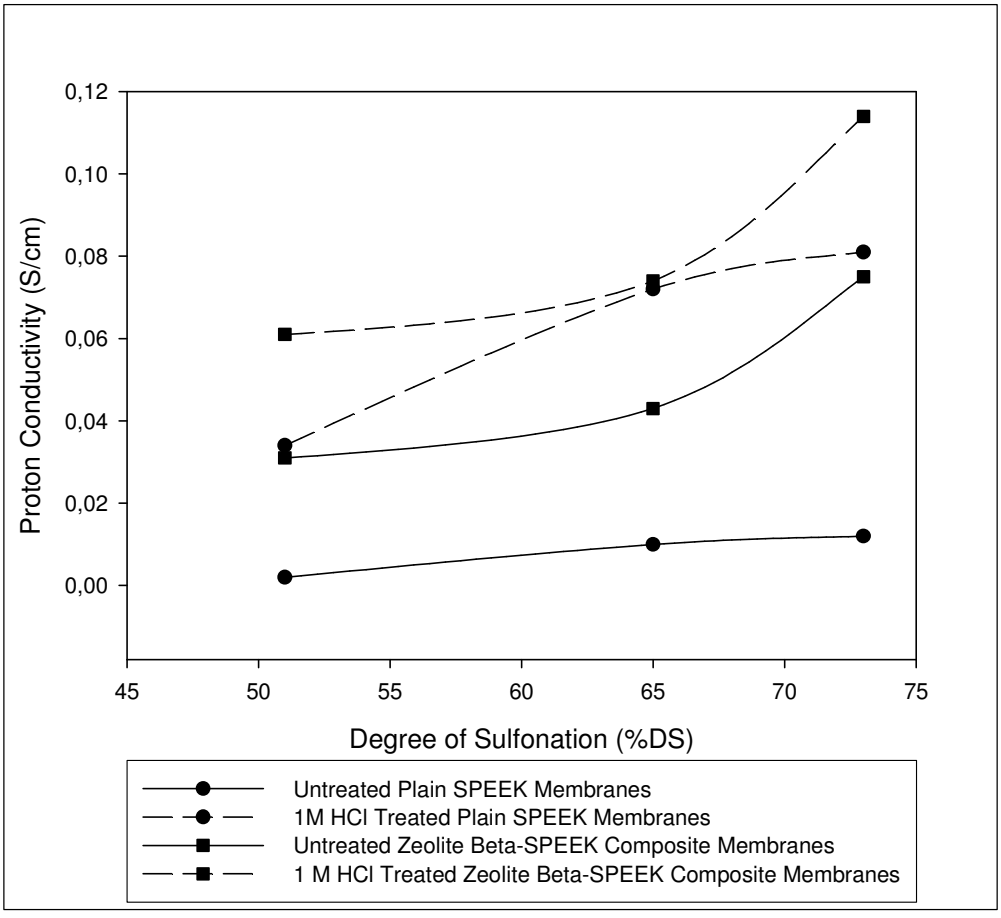

Figure 4.11: Proton conductivity of plain and composite membranes (with 10 wt% zeolite loading) at room temperature and fully-hydrated state

As shown in Figure 4.11, the membranes with higher DS were resulted in better proton conductivities. This is an expected result, since increasing the number of acid sides enhances the proton transfer. A similar result was reported by Zaidi and co-workers in Figure 2.17 [27] However, the reported conductivity value corresponding to SPEEK membrane with DS 70% was ten fold less than the value that was shown in Figure 4.11. This discrepancy is due to the differences in the measurement techniques. In the work of Zaidi and co-workers, the proton conductivity was measured in transversal direction, on the other hand, in this work the measurements were carried out in longitudinal direction. In another work [32], one order of magnitude difference in proton conductivities were observed for this two measurement techniques as shown in Figure 2.21. Keeping those in mind, the proton conductivities shown in Figure 4.11 were comparable with literature [27, 28, 32].

Moreover, the effect of acid treatment on proton conductivity was explored in Figure 4.11 and improved proton conductivities were observed after the acid treatment of the membranes. Thus, from this point on, the membranes were treated with 1M HCl and washed with distilled water prior to proton conductivity measurements.

Another important observation that could be made in Figure 4.11 is the effect of zeolite particles. The composite membranes containing zeolite beta have shown improved proton conductivities and 0.11 S/cm was achieved for the composite membranes with DS 74% after acid treatment. This is a promising result, since it is comparable with the conductivity of Nafion 112 membrane (0.1 S/cm).

However, at high temperatures, the membranes with high DS lose their hydro-thermal stability and become soluble in hot water. For this reason, PEEK polymer with a lower DS of 68% is chosen instead of the polymer with DS 74%. Moreover, to overcome the solubility and swelling problems at high temperatures, the conductivity measurements were performed in air instead of water. The effect of temperature on proton conductivity could be seen on Figure 4.12.

According to the Figure 4.12, the proton conductivity of SPEEK membrane with DS 68% increased with increasing temperature up to 0.05 S/cm at 40°C then decreased slightly. The composite membranes showed increased proton conductivities especially at higher temperatures. The composite membranes were prepared by using zeolite beta crystals synthesized at different SiO_2/Al_2O_3 ratios and the influence of this ratio on proton conductivity can be considered from Figure 4.12. There is a trend of increasing proton conductivity with increasing SiO_2/Al_2O_3 ratio of the zeolite except for the composite membrane containing zeolite synthesized at SiO_2/Al_2O_3=20. However, the opposite was stated in literature [41]. It was reported that, by the decreasing SiO_2/Al_2O_3 ratio, the zeolite becomes more hydrophilic thus retains more water within the membrane.

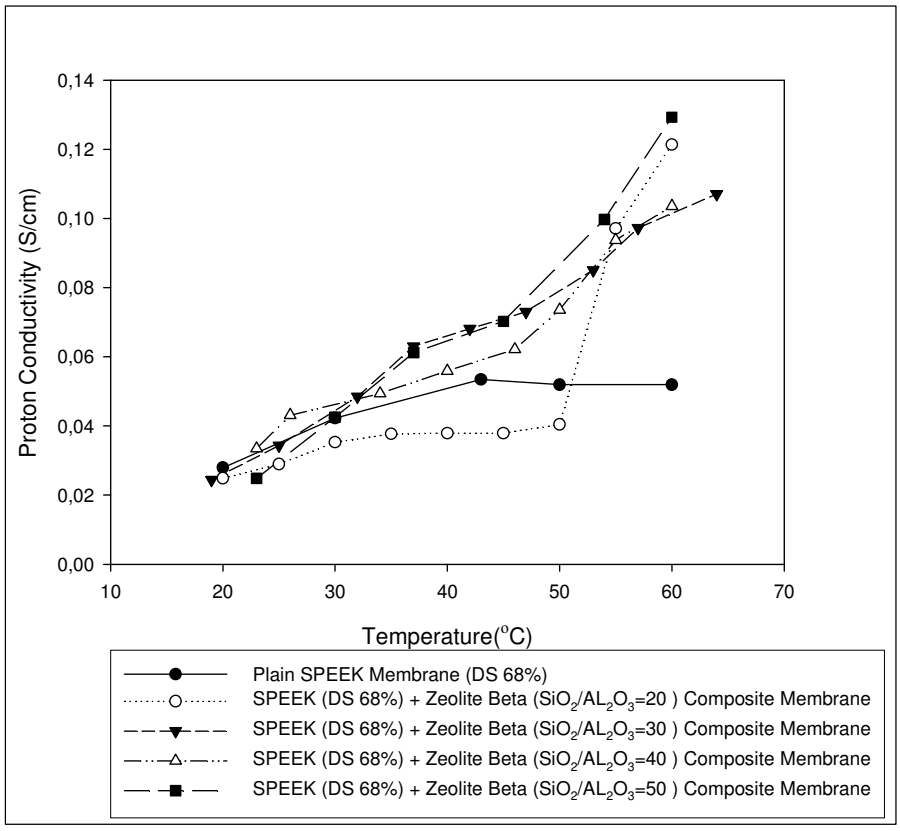

Figure 4.12: Proton conductivity of SPEEK and Composite membranes (10 wt% zeolite loading) as a function of temperature (in air, at 100% relative humidity)

In the work of Holmberg and co-workers, the zeolite beta crystals were containing an additional organic group to which sulfonic acid groups were attached, where as in this work pure zeolite beta crystals were used. This discrepancy may be due to the differences of the zeolite beta crystal structures utilized.

Moreover, at low SiO_2/Al_2O_3 ratios, the acid strength of zeolite beta is poor and the acid strength improves with increasing SiO_2/Al_2O_3 ratio. Thus, the structure of the zeolite synthesized at low SiO_2/Al_2O_3 ratios may be affected from the acidic environment of the fuel cell; so zeolites with high SiO_2/Al_2O_3 ratios could give better results.

The increase in the proton conductivity of the composite membrane containing zeolite beta synthesized at SiO_2/Al_2O_3 =20 above 50°C can be explained by swelling phenomena. Swelling causes the formation of ionic clusters which enhances the proton transfer but if swelling is too much, the membrane loses its mechanical strength and punctures.

The high proton conductivities observed above 50°C were results of membrane swelling. At this temperature, the membrane swelled too much, and not only the proton transfer was enhanced but also its surface area was enlarged. However, because of swelling, the enlargement of the area could not be measured correctly, thus the proton conductivity results came out to be higher than the actual case.

The best proton conductivity result of 0.13 S/cm at 60°C was obtained for the composite membrane prepared by incorporating zeolite beta crystals synthesized at SiO_2/Al_2O_3 ratio of 50 into a SPEEK matrix with DS 68%. This result is welcomed since the target of 0.1 S/cm for commercially viable alternate membranes is reached and the zeolite beta crystals synthesized at SiO_2/Al_2O_3 ratio of 50 was chosen as the most appropriate inorganic additive among the others.

Another parameter affecting the proton conductivity of composite membranes was the zeolite loading. Proton conductivities of composite membranes prepared by using zeolite beta crystals (SiO_2/Al_2O_3 ratio of 50) at different loadings (5 wt%, 10

wt% and 20 wt %) were measured as a function of temperature as shown in Figure 4.13. The proton conductivity of composite membranes were found to increase by increasing zeolite loading from 5 wt% to 10 wt%, but decreased for the composite membrane with 20 wt% zeolite loading. This decrease may be explained by the pore formation that may occur as the amount of zeolite particles incorporated into the polymer structure is increased further. The pores created within the polymer may lead to poor proton transfer. The best conductivity obtained in this experiment was 0.08 S/cm at 80°C. This conductivity was slightly lower than the one reported in Figure 4.12. The discrepancy between these two conductivities was possibly due to different thermal treatments in the drying step. In the second case, the membranes were thermally treated at 120°C for one more day to overcome swelling problems.

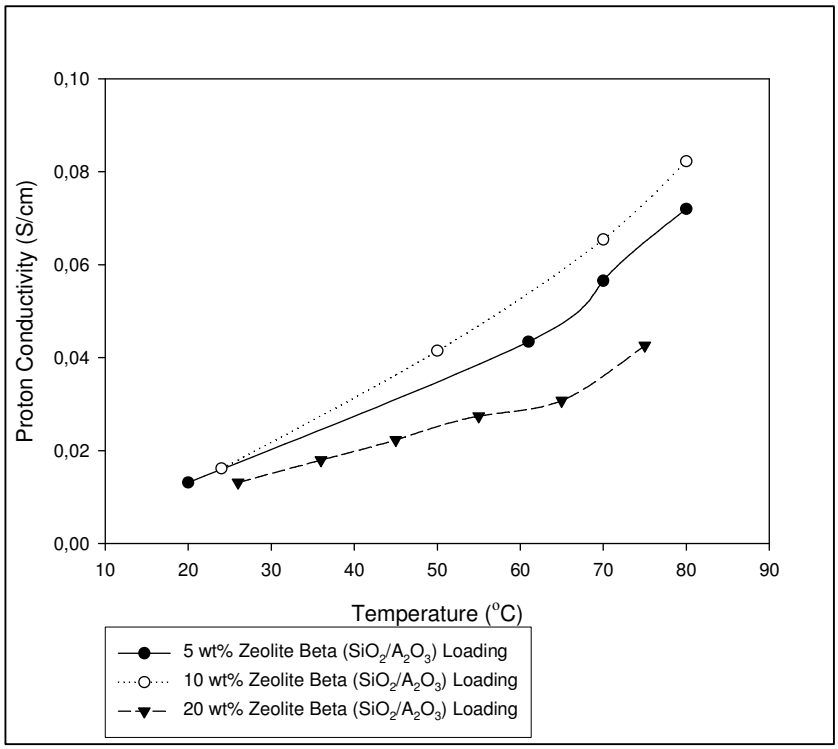

Figure 4.13: Influence of Zeolite beta loading on Proton Conductivity

By this extra thermal treatment, some of the sulfonic acid groups within the polymer were cross-linked, thus swelling problem is reduced and the measurements could be performed at higher temperatures up to 90°C. However, the cross-linking of some sulfonic acid groups led to a decrease in proton conductivity. The best conductivity of this case was 0.08 S/cm at 80°C, which is still comparable to proton conductivity of Nafion membrane.

4.4 Swelling Problem

At high degrees of sulfonation SPEEK polymer loses its crystallinity and becomes hydrophilic. Due to its new hydrophilic character, it absorbs water resulting in very high water uptakes and swollen membranes. Swelling problem can be minimized by either thermal cross-linking or blending with a more stable polymer. In thermal cross-linking, some of the hydrophilic chains (sulfonic acid groups for SPEEK polymer) within the polymer structure make bonds with the polymer backbone, thus reduces the hydrophilicity of the polymer and prevents swelling (Hogarth, 2001). On the other hand, this decline in the acidic sites hinders the proton transfer causing lower proton conductivities.

Another way to prevent swelling is blending with a more stable polymer. The properties of the blend membranes will depend upon the share and contribution of each separate polymer in the blend. The thermo hydrolytic stability and the water uptake of the resulting membrane could be controlled by adjusting the proportion of each polymer in the blend.

4.5 Blend Membranes

In order to overcome the swelling problems observed in the pure and composite SPEEK membranes, SPEEK polymer was blended with a more hydrophobic polymer, sulfonated polyether sulfone (SPES). The PES polymer was post-sulfonated as described before (experimental part 3.2.2) and blended with SPEEK polymer at predetermined proportions before membrane casting (experimental 3.6).

The incorporation of SPES polymer into SPEEK polymer improved the thermal stability of the resulting membrane. An increase in thermal decomposition and initial weight loss temperatures were observed with increasing proportion of SPES polymer in the polymer blend as given in Figure 4.14-4.16.

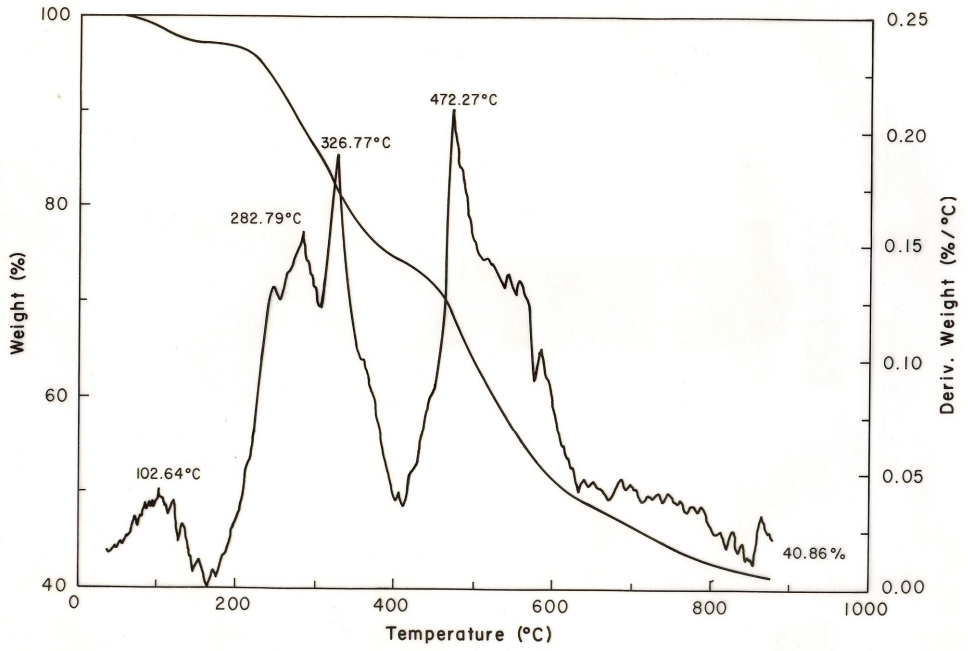

Figure 4.14: TGA graph of 25 wt % SPES+ 75 wt % SPEEK blend membrane

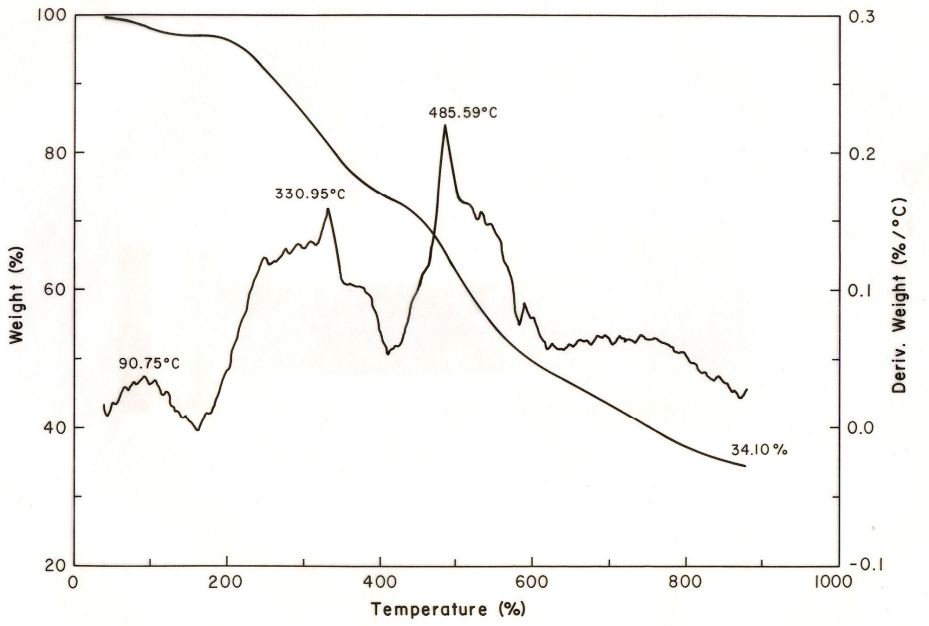

Figure 4.15: TGA graph of 50 wt % SPES+ 50 wt % SPEEK blend membrane

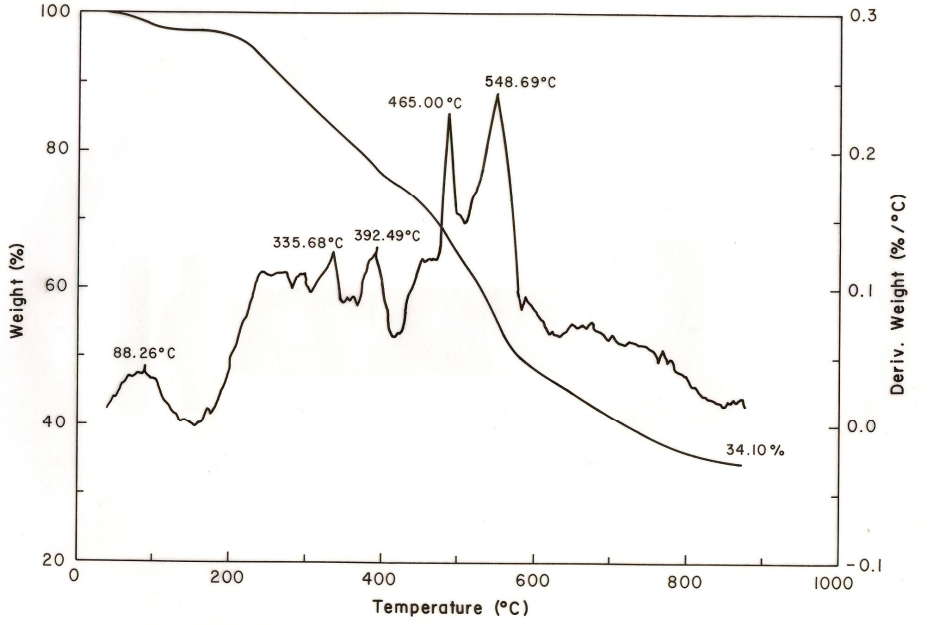

Figure 4.16: TGA graph of 75 wt % SPES+ 25 wt % SPEEK blend membrane

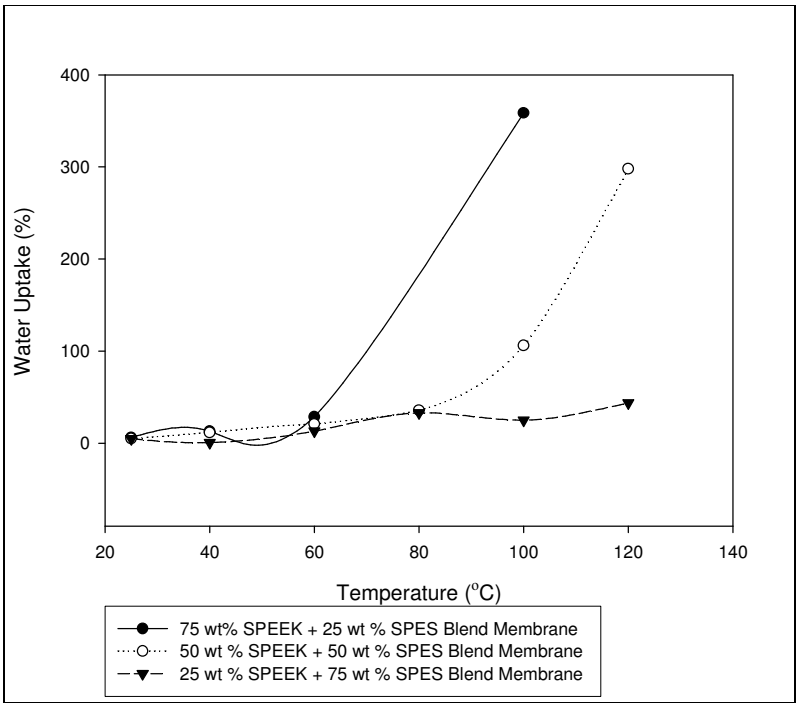

Figure 4.17: Water Uptake Capacity of Blend Membranes

Water uptake analysis proved that, the swelling problem of SPEEK membranes could be solved by blending with SPES polymer. As SPES content of the blend increased, the amount of water retained within the polymer is decreased as shown in Figure 4.17. The blend membranes posses lower water uptakes at even higher temperatures, thus conductivity measurements could be performed at higher temperatures up to 100°C without any deformation in the membrane structure. However, owing to the poor proton transfer mechanism of SPES polymer, lower conductivities were obtained for blend membranes compared to the pure and composite SPEEK membranes. The proton conductivity measurements of pure SPEEK, SPES and blend membranes are given in Figure 4.18.

The blend membrane containing 75 wt% SPEEK and 25 wt% SPES has shown good thermal stability over the operating temperature range of a PEMFC and possessed comparable proton conductivity of 0.75 S/cm at 95°C with Nafion® 112 membrane. Thus, this blend membrane could be another cheaper alternative to Nafion® 112 membrane.

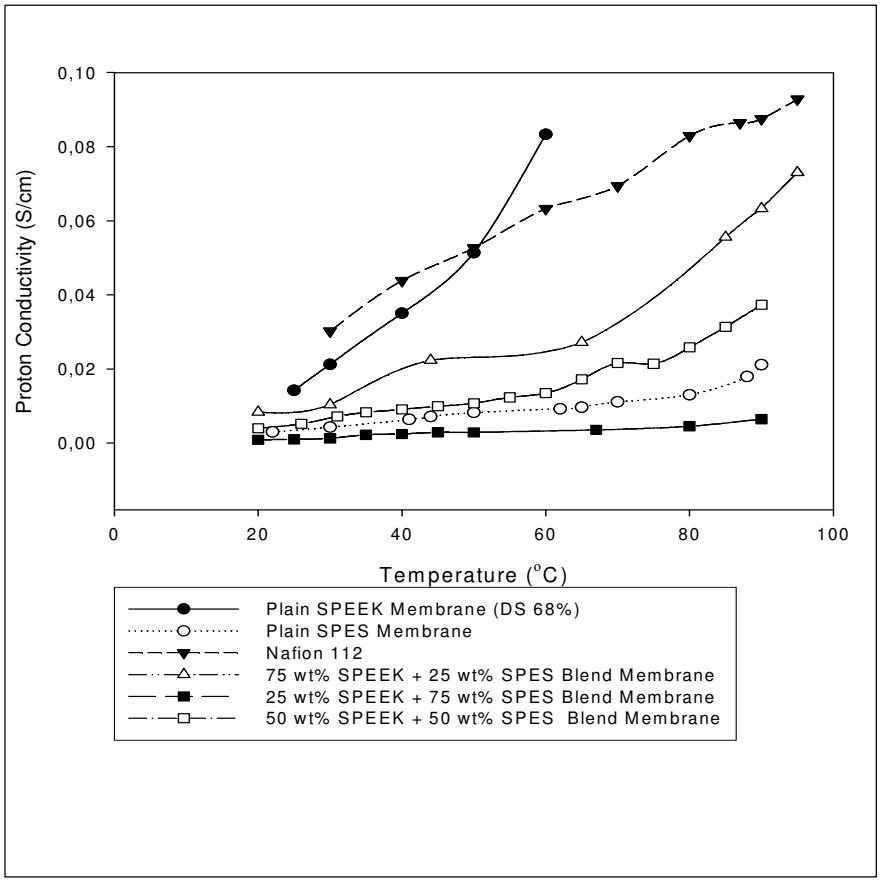

Figure 4.18: Proton Conductivities of plain and blend membranes

4.6 Fuel Cell Performance Tests

The fuel cell performances of the membranes were tested in a single cell (Electrochem) with an active area of 5cm x 5cm in which pure hydrogen was supplied as the fuel and pure oxygen as the oxidant. The membrane electrode assemblies (MEA) were prepared as described in experimental part (section 3.7.6).

First of all, the effect of using different catalyst ink solutions on the membrane performance is explored. The MEAs could be either prepared by using Nafion® solution or the original SPEEK solution.

The comparison of two MEAs prepared by both Nafion® and SPEEK solutions are given in Figure 4.19. It is apparent that the utilization of Nafion® solution in the catalyst ink resulted in higher performance. Thus, Nafion® solution is utilized in the preparation of all MEAs.

Secondly, the effect of operating temperatures on the performances of MEAs prepared by using SPEEK membranes (DS 56%) was examined and the results are given in Figure 4.20.

SPEEK based MEAs were not stable at high temperatures and they have punctured above 90°C. The best operating temperature of SPEEK based MEAs was found to be 70°C as demonstrated in Figure 4.20. The thermal stability of the membranes could be improved by blending with SPES polymer. It was noticed that, after the incorporation of 10wt % SPES into SPEEK membrane, the cell operating temperature could be increased up to 90°C without any damage to the membrane. As shown in Figure 4.21, the highest power output could be obtained at 80°C for SPES-SPEEK blend membranes.

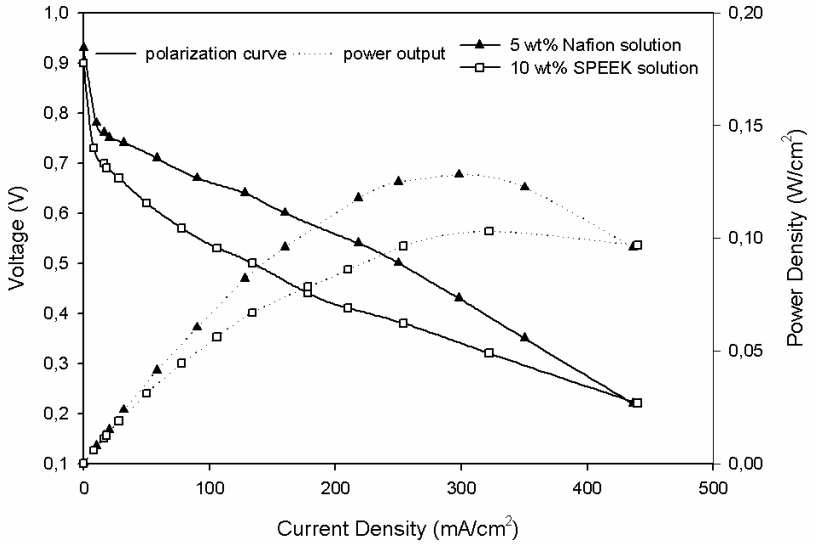

Figure 4.19: Comparison of Nafion® solution and SPEEK solution for SPEEK based MEAs (Cell temperature 70°C).

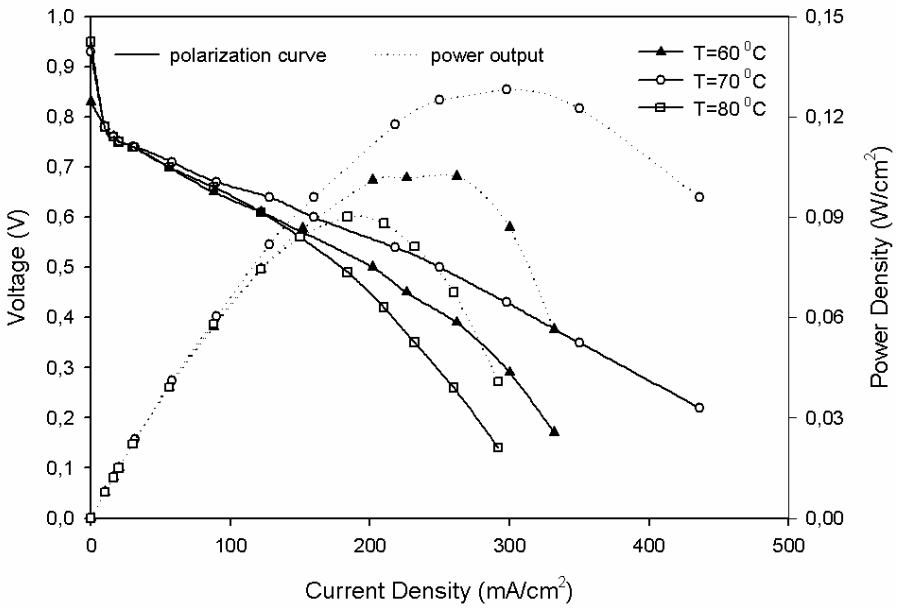

Figure 4.20: Effect of operating temperature on the performance of SPEEK (DS 56%) based MEAs.

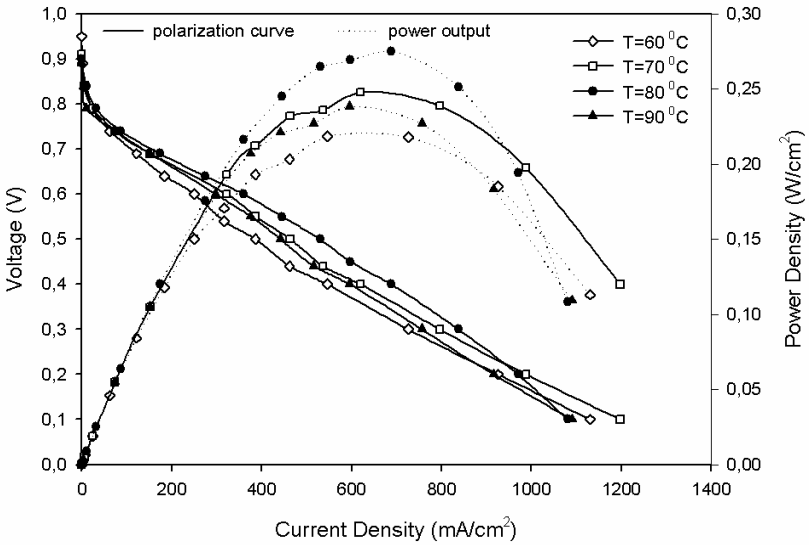

Figure 4.21: Effect of operating temperature on the performance of blend membranes

Thirdly, in order to understand the effect of sulfonation level on membrane performance, MEAs were prepared by using two membranes with different DS and the test results are displayed in Figure 4.22.

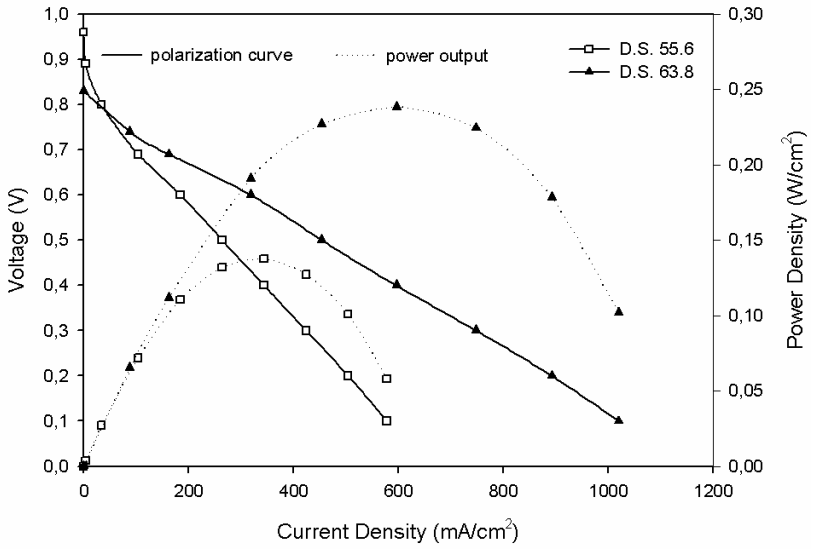

Figure 4.22: Effect of sulfonation level on the performance of SPEEK based MEAs (Cell Temperature 70°C)

It was not surprising to observe higher performance results for the MEA prepared by using the membrane at higher DS, since the proton transfer facilitates more easily with increased sulfonic acid group contents.

Another important parameter affecting the MEAs performance is membrane treatment. Since the proton transfer mechanism of both SPEEK and SPES membranes depend on the acidic character of the membranes, the acid treatment influences the membrane performance. The performance curves of both untreated and acid treated SPEEK based MEAs are given in Figure 4.23.

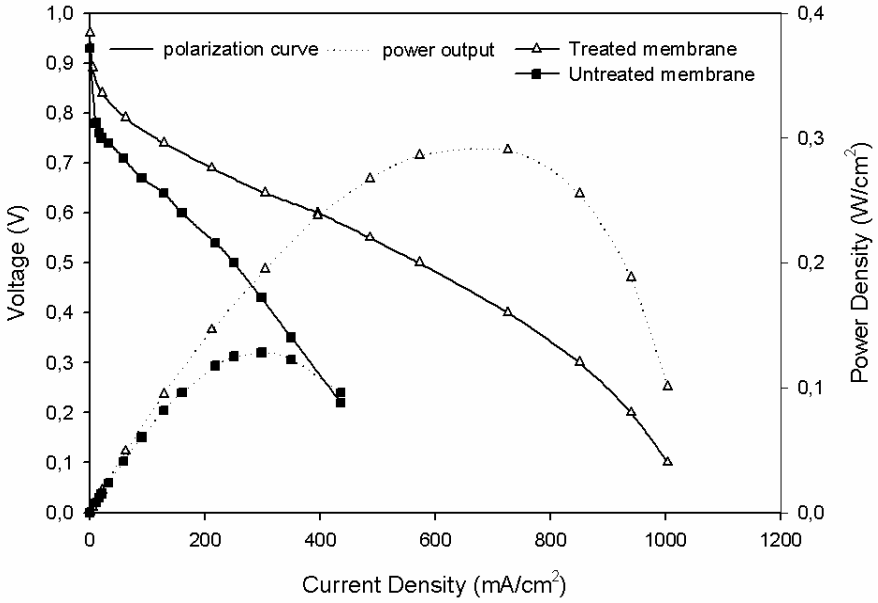

Figure 4.23: Effect of acid treatment on the performance of SPEEK (DS 56%) based MEAs (Cell Temperature 70°C)

The acid treated membrane showed almost threefold higher power density compared to the untreated membrane.

The fuel cell performance of SPEEK membrane was compared with the performance of Nafion membrane as given in Figure 4.24. The current density of plain SPEEK membrane with DS 56% was 397 mA/cm^2 at 0.6V, and it was close to the performance of Nafion 112® membrane having 660 mA/cm^2 under same conditions. Although SPEEK membrane possesses lower fuel cell performance in comparison to the Nafion membrane, the result is promising when the relatively low cost of SPEEK membrane is considered. Moreover, this result is comparable with the work of Chang and co-workers which is given in Figure 2.27 [36]. Higher performances could be obtained for the membranes with higher DS values and for composite membranes.

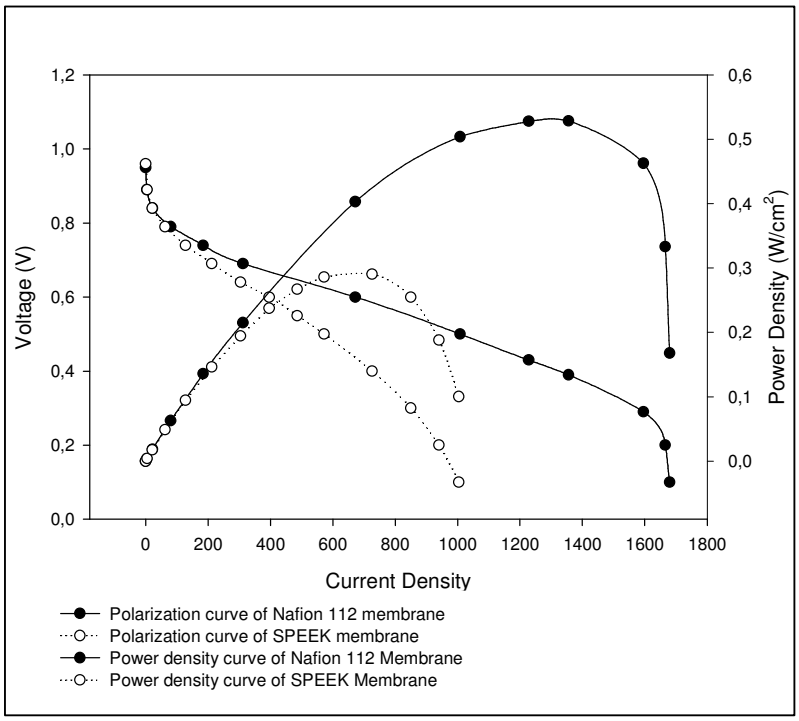

Figure 4.24: The comparison of performances of Nafion and SPEEK Membranes

CHAPTER 5

CONCLUSIONS

The aim of this study was to develop alternative membranes that have suitable thermal and chemical stability, mechanical strength, comparable proton conductivity and fuel cell performance with the commercial PEM fuel cell membranes at a relatively low cost. In this respect, organic-inorganic composite and blend membranes were developed. Polyether ether ketone polymer (PEEK), which consists of a polyaromatic hydrocarbon backbone with hydrophilic side chains, was proven to be a good membrane matrix for its high thermal and mechanical stability. The proton conductivity of this polymer could be improved by post-sulfonation and the membranes prepared from sulfonated derivative of PEEK polymer with a sulfonation level of 68% has shown good proton conductivities over a wide temperature range of 20°C-80°C. The proton conductivity of these membranes could further be increased with the addition of inorganic fillers. The objective behind the incorporation of inorganic fillers into the structure was to capture more water within the membrane and enable new water mediated pathways for the proton transfer within the membrane. Moreover, it was expected that, the inorganic fillers will contribute to the mechanical strength and thermal stability of the membrane as well as introducing their proton conductivity. Zeolite beta was chosen as the inorganic filler for its high thermal stability up to 800°C, resistance to acid environment and good proton conductivity around 10^{-4} S/cm which could be increased up to 10^{-2} S/cm via acid treatment. Zeolite beta fillers could be hydrothermally synthesized at different SiO_2/Al_2O_3 ratios and the acid strength of the zeolite increases with increasing silica content in the batch synthesis solution.

The effect zeolite beta fillers synthesized at different SiO_2/Al_2O_3 ratios were explored and proton conductivity was found to increase with increasing silica content of the zeolite. The best conductivity result of 0.13 S/cm was achieved for the composite membrane prepared by the addition of zeolite beta synthesized at SiO_2/Al_2O_3 ratio of 50 into SPEEK polymer with DS 68%. The optimum zeolite loading was found to be 10 wt% of the polymer.

On the other hand, the operating temperature of these composite membranes was limited up to 60°C because of swelling problems. The PEEK polymer lost its crystallinity and became amorphous upon sulfonation and its hydrophilicity increased. As a result, it absorbed more water leading to high water uptake of the membranes and faced with the swelling problem. Swelling problem could be solved in two ways. Firstly, some of the sulfonic acid groups within the polymer structure were cross-linked by thermal treatment at 120°C for one more day. The thermal cross-linking was successful by means of increasing the operating temperature range of the membranes which will increase their performance within the fuel cell. However, the decrease in the sulfonic acid sites available for hydrogen bonding by cross-linking caused a reduction in the proton transfer. These membranes could perform at 100°C without deformation with a proton conductivity of 0.08 S/cm that is quite close to the conductivity of Nafion® 112 membranes. Thus these membranes could still be considered as good alternatives.

Secondly, the swelling problem could be overcome by blending the SPEEK polymer with a more stable polymer. Polyether sulfone polymer has good thermal stability and lower water uptake capacity. Like SPEEK polymer the proton conductivity of PES polymer could also be altered by post-sulfonation. Thus, the sulfonated derivative of PES polymer was blended with more conductive but less stable SPEEK polymer at predetermined proportions. Introduction of 25 wt% SPES polymer into SPEEK polymer resulted in thermally stable membranes up to 100°C with conductivities of 0.08 S/cm. This blend membrane could be another promising alternative since the target is 0.1 S/cm.

In conclusion, the composite and blend membranes developed resulted in adequate thermal and chemical stability, mechanical strength and good proton conductivities comparable with Nafion membranes. Moreover, these membranes have shown promising performances in fuel cell tests. These results are welcomed when the high manufacturing cost of Nafion membranes (around 2000 $/m^2$) is compared with the manufacturing cost of composite and blend membranes which is around 1120 $/m^2$. The cost estimation calculations are given in Appendix C in detail.

CHAPTER 6

RECOMMENDATIONS FOR FUTURE WORK

For future works the following recommendations could be taken into account:

- ✓ In this work, PEEK polymer was chosen as the membrane matrix for its low cost, commercial availability, proper thermal and mechanical stability and good proton conductivity. However, due to the low molecular weight of the polymer (Aldrich, Mw= 20800) utilized in this work, swelling problems were encountered at high temperature operations. This problem was attempted to overcome by thermal cross-linking or blending with a thermally more stable polymer. Another solution could be utilizing a PEEK polymer with higher molecular weight since the increase in the molecular weight increases the crystallinity of the polymer resulting in less soluble polymer at high temperatures. In this respect, some alternatives could be higher molecular weight PEEK polymers of different brands such as Gatone™ and Vitrex™.

- ✓ In future work relative humidity could be considered as another parameter and its influence on proton conductivity and cell performance could be monitored. The composite membranes are expected to show good proton conductivities even at low relative humidity due to their high water retention capacities.

- ✓ Methanol cross-over or fuel cross-over rates of the developed membranes could be analyzed. The inorganic fillers are expected to reduce the cross-over rates of the fuel. If these membranes will result in lower methanol permeabilities than the Nafion membranes, these composite membranes could also be utilized not only in PEM fuel cells but also in direct methanol fuel cells (DMFC).

- ✓ More detailed fuel cell performance tests and durability tests over 1000 hours could be a determining step before the mass production of these membranes. The durability of these membranes must be worked out to decide on the feasibility of the mass production of these membranes.

- ✓ In future, these membranes will be further improved for higher temperature fuel cell applications which will have enhanced reaction kinetics leading to better fuel cell performances. The only drawback of these higher temperature applications is the swelling problem of the developed membranes. More stable composite membranes could be developed by incorporating zeolite beta fillers into a thermally more stable polymer with good proton conductivity. The polymers with fluorinated backbones or more stable polyaromatic hydrocarbon polymers such as polybenzimiadazole could be good alternatives.

REFERENCES

[1] Barbir F., "PEM Fuel Cells theory and Practice", Elsevier Academic Press, 2005.

[2] Fuel Cells; http://en.wikipedia.org/wiki/Fuel_cell, last accessible June, 2007

[3] Rogers., MSc. Thesis in Chemical Engineering, Northeastern University, Boston, Massachusetts, 2004

[4] Ballard Power Systems Manual, January 2003

[5] Ballards Company, www.ballard.com/be_informed/fuel_cell_technology/how_the_technology_works, last accessible June, 2007

[6] Rikukawa M., S. K. 'Proton-conducting polymer electrolyte membranes based on hydrocarbon polymers', Progress in Polymer Science, 25, 1463-1502, (2000).

[7] Savadogo O.' Emerging membranes for electrochemical systems: (I) solid polymer electrolyte membrane for fuel cell systems, Journal of New Materials for Electrochemical Systems I, 47, (1998).

[8] Asahi Chemical Company, http://www.agc.co.jp/english/index.html, last accessible June, 2007

[9] DuPont Fuel Cells, http://www.dupont.com/fuelcells/index.html, last accessible June, 2007

[10] Dow Chemical, www.dow.com/Homepage.index.html, last accessible June, 2007

[11] P. Jannasch, Recent developments in high temperature proton conducting polymer electrolyte membranes, Current Opinion in Colloid and Interface Science 8, 96, (2003).

[12] Alberti G., Casciola M., Massinelli L., Bauer B., 'Polymeric Proton Conducting Membranes for Medium Temperature Fuel Cells (110-160°C)', Journal of Membrane Science, 185, 73-81, (2001).

[13] Kobayashi T., Rikukawa M., Sanui K., Ogata N. 'Proton-conducting Polymers derived from poly (ether-ether ketone) and poly (4-phenoxybenzoyl-1,4-phenylene)', Solid State Ionics, 106, 219-225, (1998).

[14] Zaidi S. M. J., Michailenko S.D., Robertson G.P., Guiver M.D., Kaliaguine S., 'Proton Conducting Composite Membranes from polyether ether ketone and heteropolyacids for Fuel Cell Applications', Journal of Membrane Science, 173, 17-34, (2000).

[15] Michailenko S.D., Zaidi S.M.J., Kaliaguine S., 'Sulfonated polyether ether ketone based composite polymer electrolyte membranes', Catalysis Today, 67, 225-236, (2001).

[16] J.F. Blanco, Q.T. Nguyen, P. Schaetzel. 'Novel hydrophilic membrane materials: sulfonated polyethersulfone Cardo', Journal of Membrane Science, 186, 267-279, (2001).

[17] Lufrano F., Gatto I., Staiti P., Antonucci V., Passalacqua E. 'S**ul**fonated polysulfone as promising membranes for polymer electrolyte fuel cells', Journal of Applied Polymer Science, 77, 1250-1257, (2000).

[18] Lufrano F., Gatto I., Staiti P., Antonucci V., Passalacqua E. 'Sulfonated polysulfone ionomer membranes for fuel cells', Journal Solid State Ionics, 145, 47-51, (2001).

[19] Genova-Dimitrova P., Baradie B., Foscallo F., Poinsignon C., Sanchez J.Y . 'Ionomeric membranes for proton exchange membrane fuel cell (PEMFC): sulfonated polysulfone associated with phosphatoantimonic acid', Journal of Membrane Science, 185, 59-71, (2001).

[20] Jones D.J., Rozière J., **'**Recent advances in the fictionalization of polybenzimidazole and polyetherketone for fuel cell applications', Journal of Membrane Science, 185, 41-58, (2001).

[21] Staiti P., Lufrano F., Aricò A.S., Passalacqua E., Antonucci V., (2001). 'Sulfonated polybenzimidazole membranes — preparation and physico-chemical characterization', Journal of Membrane Science, 188, 71-78, (2001).

[22] Wycisk R., Pintauro P.N., 'Sulfonated polyphosphazene ion-exchange membranes', Journal of Membrane Science, 119, 155-160, (1996).

[23] Honma I., Nomura S., Nakajima H., 'Protonic conducting organic/inorganic nanocomposites for polymer electrolyte membrane', Journal of Membrane Science, 185, 83-94, (2001).

[24] Staiti P., Aricò A.S., Baglio V., Lufrano F., Passalacqua E., Antonucci V., 'Hybrid Nafion–silica membranes doped with heteropolyacids for application in direct methanol fuel cells', Solid State Ionics, 145, 101-107, (2001).

[25] Bac N., Nadirler S., Ma C., Mukerjee S. "Inorganic-Organic Composite Membranes for Fuel Cell Applications", Proceedings International Hydrogen Energy Congress and Exhibition IHEC 2005 Istanbul, Turkey, (2005).

[26] Mikhailenko S.D., Wang K., Kaliaguine S., Xing P., Robertson G., Guiver M., 'Proton conducting membranes based on cross-linked Sulfonated poly(ether ether ketone) (SPEEK)', Journal of Membrane Science,233, 93-99, (2004).

[27] Zaidi S.M.J., 'Polymer Sulfonation- A Versatile Route to Prepare Proton-Conducting Membrane Material for Advanced Technologies', The Arabian Journal For Science and Engineering, Volume 28, Number 2B, (2003).

[28] Cui W., Kerres J., Einberger G., ' Development and characterization of ion-exchange polymer blend membranes', Separation Purification Technology 14, 145-154, (1998).

[29] Bonnet B., Jones D.J., Roziere J., Tchicaya L., Alberti G., Casciola M., Massinelli L., Bauer B., Peraio A., Ramunni E., 'Hybrid organic-inorganic membranes for a medium temperature fuel cell', Journal of New Mater. Electrochem. Syst., Volume 3, Number 2, 87-92, (2000).

[30] Ise M. , Kreuer K.D., Maier J., 'Electroosmotic drag in polymer electrolyte membranes: an electrophoretic NMR study', Solid State Ionics, 125, 213-223, (1999).

[31] Kreuer K.D., 'On the development of proton conducting polymer membranes for hydrogen and methanol fuel cells', Journal of Membrane Science, 185, 29-39, (2001).

[32] Kaliaguine S., Michailenko S.D., Wang K.P., Xing P., Robertson G., Guiver M., 'Properties of SPEEK based PEMs for fuel cell application', Catalysis Today, 82, 213-222, (2003).

[33] Robertson G.P., Mickhailenko S.D., Wang K.P., Xing P., Guiver M., Kaliaguine S.,' Casting Solvent Interactions with sulfonated poly(ether ether ketone) during proton exchange membrane fabrication', Journal of Membrane Science, 219, 113-121, (2003).

[34] Xue S., Yin G., 'Methanol permeability in sulfonated poly(ether ether ketone) membranes: A comparison with Nafion membranes', European Polymer Journal, 43, 776-785, (2006).

[35] Hogarth M., Glipa X., 'High temperature membranes for solid polymer fuel cells', Johnson Matthey Technology center. Crown Copyright, 2001.

[36] Chang J.H., Park J.H., Park G-G., Kim C-S., Park O-O., 'Proton –conducting composite membranes derived from sulfonated hydrocarbon and inorganic materials', Journal of Power Sources, 124, 18-25, (2003).

[37] Eapen M.J., Reddy K.S.N., Shiralkar V.P., 'Hydrothermal Crystallization of Zeolite Beta Using Tetraethyl Ammonium Bromide', Zeolites, Volume 14, 295-302, (1994).

[38] Picture, struktur.kemi.dtu.dk/kenny/research_projects.html last accessible June 2007

[39] Akata B., Yilmaz B., Jirapnogphan S. S., Warzywoda J., Sacco, Jr., A.. "Characterization of zeolite Beta grown in microgravity", Microporous and Mezoporous Materials, 71, 1-9, (2004).

[40] Schmidt W., Toktarev A., Schüth F., Ione K.G., Unger K., ' The influence of Different Silica Sources on the Crystallization Kinetics of Zeolite Beta ', 13th Zeolite Conference, Montpellier, (2001).

[41] Holmberg B.A., Hwang S-J., Davis M. E., Yan Y., 'Synthesis and Proton Conductivity of Sulfonic acid functionalized Zeolite BEA Nanocrystals', Microporous and Mezoporous Materials, Volume 80, 347-356 (2005).

[42] Berry M.B., Libby B.E., Rose K., Haas K.-H., Thompson R.W., ,'Incorporation of zeolites into composite matrices', Microporous and Mezoporous Materials, 39, 205-217, (2000).

[43] Gür N., MSc. Thesis in Chemical Engineering, Middle East Technical University, Ankara, Turkey., 2005

[44] Şengül E., Proceeding MSc. Thesis in Chemical Engineering, Middle East Technical University, Ankara, Turkey, 2007

[45] GAMRY Instruments Manual, http://www.gamry.com, last accessible June, 2007

APPENDIX A

ELECTROCHEMICAL IMPEDANCE SPECTROSCOPY (EIS)

A.1. Concept of Impedance

Electrical resistance is the ability of a circuit element to resist the flow of electrical current and defined by the Ohm's law as the ratio between voltage E and current I.

$$R = \frac{E}{I} \tag{A.1}$$

This is a well known relationship but its usage is only limited to the ideal resistor; which obeys the following assumptions [45];

- It obeys Ohm's Law at all current and voltage levels.
- Its resistance value does not depend of frequency.
- AC current and voltage signals through a resistor are in phase with each other.

However, the real world circuit elements show a much more complex behavior and do not follow these simplifications [45]. Hence, a more general concept of resistance is required and impedance concept is introduced. Like resistance, impedance is a measure of the ability of a circuit element to resist the flow of electric current; but it is not limited with the above listed simplifications [45].

Electrochemical impedance is usually measured by applying an AC potential to an electrochemical cell and measuring the circuit through it. A small sinusoidal potential excitation is applied to the electrochemical cell [45]. The response to this potential is an AC current signal which can be analyzed as a sum of sinusoidal functions [45]. In a linear pseudo-linear system, the current response to a sinusoidal function is a sinusoid at the same frequency but shifted in phase as shown in Figure A.1 [45].

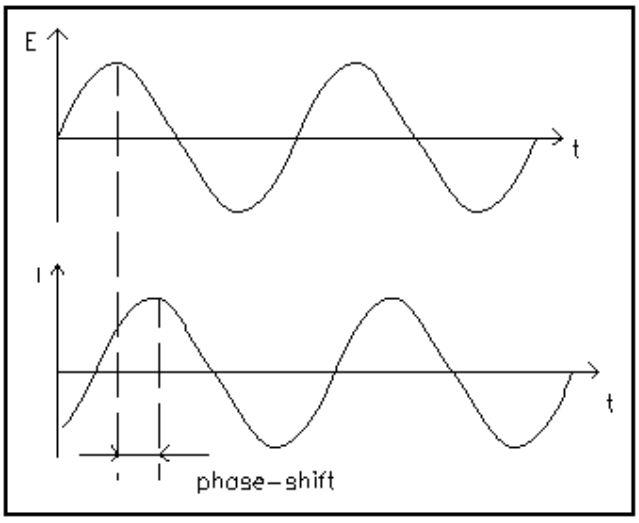

Figure A. 1: Sinusoidal Current response in a Linear System [45]

The excitation signal has the form [45],

$$E_t = E_0 \sin(\omega t) \tag{A.2}$$

Where E_t is the potential at time t and E0 is the amplitude of the signal and ω is the radial frequency (expressed in radians/second) and frequency f (expressed in hertz) [45];

$$\omega = 2\pi f \tag{A.3}$$

In a linear system, the response signal, I_t, is shifted in phase (φ) and has an amplitude [45], I_0 .

$$I_t = I_0 \sin(\omega t + \varphi) \tag{A.4}$$

The impedance of a system can be explained with a similar expression to Ohm's Law [45];

$$Z = \frac{E_t}{I_t} = \frac{E_0 \sin(\omega t)}{I_0 \sin(\omega t + \varphi)} = Z_0 \frac{\sin(\omega t)}{\sin(\omega t + \varphi)} \tag{A.5}$$

The impedance is expressed in terms of magnitude Z_0 and a phase shift, φ. By using Euler relationship, it is possible to express the impedance as a complex function [45].

$$\exp(j\varphi) = \cos\varphi + j\sin\varphi \tag{A.6}$$

$$Z = \frac{E_t}{I_t} = \frac{E_0 \exp(j\omega t)}{I_0 \exp(j\omega t - \varphi)} = Z_0 \exp(j\varphi) = Z_0(\cos\varphi + j\sin\varphi) \tag{A.7}$$

The expression of impedance is thus composed of a real and an imaginary part. If the real part is plotted on the Z axis and the imaginary part on the Y axis of a chart, Nyquist plot is obtained [45].

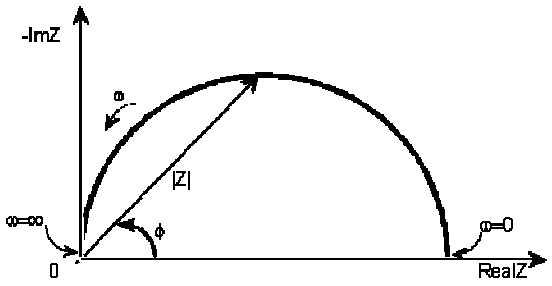

Figure A. 2: Nyquist Plot with Impedance vector [45]

Notice that in this plot Y-axis is negative. On Nyquist plot the impedance can be represented as a vector of length $|Z|$. The angle between this vector and X-axis is φ. The Nyquist plot shown in Figure A.2 is resulted from the electric circuit given in Figure A.3 [45].

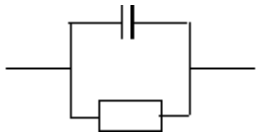

Figure A. 3: Simple Equivalent Circuit with one time constant [45]

Bode plot is another type of presentation of impedance. The impedance is plotted with log frequency on the x-axis and both the absolute values of the impedance and phase shift on the y-axis as shown in Figure A.4.

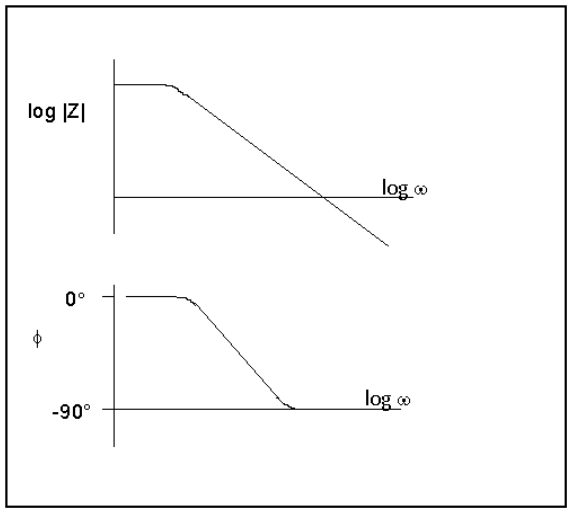

Figure A. 4: Bode Plot with one-time constant [45]

A.2 Proton Conductivity Measurements

Impedance analyses of linear circuits are much easier than non-linear ones. Although potentiostated electrochemical cells (whose input is the potential and output is current) are not linear, they behave pseudo-linearly at small potentials. Thus in normal EIS measurements, a small (1 to 10mV) AC signal is applied to the cell for which the system acts as pseudo-linear [45].

The resistance of an electrolyte can be measured by EIS technique. The resistance of an electrolyte depends on the ionic concentration, type of ions, temperature and the geometry of the area in which the current is carried [45]. In a well defined area, with area A and length L carrying a uniform current, the resistance is defined as;

$$R = \rho \frac{L}{A} \tag{A.8}$$

where ρ is the electrolyte resistivity. The reciprocal of ρ is the electrolyte conductivity (σ) and expressed as;

$$R = \frac{1}{\sigma} \times \frac{L}{A} \Rightarrow \sigma = \frac{L}{R \times A} \tag{A.9}$$

The unit of conductivity is Siemens per meter (S/m); where the siemens is the reciprocal of ohm.

APPENDIX B

EXTENDED RESULTS

B.1. Zeolite Synthesis

Zeolite beta crystals were hydro-thermally synthesized at different SiO_2/Al_2O_3 (SiO_2/Al_2O_3=20, 30, 40, 50) ratios according to the batch composition of 2.2 Na_2O: 1.0 Al_2O_3: x SiO_2: 4.6 $(TEA)_2O$: 440 H_2O (Akata, 2004). As synthesized zeolites were characterized by X-ray Diffraction and the peaks of as synthesized zeolite beta have demonstrated in Figures 1-5.

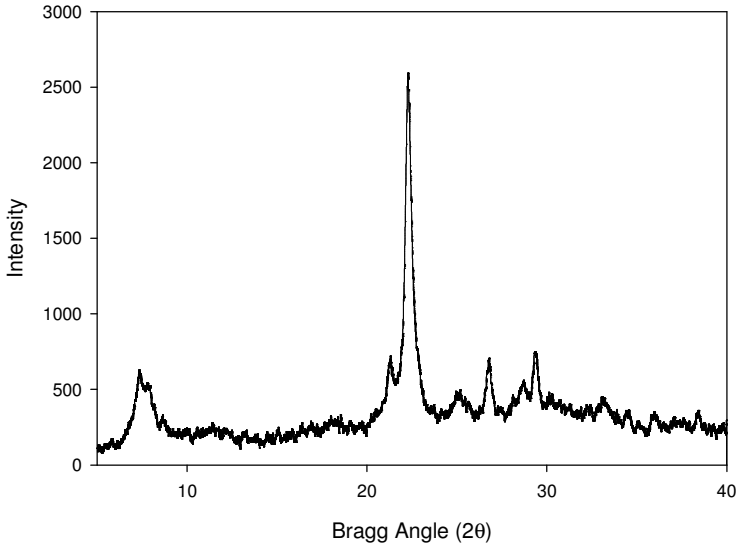

Figure B. 1: XRD pattern of as synthesized zeolite beta (SiO_2/Al_2O_3=20)

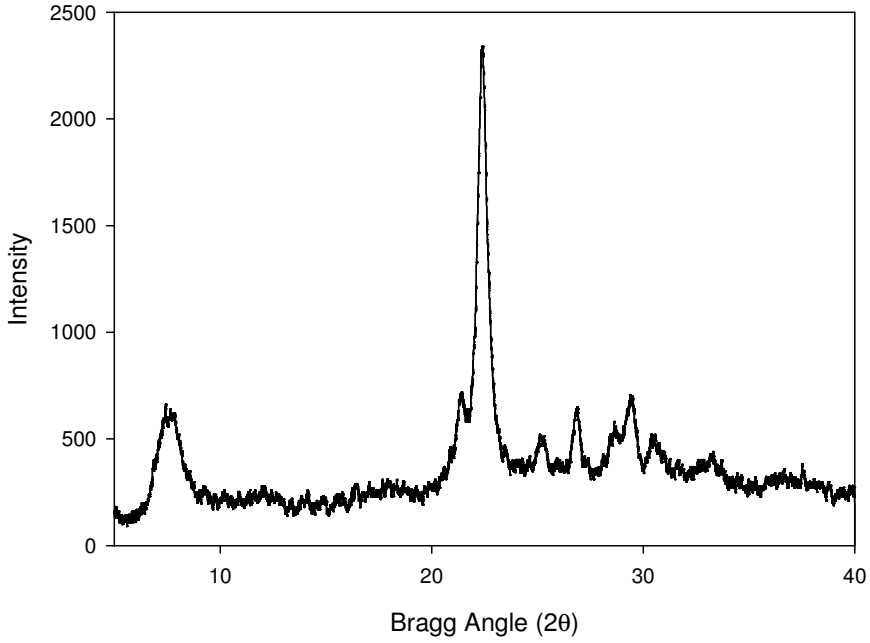

Figure B. 2: XRD pattern of as synthesized zeolite beta (SiO_2/Al_2O_3=30).

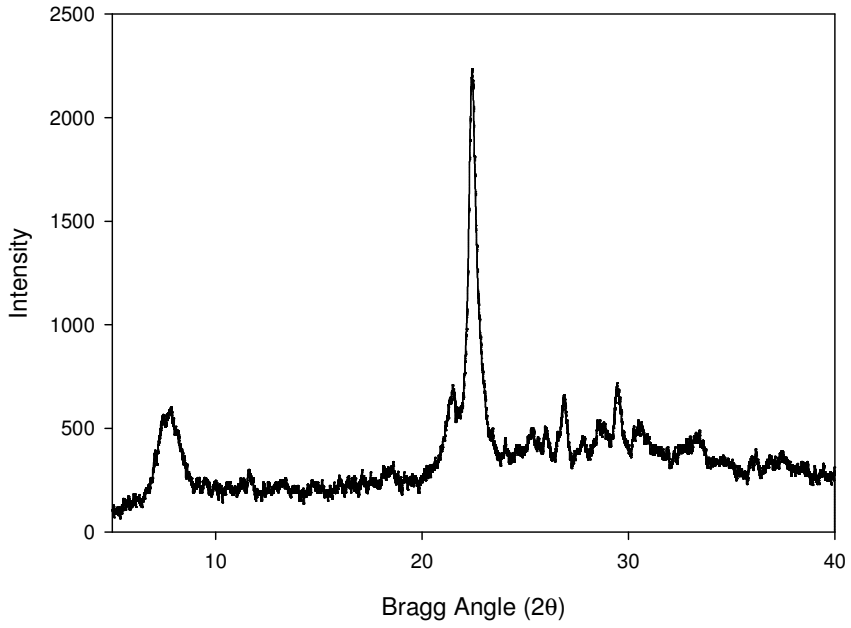

Figure B. 3: XRD pattern of as synthesized zeolite beta (SiO_2/Al_2O_3=40).

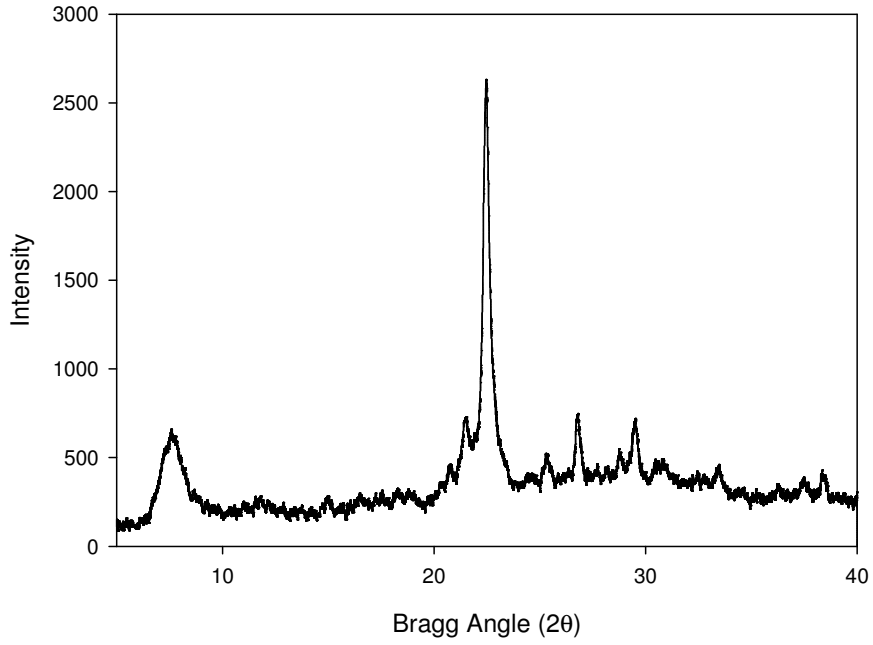

Figure B. 4: XRD pattern of as synthesized zeolite beta (SiO_2/Al_2O_3=50).

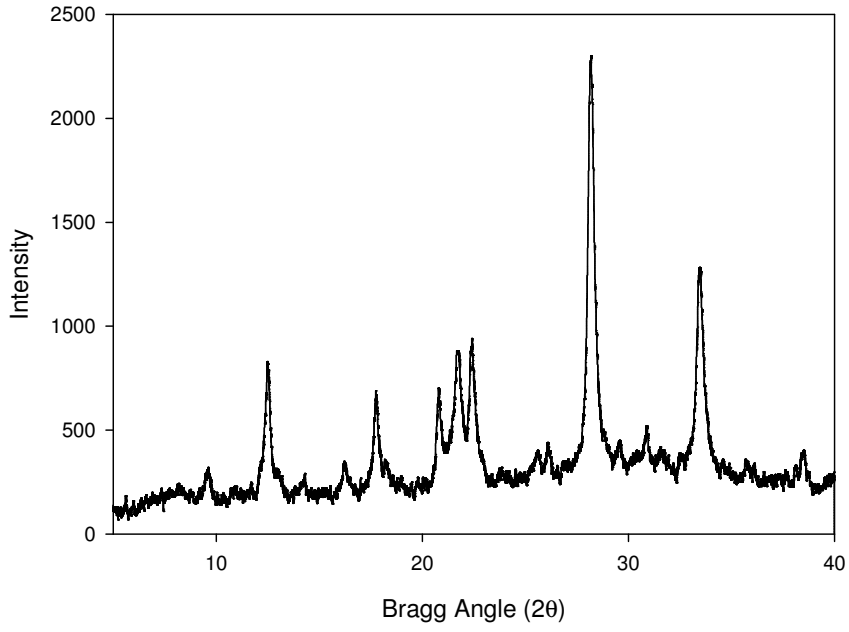

Figure B. 5: XRD pattern of as synthesized zeolite beta (SiO_2/Al_2O_3=12).

B.2. Polymer Sulfonation

The sulfonation level of PEEK polymer can be calculated from H-NMR analysis as described in the introduction part. The H-NMR results of some of the sulfonated PEEK polymer can be found in Figure 6-9.

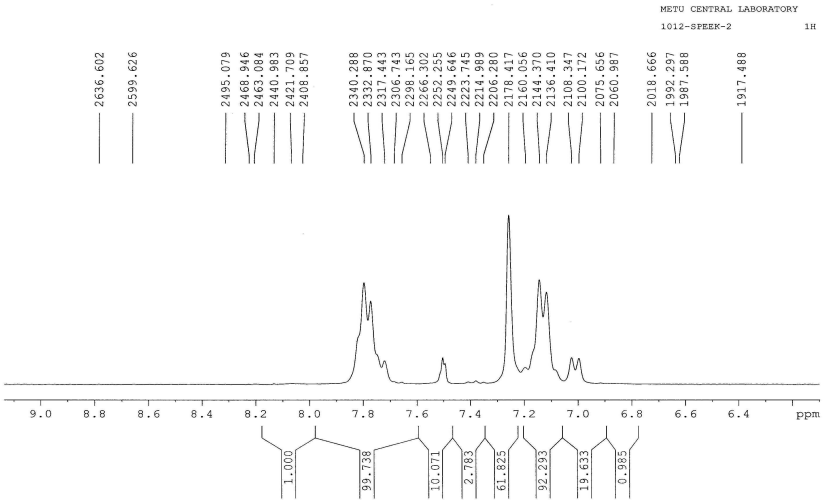

Figure B. 6: H-NMR diagram of SPEEK (DS= 41)

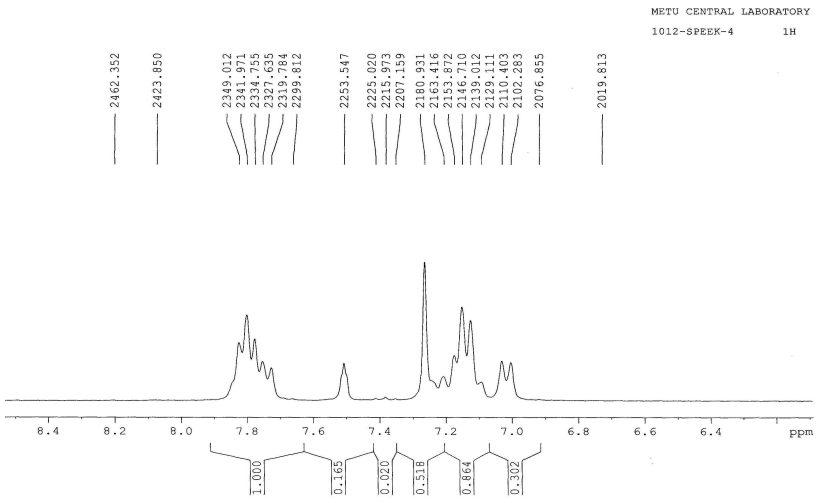

Figure B. 7: H-NMR diagram of SPEEK (DS= 65)

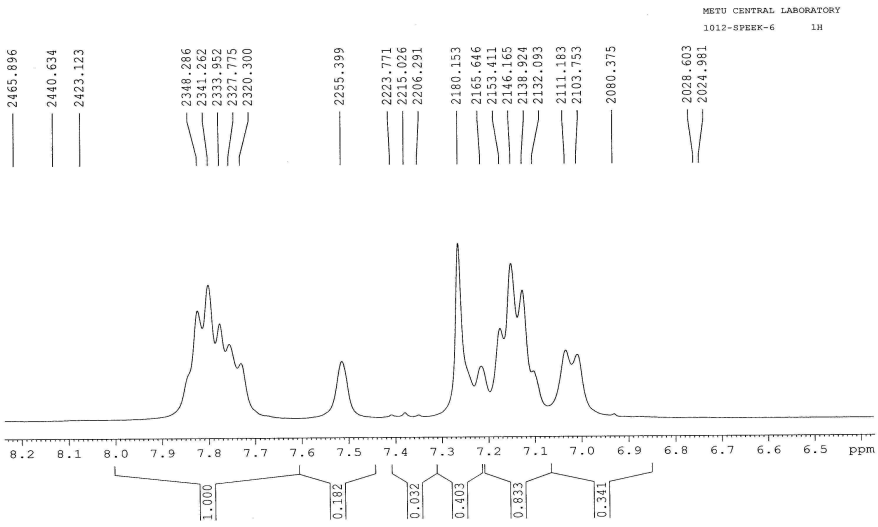

Figure B. 8: H-NMR diagram of SPEEK (DS= 68)

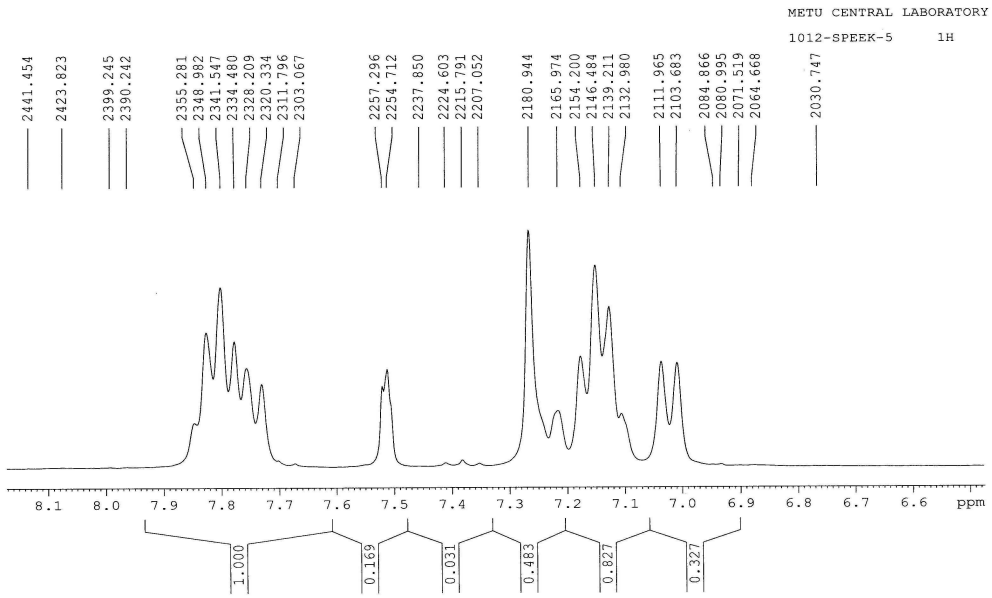

Figure B. 9: H-NMR diagram of SPEEK (DS= 74)

As demonstrated in Figures above, the sulfonation level of the polymer increases with increasing intensity of the peak at ~7.5ppm.

B.3 Thermal Analyses

The thermal stability of the casted membranes was analyzed by TGA and DSC analyses. All composite membranes were stable up to 340°C as shown in Figures 10-13.

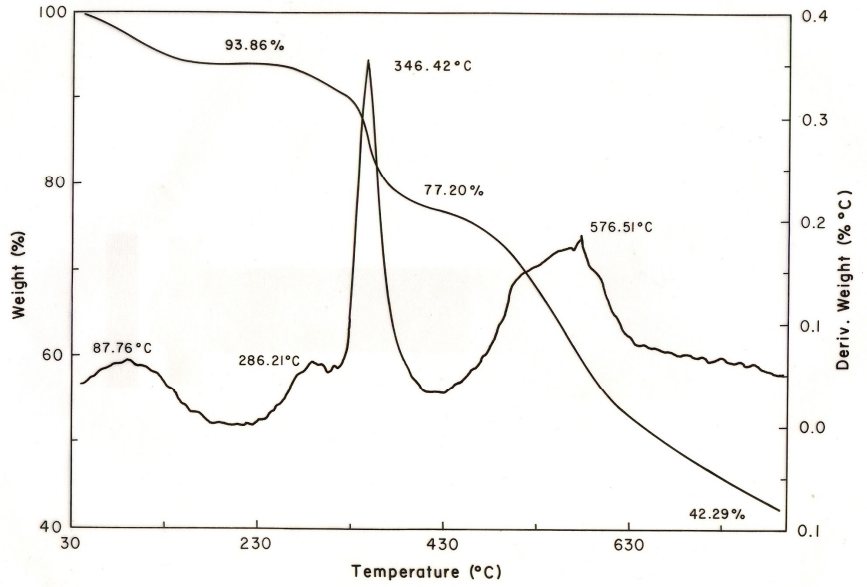

Figure B. 10: TGA graph of SPEEK (DS 68%) + Zeolite Beta (SiO_2/ Al_2O_3 = 20) Composite Membrane.

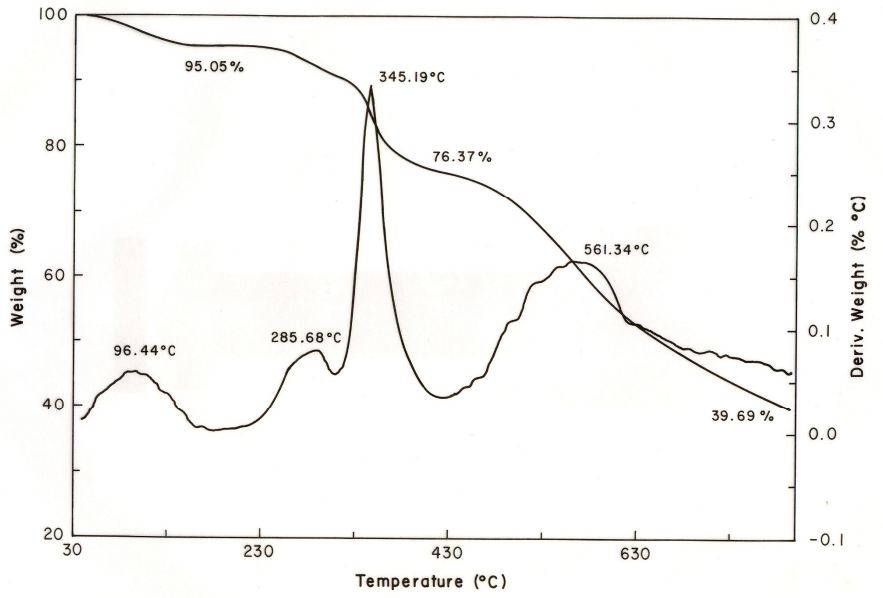

Figure B. 11: TGA graph of SPEEK (DS 68%) + Zeolite Beta (SiO_2/ Al_2O_3 = 30) Composite Membrane.

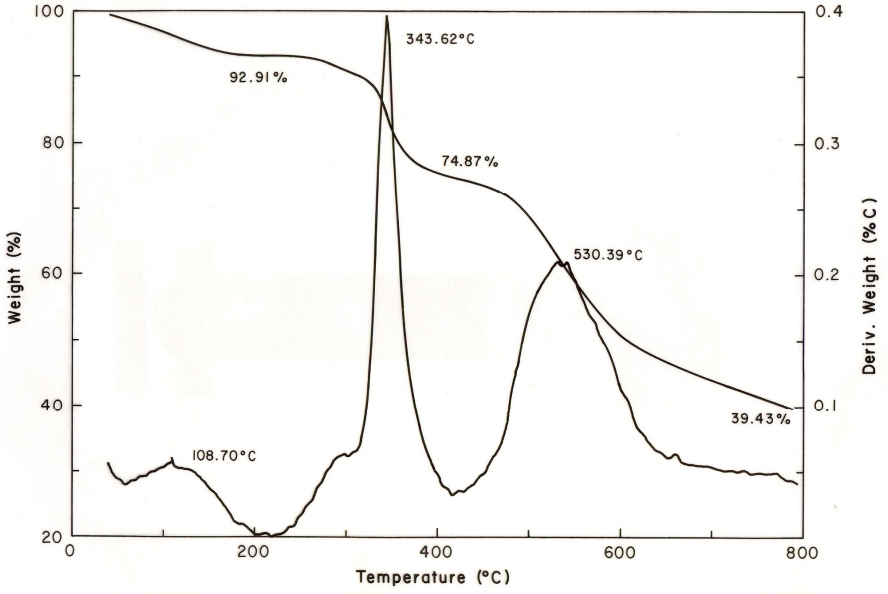

Figure B. 12: TGA graph of SPEEK (DS 68%) + Zeolite Beta (SiO_2/ Al_2O_3 = 40) Composite Membrane.

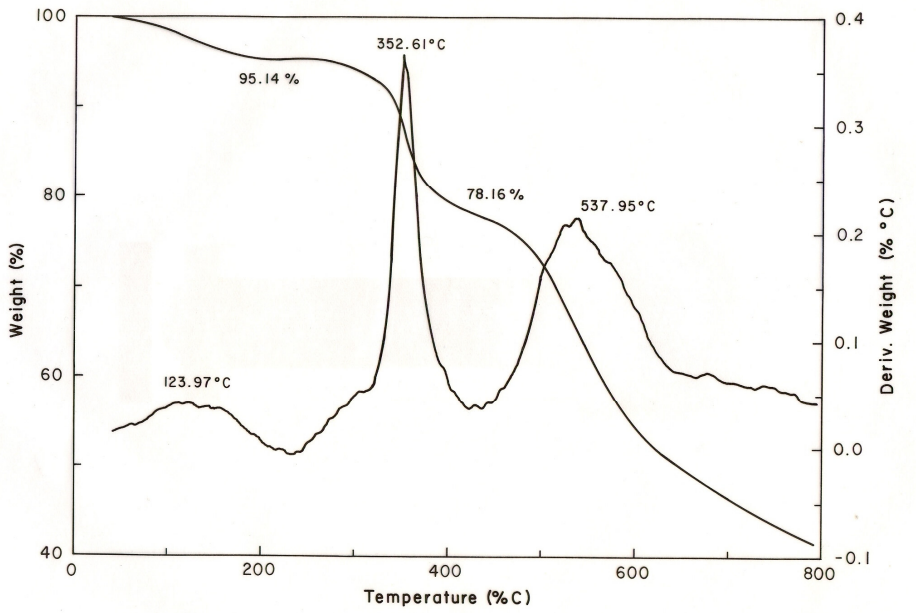

Figure B. 13: TGA graph of SPEEK (DS 68%) + Zeolite Beta (SiO_2/ Al_2O_3 = 50) Composite Membrane.

The thermal stability of SPEEK membranes could further be increased from 340°C to 465°C by blending with a more stable polymer, SPES. The TGA graphs of these blend membranes are given in Figures 14-16.

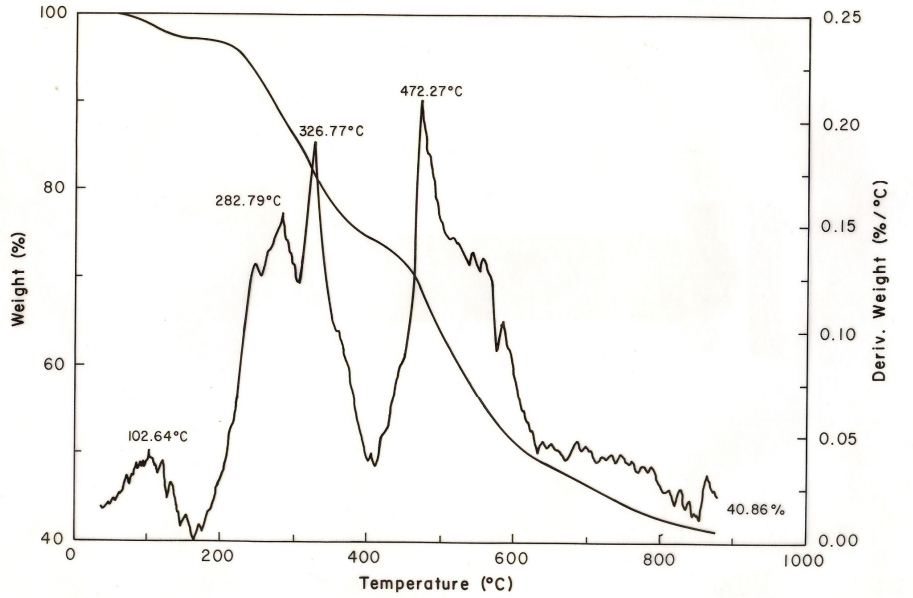

Figure B.14: TGA graph of (75 wt %) SPEEK+ (25 wt %) SPES Blend Membranes

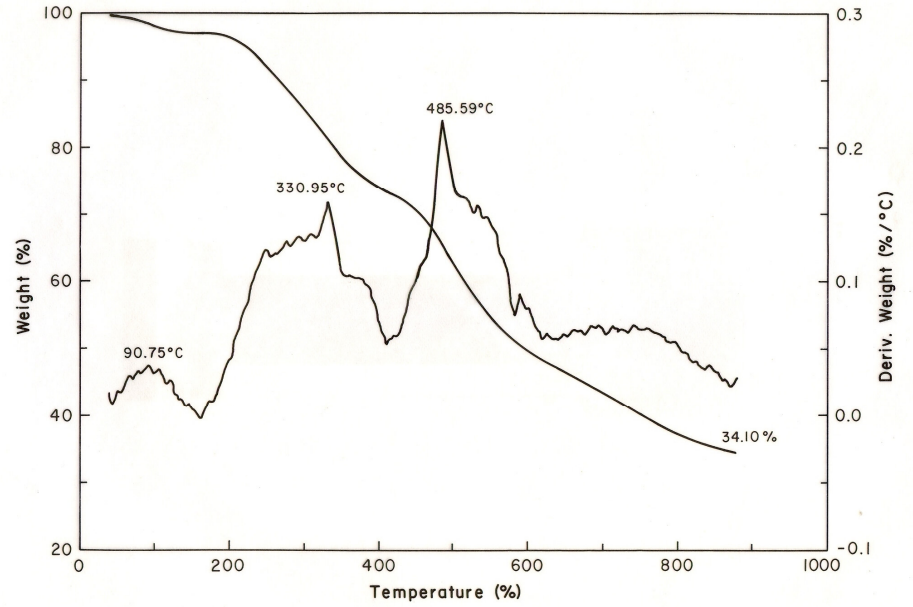

Figure B.15: TGA graph of (50 wt %) SPEEK+ (50 wt %) SPES Blend Membranes

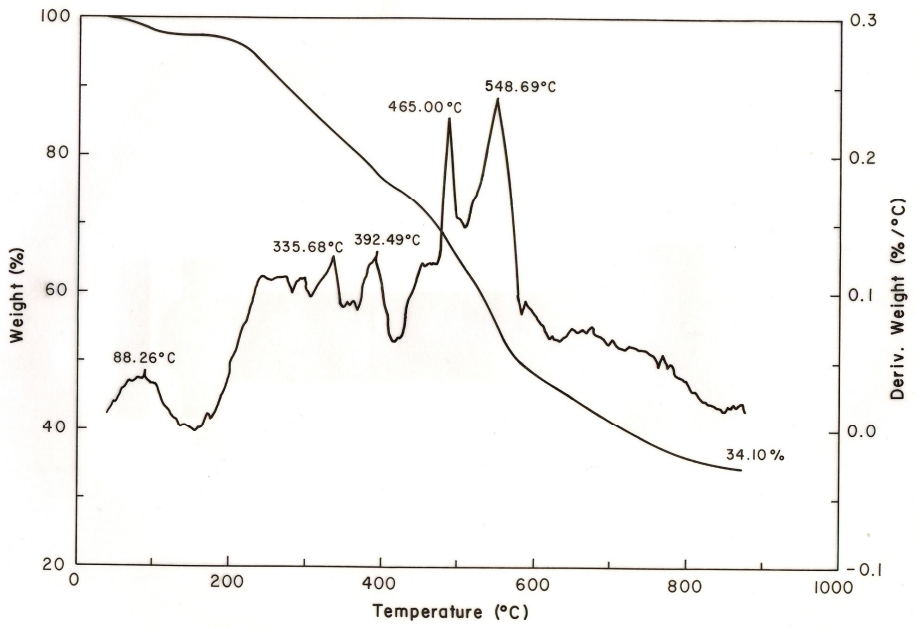

Figure B.16: TGA graph of (25 wt %) SPEEK+ (75 wt %) SPES Blend Membranes

The differential scanning calorimetry graphs some casted membranes are given in Figure 17-21. The glass transition temperatures of these membranes are in the range of 180°C to 250°C, which are quite high compared to the operating temperature of the fuel cell which is around 80°C and tends to increase after thermal treatment as shown in Figure 17 and 18.

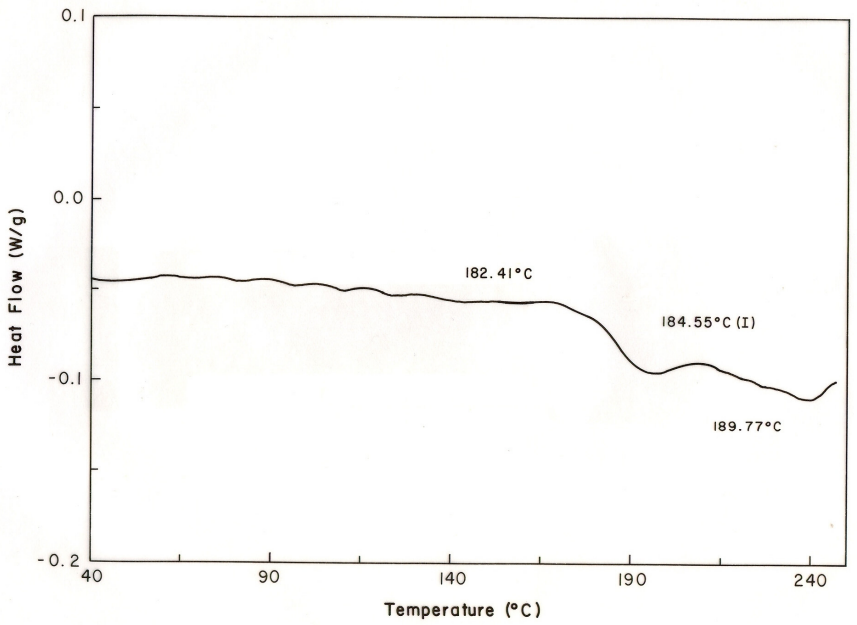

Figure B.17: DSC graph of SPEEK (DS 68%) membrane.

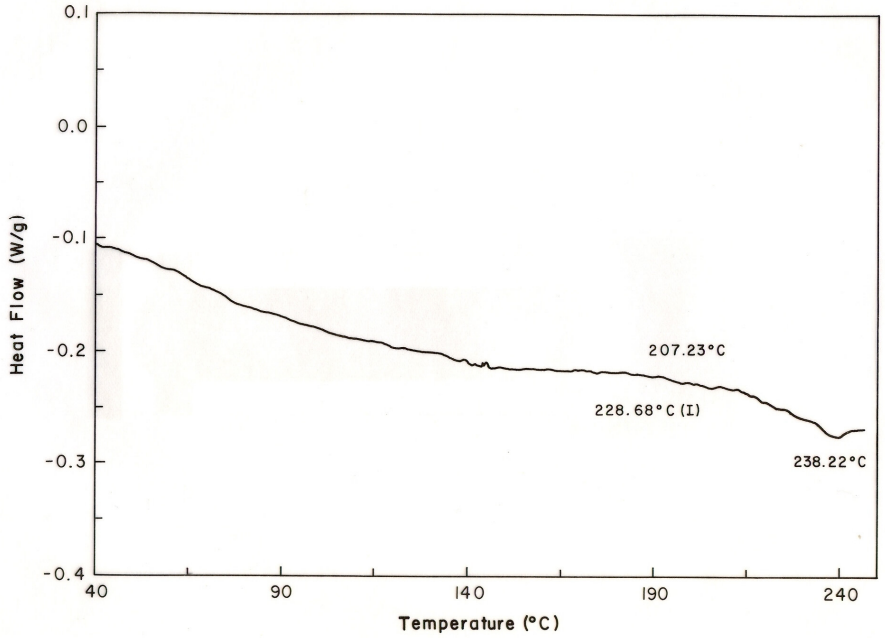

Figure B.18: DSC graph of SPEEK (DS 68%) membrane after thermal treatment at 120°C.

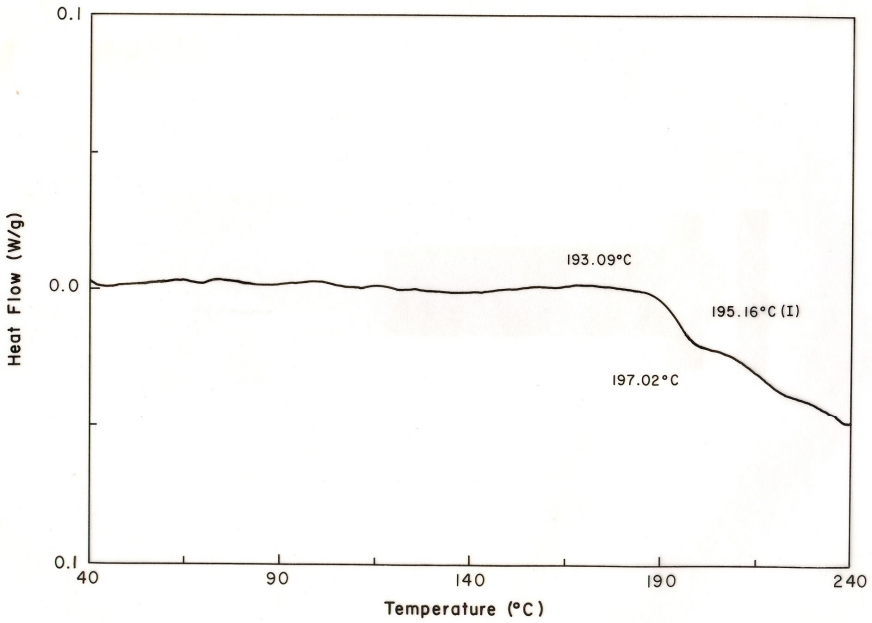

Figure B.19: DSC graph of SPEEK (DS 68%) + Zeolite Beta (SiO_2/ Al_2O_3 = 20) Composite Membrane.

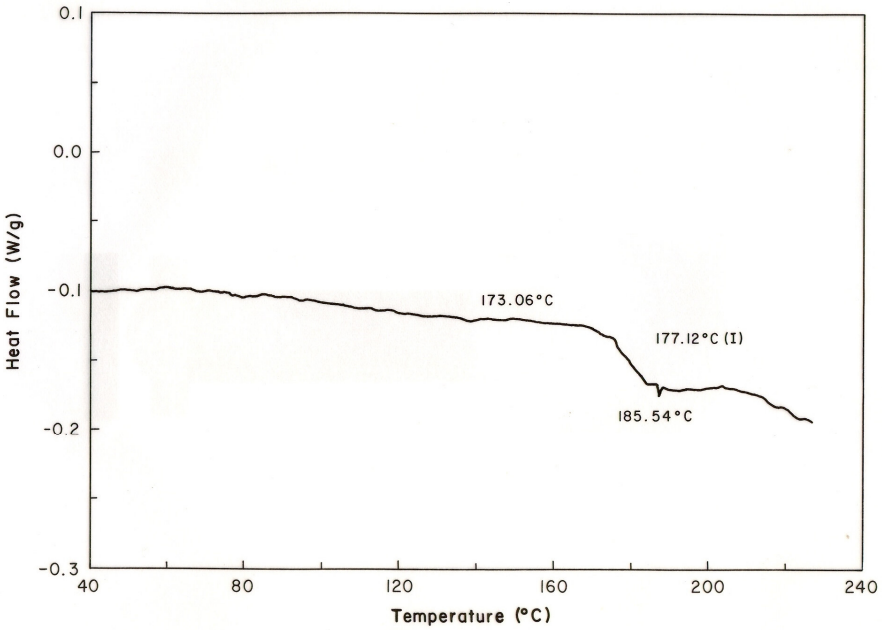

Figure B.20: DSC graph of SPEEK (DS 68%) + Zeolite Beta (SiO_2/ Al_2O_3 = 30) Composite Membrane.

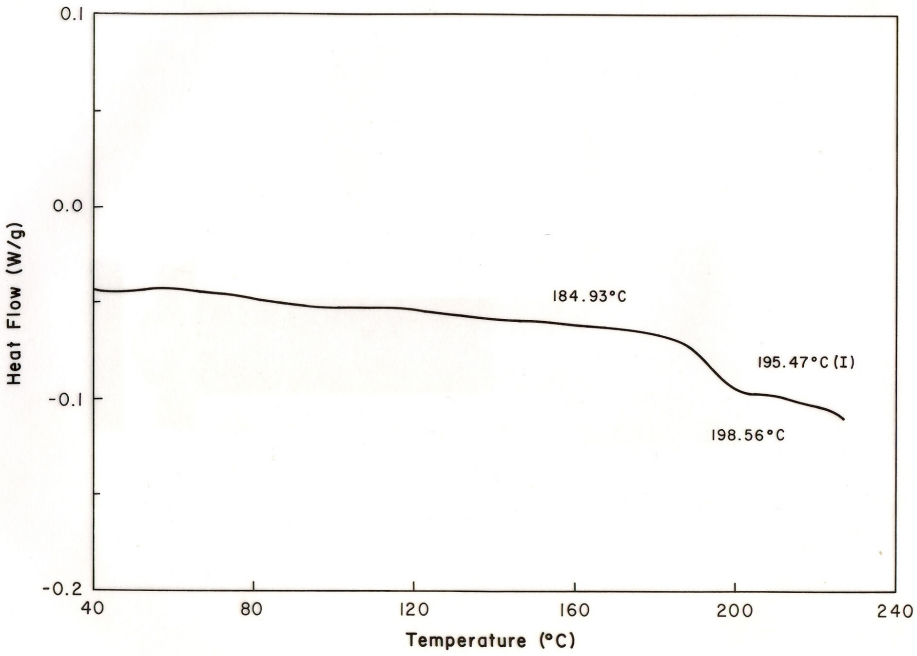

Figure B.21: DSC graph of SPEEK (DS 68%) + Zeolite Beta (SiO_2/ Al_2O_3 = 50) Composite Membrane.

B.4 SEM ANALYSIS

The SEM picture of organic-inorganic composite SPEEK membrane is shown in Figure B.22.

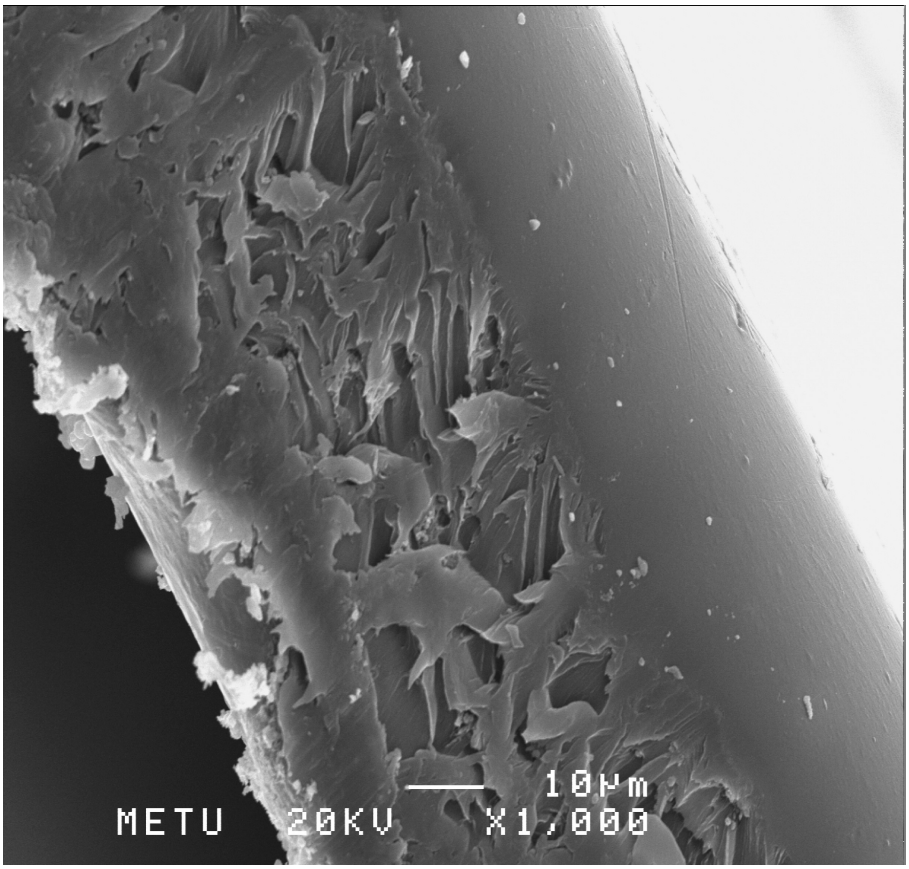

Figure B.22: SEM picture of organic-inorganic composite SPEEK (DS 68%) membrane.

APPENDIX C

COST ESTIMATION

The manufacturing cost of a composite membrane can be estimated by using the unit costs of the polymer, sulfuric acid used in the post-sulfonation process, solvent and the inorganic additives, namely zeolite beta. For simplicity the cost of commercial zeolite beta is used in the calculations.

Table C.1: The unit cost of the items used in membrane preparation

Item	Package	Unit Price
PEEK Polymer	100g.	133,70 €
N,N-Dimethylacetamide, 99%	1 L	26,90 €
SULFURIC ACID %95-97 AR	2,5 L	15,30 €
Commercial Zeolite Beta	100g.	43,60 €

In order to make a membrane 0.3 g sulfonated polymer is used. For post sulfonation 20 mL sulfuric acid is required for each gram of polymer.0.3 g sulfonated polymer is dissolved in 10 mL solvent and 0.03 gr zeolite is added to the mixture. Thus the cost of a membrane can be found as such;

The cost of PEEK polymer for a membrane;

$$0.3g\ polymer \times \frac{133.7 Euro}{100 g.} = 0.40\, Euro \quad \text{.....(C.1)}$$

The unit cost of sulfuric acid used in post-sulfonation required for one membrane;

$$0.3g\ polymer \times \frac{20\,mL\,sulfuric\,acid}{1g.polymer} \times \frac{15.30 Euro}{2500\,mL} = 0.037\,Euro \quad \text{.....(C.2)}$$

The cost of the solvent required for casting of a membrane;

$$10\,mL\,solvent \times \frac{26.90 Euro}{1000\,mL} = 0.27\,Euro \quad \text{.....(C.3)}$$

The cost of zeolite used;

$$0.03g\ zeolite \times \frac{43.60 Euro}{100\,g} = 0.013\,Euro \quad \text{.....(C.4)}$$

The total cost of the membrane;

$$0.4 + 0.037 + 0.27 + 0.013 = 0.72 Euro \quad \text{.....(C.5)}$$

The casted membrane has an area of 9 cm^2, thus the unit cost of a membrane is 0.08 Euro/cm^2, or 800 Euro/m^2 (around 1120 \$/m^2). Thus it can be concluded that the composite membranes are cheaper than the Nafion membranes which costs 2000 Euro/m^2.

The prices stated in Table C.1 were obtained from the chemical companies and these costs could be lower for bulk quantities. Hence, the manufacturing cost of these membranes might further be reduced in the mass production stage.